Su-PM-G5

GEOMETRY AND FLEXIBILITY OF BULGED THREE-WAY DNA JUNCTIONS. ((D. P. Millar and M. Yang)) Department of Molecular Biology, The Scripps Research Institute, La Jolla, CA 92037.

Branched three-way DNA junctions occur as intermediates in various cellular rearrangements of DNA. The overall structure of three-way DNA junctions is strongly perturbed by the presence of unpaired bases at the point of intersection between helices. Unpaired bases at the branch may also introduce a point of increased flexibility in the structure. We have used time-resolved fluorescence resonance energy transfer to assess the impact of bulged bases on the static and dynamic structure of a three-way DNA junction. Donor (D) and acceptor (A) dyes were attached to the arms of a synthetic three-way junction in all pairwise combinations. Donor decay profiles were analyzed using a gaussian distance distribution model. The recovered D-A distance distributions reveal the average distance between each pair of helices, as well as the range of distances that exists between each pair. In a perfectly base-paired junction, the three inter-helix distances are approximately equal, indicating that the perfect junction adopts an extended structure. The addition of two additional non-complementary nucleotides in one of the junction strands, at the point of connection between two helices, results in a significant displacement of one of the helices, while the position of the other helix remains relatively fixed. Moreover, the nature of the bulged bases dictates which of the flanking helices is perturbed by the bulge. Thymine, cytosine and adenine bulges specifically perturb the helix on the 3' side of the bulge, whereas a guanine bulge perturbs the helix on the 5' side of the bulge site. In addition, there is a broad range of distances between the perturbed arm and each of the two fixed arms in the bulged junctions, indicating that the perturbed arm has high mobility. Supported by NSF grant MCB-9317369.

Su-PM-G6

THE SEARCH FOR RIGIDITY IN DNA NANOCONSTRUCTION. ((Jing Qi, Xiaojun Li, Xiaoping Yang, and Nadrian C. Seeman)) Department of Chemistry, New York University, New York, NY 10003.

We have synthesized a cube and a truncated octahedron from DNA in the past. We wish to extend this capability to the construction of periodic matter, which entails translational symmetry. Molecular construction that involves high symmetry requires at least 3 elements: [1] Predictable specificity between components, [2] structural predictability of intermolecular products; and [3] structural rigidity of components. DNA branched junctions satisfy the first two requirements, but lack rigidity. A rigid DNA component is one in which the directions of double-helix axes (and hence the angles between them) vary within limits of flexibility no greater than those of linear DNA. We have tested the rigidity of triangles constructed from bulged 3-arm branched junctions. Triangles that alternate bulges on the inside and outside strands provide a reporter strand (thick strand below) for cyclization experiments.

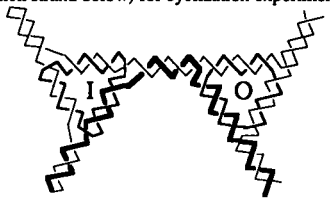

Supported by grants from ONR, NIH and W.M.Keck.

Su-PM-G7

STABILITY AND CONFORMATION OF $[d(T)-d(A)-d(T)]_n$. ((Y.Z. Chen and E.W. Prohofsky)) Purdue University, Dept. of Physics, W. Lafayette, IN 47907-1396.

A statistical mechanical variation of a vibrational mode, internal fluctuations, and hydrogen bond disruption of a DNA triplex was performed on both the fiber diffraction model with N-type sugar conformation and a proposed model with a S-type sugar conformation. Our modes for the S-type structure are in good agreement with observed IR spectra. Large discrepancies are found between observed modes for the N-type structure. The contribution of internal fluctuations to free energy, premelting hydrogen bond disruption probability and hydrogen bond melting temperatures for the Hoogsteen and Watson-Crick hydrogen bonds all show that the S-type structure is dynamically more stable than the N-type structure. Our calculation indicates $[d(T)-d(A)-d(T)]_n$ most likely adopts a S-type sugar conformation in solution.

Su-PM-G8

NON-CONTACT HANDLING OF μm-SIZED PARTICLES USING ULTRASOUND. ((K. Yasuda, +K. Takeda and S. Umemura)) Advanced Research Lab., HITACHI Ltd., 2520 Akanuma, Hatoyama, Saitama 350-03, JAPAN and +Central Research Lab., HITACHI Ltd., Kokubunji, Tokyo 185, JAPAN. (Spon. by H. Takei)

The efficacy of using an ultrasonic standing plane wave to concentrate small particles in a liquid was theoretically estimated and compared with experimental results [1]. The theory predicts that the effect of diffusion is negligible in concentrating polystyrene spheres larger than 5 μm in diameter when they are subjected to 4 J/m^3 ultrasound at 500 kHz. The halfwidth of the steady-state particle distribution in the experiment was in the same order of magnitude as in the theory. This technique was applied to concentration of biomaterials like DNA, red blood cells and liposomes. After the ultrasonic irradiation started, 3kbp DNA clusters in ethanol solution started moving toward the pressure node of the ultrasonic stationary standing wave and then gathered to form a larger cluster [2]. Liposomes also gathered to the pressure node by the acoustic radiation force. The halfwidth of the liposome distribution depended on the difference between the density of the solutions outside and inside the liposome. The separation of particles in liquid by competition between acoustic radiation force and electrostatic force was also tested. The displacement of particles from the pressure node of an ultrasonic standing wave is expected to vary according to the effective charge, radius and stiffness of the particles. By application of this technique, a mixture of polystyrene spheres with two different radii was successfully separated according to their radii.

1) Yasuda, K. et al (1995) Jpn. J. Appl. Phys. **34**, 2715-2720.

2) Yasuda, K. et al (1996) J. Acoust. Soc. Am. in press.

ACTIN AND ACTIN BINDING PROTEINS

Su-Pos1

THE STRUCTURE OF YEAST F-ACTIN. ((A. Orlova[1], P. Rubenstein[2] and E.H. Egelman[1])) [1]Dept. of Cell Biology and Neuroanatomy, Univ. of Minn. Medical School, Minneapolis, MN 55455; [2]Department of Biochemistry, Univ. of Iowa College of Medicine, Iowa City, Iowa 52242.

While there is a strong tissue-specificity to the different isoforms of actin, little structural data exists on the differences between filaments formed by these different isoforms. We have used electron microscopy and three-dimensional reconstruction to study yeast actin, as well as a mutant yeast actin. While all actins are substantially conserved across evolution, yeast and rabbit muscle actins are only 87% conserved in primary sequence. We have found that under different conditions (with either Mg^{2+} or Ca^{2+}) the yeast actin appears to display less extensive contact between the two long-pitch helical strands when compared to muscle actin. The S14A mutation in yeast actin (Chen and Rubenstein, JBC **270**, 11406-11414, 1995) involves a mutation at a residue that is assumed to bind to the γ-phosphate of ATP. It has been shown that this mutation has a 40-60 fold decrease in actin's affinity for ATP (Chen *et al.*, JBC **270**, 11415-11423, 1995). We show that this single substitution appears to modulate the cleft between the two lobes of the actin subunit. We have also found that the yeast actin displays the large-scale cooperativity that we previously observed for muscle actin (Orlova *et al.*, JMB **245**, 598-607, 1995).

Su-Pos2

MICROSECOND ROTATIONAL DYNAMICS OF F-ACTIN IN ACTO-S1 COMPLEXES DURING STEADY STATE ATP HYDROLYSIS. ((C.A. Rebello & R.D. Ludescher)) Department of Food Science, Rutgers-The State University of New Jersey, New Brunswick, NJ 08903-0231.

We have monitored the microsecond rotational dynamics of rabbit skeletal muscle F-actin, in acto-S1 complexes in rigor and during steady state ATP hydrolysis, by using the steady state phosphorescence emission polarization from a phosphorescent probe, erythrosin-5-iodoacetamide, covalently attached to cys-374 of actin. This probe is sensitive to rotational motions in F-actin on the micro- to millisecond time scale. For the 1:1 acto-S1 complex the anisotropy of the rigor complex and of the complex during steady state ATP hydrolysis were 0.135±0.004 and 0.064±0.006, respectively. The corresponding values for a 10:1 acto-S1 complex were 0.137±0.002 and 0.067±0.002 respectively. The emission anisotropies of these two complexes during active ATP hydrolysis were lower than that of the F-actin filament, 0.077±0.003, suggestive of S1 induced rotational motions in F-actin during ATP hydrolysis. Since even at sub-stoichiometric acto-S1 ratios, i.e. 10:1, the phosphorescence emission anisotropies were not significantly different from that of the 1:1 acto-S1 complex, both in rigor and during steady state ATP hydrolysis, we conclude that F-actin undergoes some degree of cooperative rotational motions during steady state ATP hydrolysis. (Research supported by the Muscular Dystrophy Association).

Su-Pos3

TORSIONAL RIGIDITY AND STRENGTH OF SINGLE ACTIN FILAMENTS MEASURED DIRECTLY BY *IN VITRO* MICROMANIPULATION.

((Y. Tsuda, H. Yasutake, A. Ishijima & T. Yanagida)) *Depts. Anesthesiol., Osaka Univ., Medical School & Biophysical Engineering, Osaka Univ., Yanagida Biomotron Project, ERATO, Mino, Osaka, Japan.*

The torsional rigidity and breaking strength of actin filaments were determined directly by measuring the rotational Brownian motion and tensile strength using optical tweezers and microneedles, respectively. Rotational angular fluctuations of filaments supplied the torsional rigidity as $8.0\pm1.2\times10^{-26}$ Nm^2. The torsional breaking strength was determined by twisting a filament through various angles using microneedles. The tensile strength decreased greatly under twist, e.g., from 650 to 320 pN when filaments were turned through 90°, independent of the rotational direction. Our results show that an actin filament exhibits comparable flexibility in the rotational and longitudinal directions, but breaks more easily under torsional load.

Su-Pos4

DIRECT MEASUREMENT OF THE TORSIONAL RIGIDITY OF SINGLE ACTIN FILAMENTS

((R. Yasuda, H. Miyata and K. Kinosita Jr.)) Dept. Phys., Fac. Sci. Tech., Keio Univ., Hiyoshi, Yokohama 223, Japan.

The elastic properties of actin filaments are important in cell motility and muscle contraction. But the magnitude of the torsional rigidity has remained ambiguous. We developed a novel method that allowed direct visualization of the torsional Brownian motion of a single actin filament: a duplex of beads were attached to the filament of which both ends were fixed to beads on a glass surface. The torsional motion of the filament was observed, under an optical microscope, as the rotation of the bead duplex around the filament. The torsional rigidity was found to depend on the kind of tightly-bound divalent cation: $(9.7\pm2.9)\times10^{-26}$ N•m^2 (n=27) for F-Ca^{2+}-actin and $(2.3\pm0.8)\times10^{-26}$ N•m^2 (n=18) for F-Mg^{2+}-actin. In contrast, the flexural rigidity was almost independent of the bound metal, $(6.0\pm0.2)\times10^{-26}$ N•m^2 for both actin. The torsional rigidity above, in both Ca^{2+} and Mg^{2+} forms, is an order of magnitude larger than previous, indirect estimates. The fact that the torsional and flexural rigidities are of the same order of magnitude implicates that an actin filament may be regarded as a homogenous and isotropic thin rod.

Su-Pos5

Measurement of interaction force between actin and α actinin from skeletal muscle

((H.Miyata, R. Yasuda and K. Kinosita, Jr.)) Dept. Phys., Fac. Sci. Technol., Keio Univ., Hiyoshi, Yokohama 223, Japan.

Force required to break the skeletal muscle actin-α actinin bond (unbinding force) was measured at the level of individual molecules with an optical trapping technique. An actin filament, attached to a gelsolin-coated polystyrene bead, was bound to α actinin molecules on the nitrocellulose-coated glass surface (~ 1 α actinin molecule per 1 μm actin filament). The unbinding force, applied by pulling the bead, ranged from 1.4 to 44 pN, with the average of ~18 pN. The time required to break the bond (unbinding time) ranged from ~ 0.1 to ~20 sec., and tended to become shorter as the unbinding force became larger. The unbinding time seemed to be classified into two major groups: one group had the time of 1 sec or less and the other had the time ranging from several to 20 seconds, suggesting the existence of at least two classes of the bond between actin and the surface-bound actinin. Supported by grants-in-aid from the Ministry of Education, Science and Culture of Japan, grants from KAST, and Keio Univ., and by Special Coordination Funds for Promoting Science and Technology from the Agency of Science and Technology of Japan.

Su-Pos6

IMAGING OF COOPERATIVE BINDING OF TROPOMYOSIN ALONG AN ACTIN FILAMENT AND BETWEEN THE TWO ACTIN STRANDS

((Y. Ishii, J. Watai and T. Funatsu)) Yanagida Biomotron project, ERATO, JRDC. Mino, Osaka, Japan

Rhodamine-labeled tropomyosin bound to single actin filaments was visualized by fluorescence microscopy. At low saturation with tropomyosin, the binding was localized in small area, forming tropomyosin blocks, rather than homogeneously distributed. The tropomyosin blocks reflect the cooperative nature of the binding and hence their length was a measure of the cooperativity along the filaments. The quantitative measurement of the fluorescence intensity along single actin filaments could distinguish whether tropomyosin was bound to only one strand or both. The fraction that both strands were saturated with tropomyosin was greater than that expected for random binding to two actin strands, indicating cooperativity between the actin strands. In the presence of troponin, the binding of Ca^{2+} to troponin modified the cooperativity. Thus, the cooperative binding of tropomyosin both along the actin filament and between the actin strands was directly demonstrated.

Su-Pos7

DYNAMICS AND STABILITY OF G-ACTIN

((W. Wriggers and K. Schulten)) Beckman Institute and Department of Physics, UIUC, Urbana, IL 61801.

Molecular Dynamics simulations have been performed on solvated G-actin bound to ADP or ATP, starting with the structure of the actin-DNase1 complex (Kabsch et al., *Nature* (1990) 347: 37), with Ca^{2+} or Mg^{2+} at the the high-affinity divalent cation binding site. The Mg^{2+}-actin structures exhibit a closure of the nucleotide binding cleft relative to Ca^{2+}-actin, consistent with the suggested role of cleft separation in nucleotide dissociation and actin polymerization. We have examined the hydrogen-bonding contacts of nucleotide and ion in the simulated structures. Water molecules are found to enter the vicinity of the phosphates, which is water-free in the crystal structure. The divalent cation appears α-β-(γ)-coordinated to the phosphates, deviating from the crystal. Consistent with new biochemical evidence for a K$^+$-ion interaction with ATP (De La Cruz and Pollard, pers. comm.) and a recent high-resolution structure of the actin-like 44 kDa ATPase fragment of the chaperone Hsc70 (Wilbanks and McKay, *JBC* (1995) 270: 2251), our results suggest that the actin crystal structure needs to be augmented by waters and possibly monovalent ions for stabilization of the nucleotide. We have classified the simulated structures by their cleft separation and radius of gyration and have found two distinct clusters of Mg^{2+}-actin states: (1) states similar to the G-actin crystal structure and (2) states similar to F-actin (Lorenz et al., *JMB* (1993) 234: 826). These states show the "hydrophobic plug" loop 264-273 detached from the protein similar to the Lorenz F-actin model. Our results suggest that conformational changes attributed to actin polymerization may be promoted by Mg^{2+}-binding to the tight binding site of G-actin.

Su-Pos8

EFFECT OF LENGTH REGULATION AND CROSSLINKING ON TRACER DIFFUSION THROUGH ACTIN FILAMENTS.

((Jeffrey D. Jones and Katherine Luby-Phelps)) Department of Physiology, University of Texas Southwestern Medical Center at Dallas; Dallas, TX 75235-9040.

We have used fluorescence recovery after photobleaching (FRAP) to examine the diffusion of a small ficoll tracer probe (30 nm radius) through actin filaments as a function of filament length and crosslinking. Using gelsolin fragment px45 to regulate filament length, we found that tracer diffusion was not significantly dependent on filament length from 1 μm to 0.1 μm. This is consistent with a theoretical model that predicts tracer diffusion in filament solutions to be a function of net filament surface area (Han and Herzfeld, *Biophys. J.* 65:1155-61, 1993). The tracer diffusion coefficient in solutions of unregulated filaments was significantly higher than in solutions of length-regulated filaments. This can be explained by the tendency of long filaments to bundle, reducing net surface area. We also determined the effect of avidin-induced crosslinks on diffusion through F-actin containing from 2 to 16% biotinylated actin. We found that crosslinking does not retard diffusion although falling ball assays showed that the shear viscosity of the crosslinked solutions was increased dramatically relative to control solutions lacking avidin. Thus, the pore size of the crosslinked actin gels is substantially larger than tracer diameter. Supported by NSF DCB-89 16421 to K.L.-P.

Su-Pos9

THERMODYNAMICS AND KINETICS OF RHODAMINE PHALLOIDIN BINDING TO ACTIN FILAMENTS FROM THREE HIGHLY DIVERGENT SPECIES. ((E. M. De La Cruz and T. D. Pollard)) Dept. Cell Biology & Anatomy, Johns Hopkins Medical School, Baltimore, MD 21205.

We compared the kinetics of rhodamine phalloidin binding to actin purified from rabbit skeletal muscle, *Acanthamoeba castellanii* and *Saccharomyces cerevisiae*. The association rate constants for rhodamine phalloidin binding in 50 mM KCl, 1 mM $MgCl_2$, pH 7.0 buffer at 22° C are 2.9 (± 0.2) x 10^6 M^{-1} s^{-1} for rabbit skeletal muscle actin filaments, 3.4 (± 0.3) x 10^6 M^{-1} s^{-1} for *Acanthamoeba* actin filaments and 5.1 (± 0.2) x 10^6 M^{-1} s^{-1} for *S. cerevisiae* actin filaments. The dissociation rate constant from *S. cerevisiae* actin (1.6 (± 0.2) x 10^{-3} s^{-1}) is an order of magnitiude faster than from rabbit skeletal muscle actin (2.6 x 10^{-4} s^{-1}) and *Acanthamoeba* actin (1.7 (± 0.2) x 10^{-4} s^{-1}). The temperature dependence of the rate constants was interpreted according to transition state theory. There is a small enthalpic difference ($\Delta H^{\ddagger}$) between the ground states and the transition state. As a result, the free energy of activation ($\Delta G^{\ddagger}$) for association and dissociation of phalloidin is dominated by entropic changes ($\Delta S^{\ddagger}$). At equilibrium, phalloidin binding generates a positive entropy change (ΔS°). Several amino acid substitutions in *S. cerevisiae* actin (A114S, T194S and V201S) may alter the dimensions of the phalloidin binding site, allowing phalloidin to associate and dissociate more readily.

Su-Pos10

Interaction of Profilin with Proline Peptides

Eugene C. Petrella, Laura M. Machesky, and Thomas D. Pollard. Dept. of Cell Biology and Anatomy, Johns Hopkins University School of Medicine, Baltimore, MD.

The actin and polyphosphoinositide-binding protein, profilin, also binds to poly(L-proline) {pLp}. pLp binding to profilin increases the intrinsic fluorescence two-fold and shifts the emission maximum from 333 to 318 nm. Using this fluorescence assay we determined dissociation equilibrium constants (K_d) for various profilin isoforms and pLp: recombinant and wild-type *Acanthamoeba* profilin isoforms (K_d=100μM proline residues); and human platelet or recombinant human profilin (K_d= 232 and 359 μM, respectively). Poly(L-proline) with ≥ 10 residues binds with these affinities. The affinities of $proline_8$ and $proline_6$ are lower by 10- and 100-fold. D-$proline_{11}$ does not bind. Insertion of glycine (or alanine) in $proline_{11}$ peptides reduces the affinity for profilin. Each glycine increases $\Delta G'_{bind}$ by about 1 kcal/mole. Similarly, insertion of 5 glycines and hydroxy-proline *e.g.*, $(PPG)_5$ and $(PP^{OH}G)_5$, reduces the affinity of $proline_{15}$ by 100- and 500-fold, respectively. By titration calorimetry the binding enthalpies of $proline_{11}$, P_5GP_5, and P_5AP_5 are similar indicating that the lower affinity of the substituted peptides compared with $proline_{11}$ is due predominantly to the entropic cost for binding a more flexible substituted peptide. Differences in circular dichroism spectra indicate that substituted peptides do not fully adopt the rigid polyproline type II helical structure. Therefore we expect that the affinity of substituted peptides for profilin will be much lower than proteins that immobilize these peptides as part of their structure. (supported by NIH grant GM26338).

Su-Pos11

INTERACTION BETWEEN NEBULIN AND ACTIN. ((L. King and C. C. Chang)) Chang Gung Medical College, Taiwan, Republic of China

Nebulin is a massive protein (about 700-900 kDa) abundant in vertebrate skeletal muscle. Most of the information available have stemmed from antibodies produced against the nebulin purified through denaturing process. We have purified nebulin under non-denaturing conditions. The conformation of the native nebulin is different from that of denaturing preparation, indicating the necessity of using native preparation for property studies. Our co-sedimentation experiments show that each nebulin molecule binds approximately 200 actin monomers, suggesting that each sequence module (about 35 amino acids) of nebulin composes one actin binding domain. The results also indicate that G-actin is able to polymerize in G-buffer (monomer buffer) in the presence of nebulin and the binding curve exhibits cooperativity. This nebulin induced actin polymerization phenomenon supports the hypothesis that nebulin serves as the template for actin filaments. The effects of tropomyosin and troponin on actin-nebulin interaction will also be discussed. Supported by Chang Gung Medical College and The National Science Council, Republic of China.

Su-Pos12

CHARACTERIZATION AND EXPRESSION OF NEBULIN CLONES FROM MOUSE SKELETAL MUSCLE. ((J.Q. Zhang, G. Luo and R. Horowits)) NIAMS, NIH, Bethesda, MD 20892.

We have further characterized three cDNA clones encoding nebulin from mouse skeletal muscle (Biophys J., A285, 1995). Using RT-PCR, we have confirmed a physical continuity between two of the three clones (7a and 8c). While the third clone (4b) shares sequence identity with clone 7a over 798 base pairs, the two sequences diverge outside this region. This data indicates clone 8c and 7a form a contiguous sequence, while clone 4b is derived from a transcript encoding a different isoform of nebulin. All of these clones showed over 80% identity with the full length human nebulin cDNA sequence (Labeit and Kolmerer, J. Mol. Biol. 248: 308, 1995), indicating a high conservation of nebulin among species. Furthermore, clones 7a and 8c were successfully expressed as thioredoxin fusion proteins (126.7 kDa and 89.7 kDa respectively) at a high level in E. coli cells. To our knowledge, these are the longest nebulin fragments expressed to date. On Western blots, antibodies raised against the fusion proteins reacted with the nebulin fragments expressed in E. coli as well as with full length nebulin in mouse muscle. The fusion proteins were also detected by a monoclonal anti-thioredoxin antibody. A purification procedure for the expressed proteins is currently under development for the purpose of using the nebulin fragments in biochemical studies.

MOTOR PROTEINS

Su-Pos13

CIRCULAR DICHROISM SPECTROSCOPIC STUDY OF ncd MOTOR DOMAIN. ((T. Shimizu and H. Morii)) N.I.B.H., Tsukuba, Ibaraqi, 305 Japan (spon. by Y. Umazume)

ncd from *Drosophila* is a microtubule motor, having a 40 kDa domain homologous to kinesin motor domain. The ncd motor domain contains tightly bound ADP at the active site just as that of kinesin does. Here, we removed this ADP from the ncd motor domain without denaturing the protein by gel filtration in the presence of EDTA and high salt. The resultant protein, however, was likely to be in an inactive conformation, binding ATP only slowly. This also suggests that there was an equilibrium between active and inactive conformation of ncd motor domain, and that the slow ATP-binding was governed by the slow transition from inactive to active conformation. The far UV circular dichroism (CD) spectrum of the ADP-free ncd motor domain was superimposable to that of normal ncd motor domain with bound ADP. This suggests that removal of ADP did not affect the backbone structure of the ncd motor domain in the presence of high salt. On the other hand, the near UV CD spectrum of the ADP-free ncd motor domain differed from that of ncd motor domain ADP complex, suggesting that the local conformation was changed. The CD spectra were also investigated with K349, a human kinesin motor domain. The near UV CD spectra of K349 also showed a difference between two forms; ADP-binding form and nucleotide-free form. The far UV CD spectrum of K349 was considerably different from that of ncd motor domain.

Su-Pos14

REALTIME IMAGING OF INDIVIDUAL MOLECULAR ORIENTATIONS; SINGLE-FLUOROPHORE POLARIZATION IMAGING. ((I.Sase, H. Miyata, J.E.T.Corrie*, J.S.Craik* and K. Kinosita Jr.)) Det. Phys., Fac. Sci Tech., Keio Univ., Hiyoshi, Yokohama 223, Japan; *Natl. Inst. Med. Research, Mill Hill, London NW7 1AA, U.K..

Single fluorophores in an aqueous medium have been imaged using an ordinary epi-fluorescence microscope. Fluorophores bound to actin were imaged, in an *in vitro* motility system, as moving spots[1]. By decomposing the fluorescence into polarized components, we have now succeeded in imaging the orientation of a single fluorophore continuously and in real time. 5-iodoacetamido-tetramethylrhodamine was rigidly attached to Cys-374 of actin. Vertically and horizontally polarized components of fluorescence were imaged simultaneously at the video rate of 30 frames/sec. In rigor where actin filaments were held immobile by surface-bound heavy meromyosin, each fluorophore gave a pair of spots (*V* and *H* components) with stationary intensities. When ATP was added and the filaments started to slide, the intensities of the two spots alternated with time, showing rotation of the fluorophore and thus of actin. This is most probably the rotation of an actin filament around its axis, suggesting the presence of a torque component in the sliding force. The detection of axial rotation would not have been possible if the filament had carried many fluorophores as in usual assays.

1) I. Sase et al., 1995. *Biophys. J.* 69:323-328

Su-Pos15

A SYSTEM FOR MOLECULAR FORCE MEASUREMENTS USING MICROFABRICATED DEVICES ((M. Fauver, C. Galambos, M.L. Bartoo, G.H. Pollack)) University of Washington Center for Bioengineering Seattle, WA 98195

An apparatus has been built for measuring the intermolecular forces generated by actin-myosin interactions. Microfabrication processes were used to produce micron-sized cantilever beams. Cantilevers have been made with compliance ranging between the high values of optical traps, to values low enough for use with preparations such as single myofibrils. To measure deflection, the cantilevers are used with a linear photodiode array (LPD) mounted on an optical microscope. A single actin filament is suspended between a reference cantilever and a more flexible cantilever. An actin filament is attached to one cantilever at a time by 'fishing' around in solution via hydraulic micromanipulators. Fluorescence microscopy is used to determine when the filament is properly suspended between the beams. Ordinary optical microscopy is then used to project the image of the cantilever tips onto the LPD. The output from the LPD is processed by a custom spot-position-detector board to track the motion of each tip. Reasonable position detectability and highly compliant cantilevers make resolution of piconewton forces possible. We are currently implementing the apparatus in a biological setting.

Su-Pos16

SINGLE KINESIN MOLECULES TWISTED BY OPTICAL TWEEZERS. ((B. S. Sorg and S. C. Kuo)) Department of Biomedical Engineering, Johns Hopkins University School of Medicine, Baltimore, MD 21205

We used optical tweezers to directly measure the torsional stiffness of a single kinesin molecule bound to a microtubule in rigor. The magnitude of torsional stiffness could prove important for maintaining the directionality of kinesin movement, particularly since dimeric kinesin should exhibit two fold rotational symmetry. We expected some measurable torsional stiffness where kinesin molecules unwind after being twisted. Instead, we observed Brownian fluctuations without unwinding in 93% of attempts (n = 183), even after as many as 30 revolutions, and all unwinding events "slipped" after additional twisting. Experiments using different rigor-like conditions, including AMP-PNP and/or apyrase, did not produce different results. These results were not due to non-functional kinesin since photoactivating DMNPE-ATP often produced motility, even after twisting molecules ~30 revolutions. "Slippage" clearly occurs when kinesin is attached by popular adsorption protocols, casting doubt on other measurements of kinesin torsional stiffness (Howard et. al. 1993, *PNAS*, **90**, 11653-11657). Preliminary results with covalent crosslinking have not yet eliminated torsional slipping, retaining the possibility of a freely jointed swivel in kinesin's structure.

Su-Pos17

CARGO-ACTIVATION OF KINESIN'S ATPASE ACTIVITY ((D.L. Coy and J. Howard)) Dept. of Physiology & Biophysics, University of Washington, Seattle WA 98195

Comparison of kinesin's ATPase rate with its speed in motility assays should provide the step size, the distance moved per ATP hydrolyzed. Assuming that the mechanical and chemical cycles are tightly coupled to one another, the step size is expected to be 8 nm, the length of a tubulin dimer in the microtubule. Paradoxically, the ATPase rate of kinesin in solution is so low as to suggest a step size of several hundered nanometers. We hypothesize that kinesin's ATPase in solution is inhibited when there is no bound cargo.

To test this hypothesis, we measured ATPase activity under conditions similar to those of motility assays. Recombinant *Drosophila* kinesin was bound onto 200-nm diameter casein-coated silica beads. The rate of ATP hydrolysis in the presence of varying amounts of taxol-stabilized microtubules and high ATP concentrations was measured spectrophotometrically using Malachite Green to assay phosphate release.

At saturating microtubule concentration, the maximal ATPase was 51 ± 11 (±SE) sec^{-1} per heavy chain at 25°C. Without beads, the corresponding ATPase was 13 ± 5 (±SD) sec^{-1} per heavy chain. For comparison, the motility rate was 754 ± 71 (±SD) nm sec^{-1} at 25°C in low density gliding assays.

Consistent with our hypothesis, binding of kinesin to cargo activates its ATPase in the presence of microtubules. We calculate a step size of 7.4 nm (=754 nm sec^{-1}/2x51 sec^{-1}) which is consistent with tight coupling. Kinesin activation by binding to transport cargos may correspond to a regulatory mechanism for transport *in vivo*. Supported by NIH AR40593 and GM08268.

Su-Pos18

FORCES AND VELOCITIES MEASURED FOR SINGLE- AND DOUBLE-HEADED KINESINS. ((Y. Inoue*, Y. Toyoshima+, H. Higuchi# and T. Yanagida*#)) *Dept. Biophys. & Engineering, Osaka Univ., Osaka. +Dept. Education, Tokyo Univ., Tokyo. #Yanagida Biomotron Project, ERATO, JRDC, Osaka, Japan.

We measured the forces and velocities caused by recombinant fragments of *Drosophila* kinesin, containing single head (K351-biotin) and double heads (K410-biotin), bound to streptavidin-coated beads using laser trapping nanometry. The velocities of both fragments decreased linearly with increasing force. Maximum velocities of single- and double-headed fragments near zero load were ~600 and ~700 nm/s, respectively. The stall forces were ~6 pN for single-headed fragments and ~7 pN for double-headed fragments at low density of fragments on beads. The velocities and forces by both kinesin fragments were similar to those by native kinesin molecules (Svoboda & Block, 1994). The results indicated that single-headed fragments can produce sliding velocity and force as large as double-headed fragments.

Su-Pos19

COOPERATIVE STEP MOVEMENT OF SINGLE KINESIN MOLECULES ((H.Kojima, E.Muto, H.Higuchi & T.Yanagida)) Biomotron Project, ERATO, JRDC and Dept. Biophys. Engineering, Osaka Univ., Osaka, Japan

We measured the stepwise movements of single kinesin molecules on an axoneme with laser trapping nanometry. Figure shows a histogram of kinesin step size; multiple peaks at 8, 16 and 24 nm can be identified. The distribution deviates from Poisson distribution, indicating that the kinesin molecule frequently undergoes multiple sequential 8 nm steps. Such a cooperative step movement was independent of load or ATP concentration.

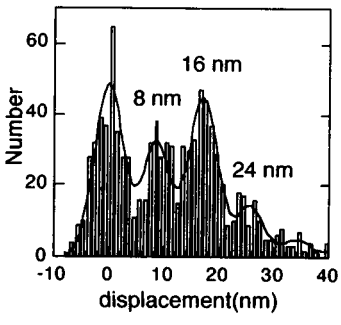

Su-Pos20

KINETICS OF FORCE DEVELOPMENT BY SINGLE KINESIN MOLECULES ACTIVATED BY LASER PHOTOLYSIS OF CAGED ATP. ((H. Higuchi*, E. Mutoh*, Y. Inoue# and T. Yanagida*#)) *Yanagida Biomotron project, ERATO, JRDC, Japan. #Dept Biophys. Engineering, Osaka University, Japan.

To understand the mechanism of force generation of kinesin, a crucial remaining problem is identification of the biochemical step corresponding to force generation. We use laser trapping nanometry, combined with laser photolysis of caged ATP, to relate transients of force and displacement by single kinesin molecules with the elementary steps of the ATPase cycle. The kinetics of the displacement transients are consistent with a two step reaction, ATP binding, with a second order rate constant of 6 x 10^5 $M^{-1}s^{-1}$, and force generation at 50 s^{-1}. The rate constant for ATP binding agrees with that determined in solution and the rate of the subsequent displacement is close to that of phosphate (Pi) release from the microtubule-kinesin.ADP.Pi intermediate, the rate limiting step of ATP hydrolysis cycle (Gilbert et al, 1995).

Su-Pos21

A ROLE FOR KINESIN IN DEVELOPING SOLEUS MUSCLE FIBERS IN THE RAT. ((C.E. Kasper)) School of Nursing, UCLA, CA 90095.

Previous studies from this laboratory have shown that, in the mature rat, the nuclei of the soleus fibers (primarily myosin slow chain oxidative fibers) align themselves in rows, often in a slight depression or furrow, along the length of the fiber. Further, this alignment of the nuclei occurs during the 14-26 day old developmental period when the second motorneuron supplying the muscle is removed, and the fiber acquires its mature myosin fiber type profile. Exactly how this nuclear movement occurs is not known but it is likely that certain molecules, 'motor molecules', are involved. The motor molecules include a group of proteins called the kinesins which act as force generating enzymes hydrolyzing ATP to ADP and Pi, and using the derived energy to induce movement of materials and organelles along microtubules. The kinesins have been well-characterized and have been found in almost all organisms and cell types. The aim of this study was to identify the presence of kinesin around the nuclei in the soleus fibers during the period of development including nuclear movement, and to compare these results with those from an adult rat soleus fiber in which the nuclei are aligned and stationary. Using monoclonal antibody and a secondary FITC conjugate the presence of kinesin was clearly seen surrounding and in-between the aligning nuclei in both 14 and 25 day old soleus fibers. By contrast little or no immunolocalization of kinesin was seen in soleus fibers from adult rats. These results suggest that the motor molecule kinesin may play a role in the alignment of the nuclei in certain skeletal muscle fibers. Further studies are now underway to identify other motor molecules, such as dynein, which may also play a role in the establishment of the mature muscle fiber structure. (Supported by NIH:NINR & NIAMS, RO1 NR02922)

Su-Pos22

EVIDENCE THAT INDIVIDUAL SINGLE-HEADED KINESIN MOLECULES MOVE MICROTUBULES. ((Krishnan Ramanathan and Scot Kuo)) Department of Biomedical Engineering, Johns Hopkins University, School of Medicine, Baltimore, MD 21205

Unlike strategies using monomeric motor domains, we constructed single-headed kinesin molecules by forming novel heterodimers that lack a motor domain. We co-expressed two peptides, which both retained the coiled-coil sequences of Rod I, but the "headless" peptide had a unique His_6 fusion tag to facilitate purification. Consistent with heterodimer formation, purification of "headed" peptide was strictly dependent on co-expression with the His-tagged "headless" peptide and the stokes radius as measured in a gel filtration column was 6.3 nm. We also developed a new assay to determine the functionality of individual kinesin molecules by photoactivating DMNPE-ATP after pre-forming single-kinesin-microtubule complexes in the absence of nucleotide. A significant fraction (0.25) of the single-headed attachment sites moved after photoactivating ATP, although they had shorter run lengths (1.2 μm) than wild type recombinant kinesin (motile fraction of 0.6 and run lengths 5.8 μm). These data suggest that, in contrast to the extreme cooperativity implied by a "walking" mechanism, kinesin generates force by the independent action of each head.

Su-Pos23

HIGH SPEED UNDER A NON-PARALLEL LOAD SUGGESTS THAT KINESIN IS A TIGHTLY-COUPLED CHEMICAL MOTOR . ((F. Gittes and J. Howard)) Dept. of Physiology & Biophysics, Box 357290, University of Washington, Seattle, WA 98195.

Does the slowing down of kinesin at high load result from slipping back during periods when the motor is detached from the microtubule, or is it due to slowing of the forward motion while the motor is attached? This is addressed by considering the effects of non-parallel load forces. If the motor slips back when detached, such slippage should be aggravated by a component of force pulling the motor away from the microtubule.

Motors moving along microtubules fixed at one end sometimes buckled the microtubules dramatically, so that the load became increasingly non-parallel to the motor motion (Gittes, Meyhöfer, Baek and Howard, Biophys. J., in press). Earlier measurements of microtubule stiffness were used to determine the magnitude and direction of the load force vector on the motor. Single motors slowed under parallel loading at the onset of buckling, consistent with maximum kinesin forces found in other experiments.

When kinesin motors were subject to a force pulling them away from the microtubule as well as backwards along it, we observed anomalously high motor speeds compared to parallel-loading experiments: perpendicular force appears to act as a catalytic agent for the kinesin cycle. We conclude that kinesin slowing is unlikely to result from slippage. A direct coupling of spatial force to the chemical cycle (like the Fenn effect in muscle) explains these results if a rate-limiting molecular motion is directed away from the microtubule. This rate-limiting step could be, for example, the rotation of a single kinesin head or, alternatively, the rate-limiting detachment of the trailing head in a coordinated two-headed mechanism. Supported by NIH AR40593.

CONTRACTILITY, LOCOMOTION, MOTILITY: MUSCLE REGULATORY PROTEINS

Su-Pos24

THE EFFECT OF $[Mg^{2+}]$ AND SARCOMERE LENGTH ON CALCIUM DEPENDENT DONNAN POTENTIAL MEASUREMENTS IN ISOLATED STRIATED MUSCLE FIBRES IN RIGOR. ((S.J.Coomber, G.F.Elliott & E.A.Bryson.)) The Open University Oxford Research Unit, Oxford, UK OX1 5HR.

A highly cooperative change is seen in the Donnan potentials of isolated rabbit psoas fibres in rigor with pCa (50 mM KCl, 2.5 mM $MgCl_2$, 2mM Ca-EGTA buffer, ionic strength 0.072, using KCl filled microelectrodes) (Coomber & Elliott, *J Physiol.*, 1995, in press). This occurs in both the A-band (E_A) and the I-band (E_I) potentials . Since competition exists between Ca^{2+} and Mg^{2+} for metal binding sites in EGTA and for the high affinity Ca^{2+} binding sites in TnC, a shift in pCa_{50} to lower $[Ca^{2+}]$ is expected in zero Mg^{2+} rigor solution and to higher $[Ca^{2+}]$ in 4mM Mg^{2+} rigor solution, especially in the I-band potentials (Rüegg, 1992, *Calcium in Muscle Contraction*, 2nd Edition, Springer Verlag, Heidelberg).

At sarcomere lengths of 3.4μm (*ie* just at overlap) both ΔE_I and ΔE_A (pCa 2.8 - 7.69) ~ 2.4 mV. Beyond overlap (SL ≈ 4.2 μm) this value decreases to ~ 1.7mV. When the muscle is stretched still further (SL>4.3 μm), no significant difference is seen between the pCa's. The degree of cooperativity also changes with increasing sarcomere lengths. Addition of 1% Triton X100 at 3.4 μm appears to produce an incubation-time dependent effect analogous to that of increasing SL. The reason is unclear: SDS PAGE indicates that there is no differential loss of proteins between the incubation media.

We shall report on these experiments, and on measurements of the electric charge in regulated and unregulated actin gels, as a function of pCa.

Su-Pos25

TWO DIMENSIONAL FOURIER ANALYSIS OF I-BAND PERIODICITY IN FROG SEMITENDINOSUS MUSCLE FIBER SEGMENTS ((M.P. Slawnych, L. Morishita, L. Mornin and B.H. Bressler)) Department of Anatomy, University of British Columbia, Vancouver, B.C., Canada

The periodicity of the troponin complex (T_p) in single semitendinosus fiber segments of *Rana Pipiens* under both relaxed and activated conditions was measured by examining electron micrographs of the fiber segments using a Fourier analysis based procedure. The fibers were first incubated in 0.2% Tannic acid (pH 7.0, 4°C) for 24 hours and then post-fixed with 1% osmium tetroxide for 30 minutes. The fibers were then dehydrated, sectioned, stained with uranyl acetate and lead citrate, and examined by electron microscopy. The electron micrographs were then digitized and analyzed in a manner in which the I band regions were first identified and then subjected to Fourier analysis (Jonas et al., *Journal of Electron Microscopy* 42:285-293, 1993). The positions of the first order peaks were then related to the average T_p in the identified region.

T_p values obtained under relaxed and activated conditions were 38.0±2.1 nm and 37.9±2.6 nm, respectively, with no significant difference between the two distributions. Similar results were obtained by fitting a single Gaussian curve to the data. Interestingly, the data was better fitted by two Gaussian curves, with the peak of the second curve located at approximately 41 nm. Possible interpretations will be discussed. (Supported by the MRC)

Su-Pos26

EFFECTS OF STRIATION STABILITY AND CALCIUM ON THE RATE OF RELAXATION IN SKINNED SKELETAL MUSCLE FIBERS FROM THE FROG. ((Philip A. Wahr and Jack A. Rall)) Department of Physiology, Ohio State University, Columbus, OH 43210.

Relaxation from contraction was induced by the photolysis of the caged Ca^{2+} chelator diazo-2 at 10 °C. Relaxation occurred in two phases which were similar to those observed in intact fibers, i.e., a slow phase followed by a "shoulder" and then a fast phase. Diazo-2 photolysis produced nearly complete relaxation from a force of 76 ± 9 % (Mean ± S.D., N = 5) of F_{max}. When a fiber was stabilized by periodic release and re-stretch during force development, the time after photolysis to the onset of the fast phase ($t_{shoulder}$) was 98 ± 27 ms (N = 7). The fast phase was described by a double exponential with rate constants (k_{r1}) of 13 ± 2.4 s^{-1} and (k_{r2}) of 3.5 ± 2.6 s^{-1}. Without fiber stabilization, $t_{shoulder}$ decreased significantly by 50% whereas k_{r1} and k_{r2} increased 2.3 and 1.5 fold, respectively (N = 3). In intact fibers (N = 4), $t_{shoulder}$, k_{r1} and k_{r2} were 177 ± 34 ms, 13.4 ± 3.0 s^{-1} and 0.15 ± 0.05 s^{-1}, respectively. Fibers generating greater fractional forces due to increased Ca^{2+} activation relaxed more slowly. $t_{shoulder}$ increased linearly, while k_{r1} and k_{r2} decreased linearly, with increases in F/F_{max}. $t_{shoulder}$ was 6 fold more sensitive to the Ca^{2+} level than k_{r1}. In conclusion, the duration of the slow phase of relaxation is strongly dependent on striation stability and on the level of Ca^{2+} activation whereas the fast phase is, to a lesser extent, modulated by these factors. NIH AR20792 and AHA, Ohio Affiliate.

Su-Pos27

EFFECT OF THE ACIDIC RESIDUES OF THE N-TERMINAL DOMAIN OF TROPONIN C ON THE CALCIUM-DEPENDENT INTERACTION WITH THE INHIBITORY PEPTIDE. ((Tomoyoshi Kobayashi, Xinmei Zhao, Robert Wade, John H. Collins and Yuichiro Maeda)) IIAR, Matsushita El. Ind. Co. Kyoto, 619-02 JAPAN and Univ. Maryland Sch. Medicine, Baltimore, MD 21201.

The calcium-dependent interaction between the inhibitory region (res. 96-116) of TnI and TnC is one of the central steps of Tn function. In order to investigate the contribution of acidic residues in the N-terminal domain of TnC upon the binding to TnI, we have constructed three double-mutant TnCs; TnC(E53A/ E54A), TnC(E60A/E61A) and TnC(E85A/D86A). We have measured the affinity between TnC and mutant TnCs and the synthetic peptide which contains the sequence of the inhibitory region of TnI with elongation at its C-terminus (i.e. residues 95-124). The results showed that the each mutant TnC showed almost the same affinity for the peptide as wild type TnC in the presence of calcium, while TnC(E85A/D86A) showed half of that of wild type TnC in the presence of magnesium and EGTA. This indicates the involvement of Glu-85/Asp-86 of TnC in the binding to the inhibitory region of TnI.

Su-Pos28

MITOGEN-ACTIVATED PROTEIN KINASE (MAPK) ACTIVATION AND DE-ACTIVATION WITH MECHANICAL LOAD IN PORCINE CAROTID ARTERIES. ((L. P. Adam and M. T. Franklin)) Boston Biomedical Research Institute, Boston, MA 02114.

The activities of mitogen-activated protein kinase (MAPK) and other molecules involved in cell growth and proliferation ($p21^{ras}$, $p90^{rsk}$, PKC, c-*fos* and c-*myc*) are markedly enhanced by stretching of cultured cardiac myocytes (Sadoshima and Izumo, EMBO J 12:1681-1692, 1993). Recently, we showed that stretch activates MAPK in intact porcine carotid arteries. Because of the importance of stretch-activation of arterial smooth muscle to physiological function, we further characterized the mechanical load-dependent activation of MAPK in intact porcine carotid arteries. MAPK activity was 67 pmole/min/mg protein in unloaded arterial muscle strips immediately after attachment to force transducers; the activity increased to a maximum value of approximately 140 pmole/min/mg protein within 30 seconds of the application of a mechanical load. With continued application of mechanical load, MAPK activity remained elevated for approximately 2 hours, and then decreased over a 16 hour time span to 16 pmole/min/mg protein. (This low level of MAPK activity is equivalent to that observed in unstretched and unstimulated arteries, *in situ*, in pigs.) On the other hand, when a load was applied to muscle strips and then removed, MAPK activity decreased within an hour to the levels observed before the application of the load. The effects of mechanical load on MAPK activity were additive to the effects observed with KCl or phorbol ester stimulation, and were only slightly inhibited by reducing extracellular calcium. The application of mechanical load to smooth muscle generates myogenic tone and leads to hypertrophy. These effects are thought to be regulated, in part, by protein kinase C (PKC). In addition, MAPK activity is regulated by PKC- and mechanical load-dependent mechanisms. These data are consistent with a role for MAPK in the stretch-activation of vascular smooth muscle. Supported by National Institutes of Health grant HL56035.

Su-Pos29

A TIME-RESOLVED STUDY OF THE FLUORESCENCE OF TROPONIN C MUTANT F22W.((M. She, W.-J. Dong, P.K. Umeda and H.C. Cheung)) Departments of Physics, Medicine, and Biochemistry & Molecular Genetics, University of Alabama at Birmingham, Birmingham, AL 35294.

A single-tryptophan mutant F22W of skeletal muscle TnC was constructed by site-directed mutagenesis. The molecular graphics, CD and myofibrillar ATPase assay suggested that the mutation had no gross effects on structure and function. The tryptophan did not sense Ca^{2+} or Mg^{2+} binding to sites 3 and 4 in the C-domain, but detected and resolved the affinities of Ca^{2+} binding to sites 1 and 2 in the N-domain. Without bound Ca^{2+} at sites 1 and 2, the quantum yield (Q) was 0.33, the emission maximum was 332 nm, and the intensity decay was monoexponential and constant across the emission band, with a mean value of 5.65 ± 0.04 ns for the single lifetime from 310-400 nm. Upon saturation of sites 1 and 2 by Ca^{2+}, Q decreased to 0.24 with a small red spectral shift, and the intensity decay became biexponential. Across the emission band, the long component (τ_1) increased from 4.88 to 5.75 ns and the short component (τ_2) from 1.89 to 3.50 ns with amplitudes α_1 increasing, and the mean of the two lifetimes increased by about 0.5 ns. Decay-associated spectra (DAS) were constructed for F22W saturated with Ca^{2+} at the N-domain. Relative to the steady-state emission spectrum, the DAS associated to the long lifetime was not shifted, whereas the DAS associated to the short lifetime was red-shifted by 18 nm. These results suggest a homogeneous microenvironment of the tryptophan in F22W in the absence of bound Ca^{2+} at sites 1 and 2. Saturation of these two regulatory sites resulted in two conformations. This heterogeneity may reflect two Ca^{2+}-saturated N-domain conformations which are related to a 10-fold difference in the affinities of the two regulatory sites for Ca^{2+}.

Su-Pos30

PHOSPHORYLATION-INDUCED DECREASE IN DISTANCE IN CARDIAC TROPONIN I. ((W.-J. Dong[1], J. Xing[1], M. She[1], M. Chandra[2], R.J. Solaro[2], and H.C. Cheung[1])) Dept. of Biochem. & Mol. Genetics[1], Univ. of Alabama at Birmingham, Birmingham, AL 35294 and Dept. of Physiology & Biophysics[2], College of Medicine, Univ. of Illinois at Chicago, Chicago, IL 60612

A full-length mutant of mouse cardiac troponin I, cTnI(S5C, C81I, C98S), and a mutant of a truncated cTnI, $cTnI/NH_2$(S9C, C50I, C67S) in which the N-terminal 32 residues were deleted, were used in this study. cTnC labeled with IAANS was titrated with the $cTnI/NH_2$ mutant to obtain the following apparent binding constants for the cTnC•$cTnI/NH_2$ complex under 3 conditions: (1) 1.5×10^6 M^{-1} (EGTA), (2) 28.9×10^6 M^{-1} (Mg^{2+}), (3) 87.5×10^6 M^{-1} (Mg^{2+} + Ca^{2+}). These binding constants were less than a factor of 2 smaller than the corresponding binding constants obtained with nonphosphorylated full-length mutant, suggesting a very small contribution of the N-terminal extension of cTnI to the stability of the cTnI•cTnC complex. Cys5 in the full-length mutant was modified by IAANS, and the distance between this site and Trp192 was determined by energy transfer from Trp192 to IAANS. The following distance results were obtained with nonphosphorylated mutant (control) and mutant phosphorylated by protein kinase A (p-cTnI) under four conditions: (a) cTnI alone, (b) cTnI + cTnC, (c) cTnI + cTnC + Mg^{2+}, and (d) cTnI + cTnC + Mg + Ca:

	(a)	(b)	(c)	(d)	
control	37 Å	39 Å	41 Å	44 Å	The 5Å decrease in the Cys5-Trp192 distance resulting from
p-cTnI	32 Å	34 Å	35 Å	36 Å	phosphorylation was carried over to

the cTnI•cTnC complex. These results suggest that phosphorylation of Ser23 and Ser24 results in a folding of the N-terminal segment toward the C-terminal end.

Su-Pos31

FLUORESCENCE STUDIES OF THE N-TERMINAL SEGMENT OF CARDIAC TROPONIN I. ((W.-J. Dong[1], J. Xing[1], M. Chandra[2], R.J. Solaro[2], and H.C. Cheung[1])). Dept. of Biochem. & Mol. Genetics[1], Univ. of Alabama at Birmingham, Birmingham, AL 35294 and Dept. of Physiology & Biophysics, College of Medicine, Univ. of Illinois at Chicago, Chicago, IL 60612.

A cardiac troponin I mutant containing a single cysteine at position 5, cTnI(S5C, C81I, C98S), was generated from mouse cTnI cDNA clone and expressed in a bacterial system. Cys5 was modified with the fluorescent reagent IAANS to probe the conformation of the N-terminal segment and the effect of phosphorylation of Ser23 and Ser24 by protein kinase A on this conformation. The emission properties of the attached probe were determined with nonphosphorylated and phosphorylated cTnI mutant, each in 4 different conditions: (a) cTnI mutant alone, (b) cTnI + cTnC, (c) cTnI + cTnC + Mg^{2+}, and (d) cTnI + cTnC + Mg^{2+} and Ca^{2+}. In the absence of cTnC, phosphorylation resulted in pronounced changes in fluorescence parameters: a 7-fold reduction in quantum yield, a 13-nm red-shift of the emission spectrum, and a reduction of the mean fluorescence lifetime. These changes were carried over to its complex with cTnC ± cations [conditions (b), (c), (d)] and suggest that phosphorylation induced significant changes in the IAANS environment. The Stern-Volmer plots of the quenching of the steady-state intensity by acrylamide showed only a slight deviation from linearity with nonphosphorylated protein in all 4 conditions, but had pronounced downward curvature with phosphorylated protein. This may be indicative of static quenching which was not detected before phosphorylation. In spite of this, phosphorylation resulted in a reduction of the bimolecular dynamic quenching constant by a factor of 2-3, indicating decreased solvent accessibility. These results support the notion that phosphorylation induces considerable conformational changes in the N-terminal segment of cTnI.

Su-Pos32

THE EFFECT OF MYOSIN HEAD STATE ON THE ORIENTATION OF TROPONIN C

((H.-C. Li & P.G. Fajer)) Dept. of Biol. Sci., Florida State University, National High Magnetic Field Laboratory, Tallahassee FL 32306

The activation of the thin filament could be induced not only by Ca^{2+}, but also by myosin heads (reviewed in Lehrer, 1994, J. of Muscle Res. Cell Motil. 15,232-6). The transition of the pre- to post-power stroke myosin heads is closely coupled to the shift of tropomyosin in the thin filament. We have shown previously that troponin C reorients upon binding of calcium and/or myosin heads attachment, and the orientational distribution is different in response to Ca^{2+} and to rigor heads (Li & Fajer, 1994, Biochemistry 33,14324-32). The focus of the current effort is to establish whether the pre- and post-power stroke myosin heads have the same effect on the thin filament. Complex of A•M•ADP and aluminum fluoride is thought to be an analog of the pre-power stroke state: A•M•ADP•Pi. EPR study has shown that the pre-power stroke myosin heads are as disordered as the detached heads, but their mobility is highly restricted (Raucher & Fajer, 1994, Biochemistry 33, 11993-9). Here, we use AlF_4^- analog to investigate the effect of pre-power stroke myosin heads on spin labeled TnC reconstituted into muscle fibers. The spectrum obtained in the presence of Ca^{2+}, AlF_4^- and ATP is very similar to the one obtained without ATP suggesting similar orientational distribution. However, since the mechanical data indicated that only 40% of the myosin heads are bound to actin in the presence of AlF_4^-, the spectrum of the bound ternary complex is obtained by subtracting the spectrum of M•ADP• AlF_4^- state weighted by the fraction of detached heads. The resulting spectrum, which represents the effect of pre-power stroke state (A•M•ADP•AlF_4^-), is different from the spectrum acquired under rigor heads condition. This implies that the structure of TnC is intimately coupled with the chemical state of myosin heads.

Su-Pos33

ANALYSIS OF TWO FHC TROPOMYOSIN MUTANTS.

((Y. An, N. Golitsina, N.J. Greenfield, L. Thierfelder, J.G. Seidman, C.E. Seidman, S.S. Lehrer, S.E. Hitchcock-DeGregori)) Robert Wood Johnson Med. Sch., Piscataway, NJ; Boston Biomed. Res. Inst., Boston, MA; Harvard Med. Sch., Boston, MA.

One locus of familial hypertrophic cardiomyopathy (FHC) is the α-tropomyosin (TM) gene where D175N or E180G mutations have been identified in the striated TM isoform (Thierfelder et al., 1994, *Cell 77*, 701-712*)*. To investigate the consequences of these single changes on TM's function and conformation, unacetylated human wildtype, D175N and E180G TMs were expressed in *E. coli*. CD analysis showed that the major unfolding transition of E180G (44.4 °C, 1.5 μM, 0.5M NaCl) was similar to that of wildtype (43.2 °C) whereas D175N unfolded with two major transitions (40.4, 48.6 °C). The actin affinity in the presence of troponin and Ca^{++} of E180G was similar to wildtype (7.1 vs 10 x $10^6 M^{-1}$) whereas that of D175N was weaker (3.7 x $10^6 M^{-1}$). The differences in affinity from wildtype were maintained in the absence of Ca^{++}. The proteins were labeled at Cys 190 with pyrene maleimide to give a probe close to the sites of the mutations. The temperature dependence of formation of pyrene excimer was used as an indicator of local unfolding in the Cys190 region. Wildtype showed a large increase between 30 and 40 °C, as previously reported for rabbit TM. The excimer fluorescence D175N increased 2X between 20 and 35 °C whereas that of E180G remained high between 20 and 40 °C. The results indicate that the local unfolding (flexibility) in the region of Cys190 of both mutants is greater than wildtype. Myosin S1 induced the binding of all three TMs to actin and resulted in an 80% increase in fluorescence in wildtype, but had little effect on E180G and caused a 15-20% decrease in D175N, indicating that S1 induced a different conformation of each TM on actin in the "on-state". Troponin T interaction was similar with all three TMs. Supported by NIH.

Su-Pos34

LOCALIZATION OF CYS133 IN TROPONIN-I RELATIVE TO TROPONIN-C IN THE TERNARY TROPONIN COMPLEX

((Y. Luo, J.-L. Wu, T. Tao & J. Gergely)) Muscle Research Group, Boston Biomedical Res. Inst. 20 Staniford St., Boston, MA 02114.

Our previous work has shown that Cys133 of TnI moves away from Cys374 of actin and towards Cys98 of troponin-C (TnC) as Ca^{2+} binds to TnC. In this work we used the technique of resonance energy transfer (RET) to define the locations of Cys133 of TnI in the ternary Tn complex under different metal binding conditions. A single Cys mutant of TnI at position 133 (C48S, C64S) was made to facilitate selective probe labeling. We measured ten distances from Cys133 in TnI to Cys's at positions 5, 12, 21, 41, 49, 89, 98, 125, 133 and 158 in genetically engineered single Cys TnC mutants. The fluorescent probe 1,5-IAEDANS was used as the donor, and either DDP-Mal or DAB-Mal were used as non-fluorescent acceptors. Assuming that the conformation of TnC in the Tn complex is identical to that in the crystal structure, a distance geometry algorithm was used to localize Cys133 of TnI with respect to TnC. Our results show that in the presence of Ca^{2+}, Cys133 of TnI is located near residue 12 of TnC beneath the N-terminal lobe, and approximately 27 Å from the central helix. In the absence of Ca^{2+}, the site moves by 12 Å away to a site that is ~36 Å from the central helix. Our findings are consistent with our previous results showing that a photocrosslinker attached at residue 12 of TnC crosslinks to residues 132-141 of TnI, and is consistent with the view that the C-terminal region of TnI moves away from TnC and presumably towards actin in the Ca^{2+}-free state. In addition, this work demonstrates the viability of using a combination of RET and distance geometry analysis to characterize conformational transitions in Tn. (Supported by NIH HL05949 and AR21673).

Su-Pos35

EFFECTS OF CARDIAC TROPONIN/TROPOMYOSIN ON LOADED AND UNLOADED THIN FILAMENT SLIDING SPEED IN MOTILITY ASSAYS

((A. Bobkova, L.Tobacman*, and E. Homsher)) Dept. Physiology, UCLA, Los Angeles, CA. 90024 and *Dept. Medicine, U. Iowa, Iowa City, IA 52242.

Regulation of the sliding speed (S_f) of rhodamine-phalloidin labeled actin thin filaments by bovine cardiac tropomyosin (Tm) and troponin (Tn) has been studied at 25°C and 100 mM ionic strength. By adding 0.1 μM Tn/Tm to the assay chamber during filament motion, complete regulation of the sliding speed can be achieved; i.e., >95% of the filaments move at 5-7 μm/s at pCa 5 and none move at pCa 9.0. Hill plots having a pCa_{50} of 7.0 and a Hill coefficient of 1 accurately describe the relationship between S_f and pCa. The data suggest that the variation of filament sliding speed is a function of the number of crossbridges having access to the thin filaments. We have "loaded" the thin filaments by adding a weak-binding crossbridge analog, pPDM-treated HMM, to the usual rabbit skeletal HMM-coated assay surface. We find, as reported by Warshaw et al (J.C.B.[1990], 111:453), that S_f declines linearly with the added pPDM-HMM reaching zero speed at a pPDM-HMM/HMM ratio of 0.5. Further at ionic strengths of 100 mM or more and in the presence of Tm and Tn, the labeled thin filaments show little fragmentation when pPDM-HMM is used to "load" the thin filaments. At lower ionic strengths significant fragmentation occurs. When pPDM-HMM is added to slow the filament sliding speed to 2.5 μm/s at pCa 5, variation of pCa produces an speed-pCa plot whose pCa_{50} is reduced to 6. This rightward shift in the speed-pCa plot is consistent with a regulation produced by varying the number of crossbridges interacting with the thin filaments. (Supported by NIH grants AR-30988 [EH] and HL-38834 [LT])

Su-Pos36

THE FUNCTIONAL INTERACTION OF CALDESMON WITH CALMODULIN

((P.A.J. Huber, Z. ¶Grabarek *D.A. Slatter, *B.A. Levine and S.B. Marston))
NHLI (CM), Imperial College, Dovehouse St. London SW3 6LY, UK,
*University of Birmingham, Edgbaston, Birmingham B15 2TT, UK
¶ Muscle Research Group, Boston Biomed. Res. Inst., Boston, MA, USA

The binding of Ca^{2+}- and Ba^{2+}-calmodulin to caldesmon and its functional consequence was investigated with three calmodulin mutants whose Ca^{2+} induced transformation is altered. Two calmodulin mutants have pairs of cystein residues substituted and oxidised to a disulphide bond in either the N- or C-terminal lobe (C41/75 and C85/112). The third mutant has Phe92 replaced by Ala (F92A). Binding measurements in the presence of Ca^{2+} by separation on native gels and by carbodiimide induced crosslinking showed a lower affinity for caldesmon in all the mutants. When Ca^{2+} was replaced by Ba^{2+} the affinity of calmodulin for caldesmon was further reduced. In contrast to native calmodulin the mutants C41/75 and F92A did no prevent carbodiimide induced actin-caldesmon crosslinking in the presence of Ca^{2+}. The ability of Ca^{2+}-calmodulin to release caldesmon's inhibition of the actin-tropomyosin activated myosin ATPase was virtually abolished by mutation of Phe92 to Ala or by replacing Ba^{2+} for Ca^{2+} in native calmodulin. Both Cys mutants retained their functional ability but the increased concentrations needed for 50% release of caldesmon inhibition reflected their decreased affinity. Ca^{2+}-calmodulin produced a broadening in the signals of the nuclear magnetic resonance spectrum of the 10 kDa C-terminal Ca^{2+}-calmodulin binding fragment of caldesmon arising from Trp 749 and 779 and caused an enhancement of maximum Trp fluorescence of 49% and a 16 nm blueshift of the maximum. Ca^{2+}-calmodulin F92A produced a wavelength shift of 4 nm but no change in maximum whilst Ca^{2+}-calmodulin C41/75 binding produced a decrease in fluorescence with no shift of the maximum. We conclude that functional binding of Ca^{2+}-calmodulin to caldesmon requires multiple interaction sites on both molecules.

Su-Pos37

SMOOTH MUSCLE CALPONIN BLOCKS THE STRONG BINDING INTERACTION BETWEEN ACTIN AND MYOSIN.

((Mohammed EL-Mezgueldi and Steven B. Marston))
NHLI (CM), Imperial College, Dovehouse Street, London SW3 6LY, U. K.

We have investigated the mechanism of regulation by the thin filament regulatory protein calponin. Calponin inhibits the actomyosin ATPase activity upon binding to actin and this inhibition is reversed by Ca^{2+}-binding proteins such as calmodulin or caltropin. We have previously shown the specific interaction of calponin at Glu 334 of actin (Mezgueldi et al. 1992, J. Biol. Chem., 267, 15943-15951). Recently this region of actin, notably amino acids 332-334 and 338-348, has been proposed as being an important part of the strong myosin binding site (Rayment et al. (1993) Science 261, 58-65). Therefore from these structural studies it is reasonable to suggest that calponin inhibits the strong actin-myosin interaction. To test this hypothesis we have investigated the effect of calponin on the strong binding complexes, S-1 adenylyl imidodiphosphate (AMP.PNP) and S-1ADP, and on the weak binding complex, S-1.ATP. We found that an inhibitory concentration of calponin decreased the binding of the S-1.AMP.PNP and S-1.ADP to actin, but has no effect on the binding of S-1.ATP. In competition experiments calponin was found to displace S-1AMPPNP and S-1ADP from actin and S-1 displaced calponin from actin in the rigor state and in the presence of ADP. We conclude that the binding of calponin to actin blocks the strong binding site of myosin. Thus calponin inhibits the actomyosin ATPase by blocking the transition from the weak to the strong binding state in the actomyosin complex. Accordingly, calponin, caldesmon and troponin-I share a common mechanism of inhibition of the actomyosin ATPase activity, however calponin appears to bind directly to the myosin strong binding site on actin whereas caldesmon and troponin-I act indirectly by controlling tropomyosin position in the filament.

Su-Pos38

Thin Filament Regulation of Dephosphorylated Smooth Muscle Myosin. ((J.R. Haeberle)) Dept.Molecular Physiology and Biophysics, The University of Vermont, Burlington, VT, 05405

We previously reported that dephosphorylated smooth muscle myosin was activated in an *in vitro* motility assay by regulated thin filaments containing tropomyosin and calponin. In the present study, we have directly tested the hypothesis that dephosphorylated myosin is activated by actin filaments that have been "turned-on" by high-affinity cross-bridge binding (rigor-dependent activation). Actin-tropomyosin filaments were turned-on either by decreasing the concentration of MgATP, or by decorating the filaments with NEM-modified skeletal S1. Isometric force and velocity were measured using a standard motility assay with rhodamine-phalloidin labeled skeletal muscle actin filaments moving over chicken gizzard smooth muscle myosin immobilized on nitrocellulose-coated glass coverslips. Changes in isometric force were measured by adding NEM-modified skeletal muscle myosin to the coverslip to impose a mechanical load on the filaments. An index of relative isometric force (F_{NEM}) was determined as the minimum molar ratio of "NEM-modified myosin/smooth muscle myosin" at which filament motion was completely inhibited (i.e. isometric conditions). F_{NEM} values were normalized to F_{NEM} for fully thiophosphorylated smooth muscle myosin. The density of smooth myosin and NEM-myosin bound to the coverslip was kept as low as possible to minimize activation of thin filaments by NEM-modified myosin. Normalized F_{NEM} for control dephosphorylated myosin was <0.01, confirming that there was little or no activation under control conditions. Reducing the MgATP concentration resulted in an abrupt increase in F_{NEM} to 0.96 at 0.1 mM MgATP. This effect was dependent on the presence of tropomyosin. In the presence of NEM-S1 decorated actin-tropomyosin filaments (1 mM MgATP, molar ratio NEM-S1/actin=1/7), F_{NEM} was to 0.60. These results demonstrate that force production by dephosphorylated myosin, equal to that produced by phosphorylated myosin, is activated by actin filaments that have been turned-on by high-affinity cross-bridge binding (rigor-dependent activation).

Su-Pos39

CA^{2+}-DEPENDENT BINDING OF CALCYCLIN TO SMOOTH MUSCLE TROPOMYOSIN. ((N.L. Golitsina, J. Kordowska, C.-L.A. Wang & S.S. Lehrer)) Boston Biomedical Research Institute, Boston, MA.

The interaction of reduced calcyclin (SH-CaCY) and oxidized CaCY (SS-CaCY) with gizzard tropomyosin (Tm) and Tm.actin was studied with fluorescence titrations and photoreactive crosslinking experiments. Titrations with pyrene-iodoacetamide-labeled Tm (Tm*) showed Ca^{2+}-dependent binding with μM dissociation constants for Tm alone and Tm.actin and stoichiometry, n = 0.8 SH-CaCY (10.5 kDa monomer) / 1 Tm molecule and 1.5 SS-CaCY (21 kDa dimer) / 1 Tm molecule. CaCY cosedimented with Tm.actin only in the presence of Ca^{2+}. The location of the CaCY-binding site on Tm, was determined by UV photochemical crosslinking using Tm containing benzophenone-iodoacetamide attached to Cys36 of ββTm (BPI-Tm). In the presence of CaCY and Ca^{2+}, UV irradiation produced a new band (about 43kDa) on SDS polyacrylamide gels, consistent with crosslinking between a Tm chain and a CaCY monomer. A similar yield of Tm-CaCY crosslinked species was obtained after UV irradiation of CaCY + BPI-Tm.actin detected in the presence of Ca^{2+}. No CaCY crosslinked products were in the presence of 1mM EGTA. The crosslinked CaCY-Tm was found in the actin pellets after ultracentrifugation of the UV-irradiated BPI-Tm.actin + CaCY mixture in the presence of Ca^{2+}. Our data provide direct evidence for a Ca^{2+}-dependent Tm-CaCY interaction at or near Cys36 of Tm and also suggest that CaCY binding to Tm.actin does not cause Tm dissociation. (Supported by NIH.)

Su-Pos40

DISTRIBUTION OF CALDESMON IN CHICKEN GIZZARD SMOOTH MUSCLES. ((Katsuhide Mabuchi#, Philip Graceffa# Adelaida Carlos# and Jim J-C. Lin*)) #Muscle Research Group, Boston Biomedical Research Institute, Boston Ma 02114; *Dept. Biol. Sci., Univ. Iowa, Iowa City, IA 52242

Immunogold electron microscopy of chicken gizzard smooth muscle cells indicated that CaD was not distributed uniformly among actin filaments but rather concentrated around myosin filaments, suggesting two possibilities: 1) the presence of two types of filaments, either decorated with CaD or not; 2) CaD molecules cluster only at certain areas but not other areas on the same filaments. We found that tropomyosin gradually dissociates to form tethered molecules, and this complicated identification of CaD molecules. In order to accurately identify CaD molecules on isolated native thin filaments (NTF), NTF were first treated with 5,5'-dithiobis(2-nitrobenzoic acid) (DTNB), a very effective crosslinker for CaD and actin (Graceffa et al., Biochem. J. 294:63, 1993), then Tm was washed away in 0.5 M NaCl, and finally DTNB-treated NTF were examined with electron microscopy. Visualization of CaD molecules was aided with monoclonal anti-CaD for rotary shadowing and an additional gold-conjugated anti-antibody for negative staining. Both techniques indicated that the density of CaD molecules varies not only between different filaments but also along the same filament. Often anti-CaD molecules were found only on the same side of an actin filament with ~40 nm displacement. This arrangment appears to be very effective way for CaD molecules to face the same myosin filament. Our observation also support earlier results that CaD binds to NTF lengthwise (Supported by a grant form NIH, P01-AR41637).

Su-Pos41

SLOWED MYOCARDIAL RELAXATION WITH HIGH PRELOAD IS NOT DUE TO SLOWED DECLINE OF ACTIVATION. ((AJ Baker, EC Keung, SA Camacho, VM Figueredo & MW Weiner)). Univ. Calif. San Francisco CA 94143.

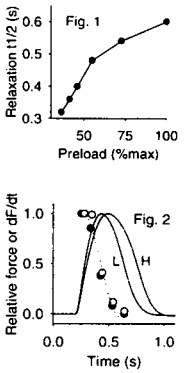

The Frank-Starling relation (increased force with higher preload) is well known; much less clear is the effect of preload on relaxation. Recent studies suggest perfused hearts relax slower with higher preload but the mechanism is unknown. **Goal:** Determine if slower relaxation with higher preload is due to slower decline in the level of activation of the contractile proteins. **Methods**: During twitches of rat right ventricular trabeculae, actomyosin cross-bridges were forcibly dissociated by a brief stretch. The subsequent rate of force redevelopment (dF/dt) indicated the instantaneous level of activation. **Results:** Fig.1 shows as preload was increased (by increasing muscle length) relaxation was slowed (time to half relaxation (t1/2) increased). Fig.2 shows force vs. time for twitches at low (L) and high (H) preload. Relaxation was slowed with high preload. In contrast, Fig.2 also shows dF/dt declined similarly with high (open circles) and low preload (filled circles). **Conclusions:** slowed relaxation with high preload is not due to slowed decline in the level of activation of the contractile proteins; suggesting therefore that slowed cross-bridge kinetics may play a role. The effects of preload and muscle length on cross-bridge kinetics may be important determinants of relaxation of the heart.

CONTRACTILITY, LOCOMOTION, MOTILITY: MOTORS

Su-Pos42

KINETICS OF ATP CLEAVAGE AND PHOSPHATE RELEASE STEPS BY ASSOCIATED RABBIT SKELETAL ACTOMYOSIN USING A NOVEL FLUORESCENT PHOSPHATE PROBE. ((Martin R. Webb and Howard D. White)) National Institute for Medical Research, Mill Hill, London, NW7 1AA, U.K. and Dept. of Biochemistry, Eastern Virginia Medical School, Norfolk Va. 23507.

We have measured the kinetics of phosphate (Pi) release during a single turnover of actomyosin (AM) nucleoside triphosphate (NTP) hydrolysis using double mixing stopped-flow fluorescence at very low ionic strength to prevent dissociation of the acto-myosin. Myosin-S1 and NTP are mixed and incubated for ~1 s to allow NTP to bind to myosin and generate a steady-state mixture of M-NTP and M-NDP-Pi. The steady state intermediates are then mixed with actin. The kinetics of Pi release are measured using a fluorescent probe for Pi, based on a phosphate binding protein (Brune et al. Biochemistry 33, 8262, 1994). The kinetics of Pi release are biphasic. At saturating [actin], there is a correlation between the amplitude of the fast phase and the size of the Pi burst in the absence of actin: the size of this phase corresponds to the M-NDP-Pi formed during the first mix and the kinetics of the phase is Pi release from AM-NDP-Pi. The slow phase corresponds to the amount of M-NTP present after the initial mix and measures the rate of the cleavage step on associated actomyosin. For ATP at 20^{o} C the rate of the Pi release step is 75 +/- 5 s^{-1}, 15 times larger than the cleavage step, which is the rate limiting step of actomyosin ATP hydrolysis at saturating actin. The rate constant of the slow phase of the Pi release (measuring cleavage) is dependent upon the structure of the NTP substrate. The rate constant of the rapid phase of Pi release is independent of substrate structure. This work was supported by MRC, U.K. and HL41776.

Su-Pos43

PROBING THE ATPases OF MYOFIBRILS AND MYOSIN BY CRYOENZYMOLOGY. ((C. Lionne, R. Stehle, F. Travers and T. Barman)) U128 INSERM, CNRS, BP5051, 34033 Montpellier Cedex 1, France.

The myofibrillar ATPases have been used as models for muscle fibre ATPases. There are 3 myofibrillar ATPases, each mimicking a muscle fibre condition: Ca-activated (isotonic contraction under zero external load), chemically crosslinked (isometric contraction) and, in particular, relaxed-myofibrils ("relaxing" conditions). Here we address the problem of the myosin head ATPase activity of relaxed myofibrils : is it identical to that of the heads alone (S1) or is it modulated by the myofibrillar environment? The overall kcat and the kinetics of ATP binding and cleavage of relaxed myofibrils and myosin (S1) are identical. The following release of products steps (Pi before ADP) are of more interest as they may be related directly to the contractile process. The Pi release kinetics are identical for the two systems (Lionne et al, 1995, *FEBS Lett 364*, 59). Here we compared the ADP release kinetics of relaxed myofibrils and S1. The traditional methods for studying ADP release with S1 (single turnovers, ADP displacement) cannot be used with myofibrils as they cause rigor activation. Another way is to obtain the temperature dependence of kcat. With S1 there is a "break" at 5°C : above, the Pi release kinetics are rate limiting (low $\Delta H^{\ddagger}$), below it is the ADP release (high $\Delta H^{\ddagger}$). Such experiments require an extensive temperature range and an antifreeze. In *40% ethylene glycol* (-15°C to 30°C) the dependences are similar but in *20% methanol* they are different. With relaxed myofibrils the dependence is linear (-15°C to 30°C, $\Delta H^{\ddagger}$ = 84 $kJ.mol^{-1}$) but with S1 there is a break at about 0°C with $\Delta H^{\ddagger}$ = 43 $kJ.mol^{-1}$ above and 120 $kJ.mol^{-1}$ below the break. This suggest that in methanol the myofibrillar environment modulates the ADP release kinetics of the myosin heads: whereas with S1 these kinetics become rate limiting below 0°C, with relaxed myofibrils they remain fast down to -15°C.

Supported by the Association Française contre les Myopathies and the European Union.

Su-Pos44

ANALYSIS OF SPONTANEOUS OSCILLATORY CONTRACTION IN SKELETAL MYOFIBRILS BY ISOTONIC FEEDBACK CONTROL. ((Y. Shindo[1], K. Yasuda[2], and S. Ishiwata[1])) Department of Physics, School of Science and Engineering, Waseda University, 3-4-1 Okubo, Shinjuku-ku, Tokyo 169, Japan[1], and Advanced Research Laboratory, Hitachi Ltd., Hatoyama, Saitama 350-03, Japan[2]. (Spon. by J. Otomo)

An isotonic control system for studying dynamic properties of single myofibrils under optical microscope was developed. This system was applied to evaluate the change of sarcomere lengths in glycerinated skeletal myofibrils under the condition of spontaneous oscillatory contraction (SPOC). Sarcomere length oscillated spontaneously under the isotonic conditions, in which the external loads were maintained constant. Moreover, the synchronous behavior of sarcomeres, that is shortening and yielding of sarcomeres occurred in concert, was observed only under isotonic conditions (we call this synchronous SPOC). The period of the sarcomere length oscillation, 1-3 s, did not largely depend on external loads. The active tension under the SPOC condition increased as the sarcomere length increased, though it was still a magnitude smaller than the tension under normal Ca^{2+} contraction. The synchronous SPOC implies that there is a mechanism transmitting information between sarcomeres such that the state of sarcomeres is affected by the states of adjacent sarcomeres. And not only the large amplitude of the oscillation of the overlap between thick and thin filaments under constant external load but also the unusual sarcomere length-tension relation indicate that in each half-sarcomere the number of force-generating cross-bridges is spontaneously regulated so as to balance the active tension with the external load.

Su-Pos45

X-RAY DIFFRACTION STUDIES OF STRUCTURAL CHANGES IN ACTIN AND MYOSIN FILAMENTS DURING CONTRACTION. ((Hugh Huxley, and Alex Stewart)) Rosenstiel Center, Brandeis University, Waltham, MA 02254, ((Tom Irving)), BioCAT, Illinois Institute of Technology, Chicago, ILL 60616-3792

Using the high flux multipole wiggler beam line at CHESS (Cornell) we have made further studies of spacings and intensities in the wider-angle X-ray diagrams from contracting frog sartorius muscle, using an imaging plate recording system. We have paid particular attention to the higher order myosin meridional reflections, which appear at successive orders of the 143Å axial repeat of the crossbridges, and might have been expected to arise from the same diffracting structure. Surprisingly, although all these reflections show the same overall ~1.5% spacing increase going from rest to full isometric contraction, there are significant differences in the time course of the changes; and the extent of the reversal of this spacing change, brought about by isotonic shortening, differs between the 143Å and the higher order reflections. Moreover, procedures such as quick release which cause a large decrease in 143Å reflection intensity have a much smaller effect on several of the higher order reflections. These findings indicate that the reflections arise from different parts of the axially repeating myosin molecules, moving relative to each other during activity. Possibly the higher order reflections come from backbone structures in the thick filaments, but if so, the changes show that the backbone is a more active and interesting component than might have been supposed. Alternatively, the reflections might arise from a part of the crossbridge structure which is not rigidly coupled to the actin-binding regions. Preliminary studies of the actin axial repeat during the early activation phase of contraction, using a spinning imaging plate technique and other methods, indicate that small initial changes in spacing are in the direction of filament shortening. Therefore mechanical experiments which involve the full release of tension in an active muscle will produce an actin filament shortening by at least the full extent seen between isometric contraction and rest (0.3-0.35%), possibly slightly more, rather than the smaller, minimum values (~0.2%) measurements during moderate tension changes (±50%) around P_o.

Su-Pos46

SEARCH FOR FUNCTIONAL DEFECTS RESULTING FROM THE 606VAL→MET MUTATION IN THE β-MHC GENE ASSOCIATED WITH HCM. ((T.Kraft*, V.Nier*, E. Thedinga*, W.J. McKenna+, B.Brenner*)). *Dept. Clin. Physiol., MHH, 30623 Hannover, FRG; +Dept. Card. Sci., St. George's Hosp. Med. School, London, U.K.

The 606Val→Met mutation of the β-myosin heavy chain gene (β-MHC) observed in familial hypertrophic cardiomyopathy (HCM) was described to result in an ≈50% reduction of in vitro sliding velocity (Cuda et al., JMRCM 15, 1994). To identify the primary dysfunction at the cross-bridge level in the structurally intact contractile system we examined isometric force, unloaded shortening velocity (v_{max}) and the rate constant of force redevelopment (k_{redev}). We used skinned soleus muscle fibers of a patient with this 606Val→Met mutation since it had been shown that the β-MHC is also expressed in soleus muscle (Cuda et al., J. Clin. Invest.91, 1993). SDS-PAGE, k_{redev} and v_{max} allowed us to identify fibers that only contained the β-MHC. To our surprise, fibers of the 606Val→Met patient did not show any difference in isometric force, v_{max} and k_{redev} when compared with normal controls. Since the apparent discrepancy with the observation of Cuda et al. (1994) could result from the basic differences between in vitro motility assay and skinned fibers (e.g. non-structured vs. structured system), we also measured the in vitro sliding velocity using the approach of Thedinga et al. (this meeting). Again, no difference was observed between the mutation and normal controls. One possible explanation for the discrepancy with Cuda's results could be that there is a large variability in the level of expression of the mutant gene among different kindreds of the same mutation. We are currently testing this possibility by quantifying the expression of wild type vs. mutant β-MHC. Our observations indicate that testing mechanical and other parameters without such quantification may be quite misleading for conclusions about the functional relevance for the myosin cross-bridge cycle.

Su-Pos47

A SINGLE FIBER IN VITRO MOTILITY ASSAY. ((E. Thedinga, Th. Kraft, B. Brenner)). Dept. of Clinical Physiology, Medical School Hannover, 30623 Hannover, Germany.

We established a micro in vitro motility assay from segments of single skinned muscle fibers to directly correlate mechanical parameters recorded from a single fiber with sliding velocity of actin filaments observed in an in vitro motility assay of the same fiber segment. Different from methods for the standard assay (e.g. Kron and Spudich, Methods in Enzymology, 1991), myosin was extracted directly from the single fiber segment by a high ionic strength buffer in the presence of MgATP and applied to a miniaturized flow cell such that the small quantity of extracted myosin was sufficient to yield a fully functional motility assay. Myosin isolated from an approximately 10 mm segment of a single skinned fiber was found sufficient to support normal ATP-driven sliding of fluorescently labelled actin filaments at maximum speed. The actin filaments were prepared and labelled with TRITC-Phalloidine according to Harada et al. (JMB, 1990).

We used this approach (1) as a straightforward way to isolate pure populations of myosin heavy chain isoforms to study their in vitro sliding velocities, and (2) to directly correlate in vitro sliding velocity with unloaded fiber shortening under identical experimental conditions by generating the in vitro assay from the same fiber segment of which the mechanical parameters were measured. Such correlation was done on rabbit psoas and human soleus muscle fibers. (3) We are using this approach to study both, various mechanical parameters and in vitro sliding velocity for characterizing functional effects of β-myosin heavy chain mutations expressed in human soleus fibers in some kindreds with hypertrophic cardiomyopathy (cf. Kraft et al., this meeting).

Su-Pos48

ORIENTATION DEPENDENT AMPLITUDES AND DURATIONS OF DISPLACEMENT SPIKES FROM SINGLE MYOSIN MOLECULES ((H.Tanaka, A. Ishijima, M. Honda, K. Saitoh, & Yanagida, T.)) *Yanagida Biomotron project, ERATO, JRCD, Mino, Osaka & Osaka Univ. Toyonaka, Osaka, Japan.*

Using dual beam laser tapping nanometry, we measured displacement spikes from single myosin molecules on a very sparse myosin–rod cofilament at various angles between the actin and myosin–rod filaments. The amplitudes and durations varied from 16 to 6 nm and from 50 to 8 ms at the trapping stiffness of 0.2 pN/nm when the angle was altered from 4 to 60°, respectively. The values indicate those after correction for the randomizing effect of thermal motion of the beads (Molloy's effect). At > 60°, no detectable spikes were observed.

Thus, the unitary step size of correctly–oriented myosin heads is 16 nm even at medium load (0–50 % of maximum force). If the 1:1 coupling is assumed, the duration, 50 ms, would be too large to explain the velocity (16nm/50ms=0.3μms^{-1}<<the expected velocity, 2μms^{-1} at medium load), suggesting that several power strokes occur during one displacement spike (one ATP cycle). Small (<10 nm) and sharp (<10ms) displacement spikes previously reported using a surface motility assay would be due to the effect of random orientation of myosin molecules.

Su-Pos49

EFFECT OF SOLUTION VISCOSITY ON CALCIUM ACTIVATED, SKINNED SKELETAL MUSCLE FIBERS. ((P.B. Chase, T.M. Denkinger and M.J. Kushmerick)) Dept. of Radiology, Dept. of Physiology & Biophysics, and Center for Bioengineering, University of Washington, Seattle, WA 98195.

Isometric force, unloaded shortening velocity (V_{US}) measured by the slack test, the rate of isometric force redevelopment (k_{TR}) after release and restretch, and the force responses to small amplitude length steps were recorded during Ca^{2+}-activation of single, skinned fibers from rabbit psoas. To vary viscosity of the bathing solutions, low MW sugars (sucrose, mannose, glucose or fructose) were added which readily permeate the myofilament lattice. As reported previously, V_{US} was more affected by this perturbation than force at maximum Ca^{2+}-activation (Chase & Kushmerick, 1988, *Biophys J* 53:935); furthermore, we found that the decrease in V_{US} was inversely proportional to viscosity. There was little effect of increased viscosity (2-fold) on phase 2 of tension transient responses to step length changes. At submaximal activation, Ca^{2+} sensitivity was decreased (shifted to lower pCa) by increased viscosity, as previously reported (Endo et al., 1979. In: Cross-Bridge Mechanism in Muscle Contraction. Sugi & Pollack, eds., Univ. of Tokyo Press, 365). Elevated viscosity also decreased k_{TR} at maximal Ca^{2+} activation, but not at submaximal force levels. These results suggest a role for cytoplasmic viscosity in modulating muscle function.

Supported by NIH HL52558, AR36281, HL31962 and AM07783.

Su-Pos50

SARCOMERE LENGTH DEPENDENCE OF STIFFNESS AND PHASE 2 TENSION KINETICS IN SKINNED SKELETAL FIBERS.

((D.A. Martyn, P.B. Chase, K. Guess, A.M. Gordon and L.L. Huntsman)). Center for Bioengineering, Dept. of Physiology and Biophysics and Dept. of Radiology, University of Washington, Seattle, WA 98195

Recent evidence indicates that the contribution of thin filaments to fiber compliance is greater than previously thought. Thin (or combination of thick and thin) filament compliance, on the order of the fiber compliance due to cycling crossbridges, could explain the difference in timecourse of stiffness and force during the rise of tension in a tetanus, as well as the difference in Ca^{2+} sensitivity of force and stiffness, and more rapid phase 2 tension recovery at low Ca^{2+} activation observed in skinned skeletal fibers. For fibers in rigor, thin filament compliance decreases as sarcomere length (SL) is decreased (Higuchi *et al., Biophys. J.* 69, 1000, 1995). To characterize the effects of thin filament compliance on sarcomere stiffness and isometric force kinetics of cycling crossbridges, we measured the activation and SL (2.5 to 2.1 μm) dependence of sarcomere stiffness in single glycerinated rabbit psoas fibers, in the presence of ATP (5.0 mM). Sarcomere stiffness was measured using rapid length steps. At each steady SL, the ratio of stiffness/force was higher at lower force (low Ca^{2+}) levels and phase 2 tension transients were faster, compared to maximum activation, as we previously reported (Martyn and Gordon, *J. Gen. Physiol.* 99, 795, 1992; Martyn and Chase, *Biophys. J.* 68, 235, 1995). Furthermore, if thin filament compliance decreases as SL decreases, the ratio of stiffness/force and rate of phase 2 tension recovery should both increase at short SL. In contrast to this prediction, at both maximal and submaximal force levels, we found no significant change in either the stiffness/force ratio or rate of phase 2 tension recovery at 2.2 μm compared to 2.5 μm SL. Supported by NIH Grants HL-51277 and HL-52558.

Su-Pos51

A NOVEL ADENOSINE TRIPHOSPHATE ANALOG WITH A HEAVY ATOM TO TARGET THE NUCLEOTIDE BINDING SITE OF PROTEINS.

((N. Naber, M. Matuska, E.P. Sablin, E. Pate and R. Cooke)) Dept. Biochem. & Biophys. & CVRI, UCSF; Dept. Mathematics, WSU; Dept. Biophys., Max Plank Inst., Heidelberg, Germany.

We have synthesized 2'-deoxy-2'-iodoadenosine-5'-triphosphate (2'-IATP), a heavy atom analog of adenosine-5'-triphosphate. This compound was made for X-ray structural studies to target the nucleotide site of ATP binding proteins. It was diffused successfully into crystals of the microtubule based motor proteins, ncd and kinesin. With ncd, the nucleotide binding site was 70% occupied and the crystals were able to diffract X-rays to 2.5Å. The iodo-analog provided a useful isomorphous derivative with overall phasing power 1.89 in the range of 25.0 - 2.5 Å. With kinesin, 2'-IATP co-crystallized with the protein. The crystals diffracted to at least 2.8 Å with a phasing power of 1.73 in the range of 20.0 - 5.0 Å. The analog was also found to be a substrate for all of the enzymes tested, including: creatine kinase, pyruvate kin-ase, hexokinase and myosin, with values of Km and Vmax that were within a factor of 10 of those for ATP. The analog supported muscle contraction, relaxing fibers and producing active tension with values not statistically different from those obtained with ATP. These results all suggest that this analog should be useful for providing a heavy atom derivative for crystals of enzymes that bind ATP. Supported by grants from the NIH AR42895 (RC) and AR39643 (EP).

Su-Pos52

Kinetics of Phosphate Release and its Implications for the Modelling of ATP Hydrolysis by Actomyosin

Leonard A. Stein, H.S.C., SUNY at Stony Brook

The recent studies of Webb et.al. show that a 'Burst' of Pi-release does not occur during pre-steady state hydrolysis of ATP by Actomyosin. Detailed quantitative studies of the actomyosin kinetics in terms of the 4- and 6-state models of Stein et. al., show that different results are predicted by the two models during a double mixing stopped flow experiment. In the proposed experiment, S-1 and ATP are initially mixed and 0.5 seconds given to achieve steady state: M + ATP --> M*ATP <---> M**ADP,Pi ---> M + ADP+Pi This mixture is then mixed with actin. The 4-state model predicts an initial burst of Pi-release that increases with the actin concentration, the six state model predicts no such burst of Pi-release. The plots come from published models at 15C, LIS, & 48uM Actin.

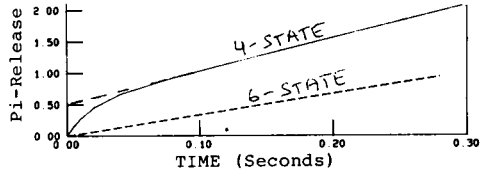

Su-Pos53

IN VITRO ACTIN FILAMENT SLIDING VELOCITIES PRODUCED BY MIXTURES OF DIFFERENT MYOSIN TYPES.

((G. Cuda, E. Pate, R. Cooke, and J. Sellers)) NHLBI, NIH, Bethesda MD; Dept. Mathematics, WSU; Dept. Biochem. & Biophys. & CVRI, UCSF.

Using *in vitro* motility assays, we have examined the sliding velocity of actin filaments generated by pairwise mixings of actively cycling myosins from 6 different sources. In isolation, the myosins translate actin filaments at differing velocities. We find that only small proportions of a more slowly translating myosin type are required to significantly inhibit the sliding velocity generated by a myosin type which translates filaments rapidly. In other experiments, addition of noncycling, unphosphorylated smooth and nonmuscle myosin to actively translating myosin also inhibits the rapid sliding velocity, but to a significantly reduced extent. The data are analyzed in terms of a model derived from the original working cross-bridge model of A. F. Huxley. We find the inhibition of rapidly translating myosins by slowly cycling myosins can be explained by a change in only a single parameter -- the cross-bridge detachment rate at the end of the working powerstroke. In contrast the inhibition induced by the presence of noncycling, unphosphorylated myosins requires a change in another parameter -- the transition rate from the weakly attached actomyosin state to the strongly attached state at the beginning of the cross-bridge powerstroke. Supported by USPHS grants AR39643 (EP), HL32145 (RC) and a grant from the MDA (RC).

Su-Pos54

DEPLETION OF PHOSPHATE IN ACTIVE MUSCLE FIBERS PROBES ACTOMYOSIN STATES WITHIN THE POWERSTROKE.

((E. Pate, K. Franks-Skiba, and R. Cooke)) Dept. Mathematics, WSU; Dept. Biochem. & Biophys. & CVRI, UCSF.

Previous studies have shown that isometric tension (Po) in skinned, rabbit psoas fibers decreases linearly with log[Pi] for 70 mM ≥ [Pi] ≥ 200 μM. The 70 mM maximum examined was due to ionic strength constraints. The 200 μM minimum resulted from an inability to buffer the diffusive buildup of Pi from ATP hydrolysis interior to the fiber. In the present study, we used the enzyme nucleoside phosphorylase (NP) with Pi and 7-methyl guanosine as substrates to reduce the [Pi] internal to contracting fibers to <10 μM. We first found that a number of commonly employed components in fiber buffers competed with Pi in the NP catalyzed reaction: ATP (Ki = 1.5 mM), ADP (Ki = 300 μM), creatine phosphate (Ki < 100 μM), and phosphoenoyl pyruvate (Ki = 800 μM). Thus our lowest fiber Pi levels were obtained using very thin muscle fibers, and a buffer containing 1 mM ATP (no regenerating system) and high [NP] (up to 300 U/ml). We found that Po continued to increase as the [Pi] decreased from 200 μM to approx. 100 μM. Further decreases in [Pi] did not result in additional increases in Po. The data were analyzed using spatially-dependent models for cross-bridge function. Supported by USPHS grants AR39643 (EP) and HL32145 (RC).

Su-Pos55

RADIAL FORCES IN THE A-BAND OF VERTEBRATE STRIATED MUSCLE.

((Barry M. Millman)) Biophysics Group, Dept. of Physics, University of Guelph, Guelph, ON, N1G 2W1.

Radial forces or lateral pressure between filaments in the A-band of frog sartorius muscle have been analysed under conditions of relaxation, isometric contraction, and rigor over a range of lattice spacings. The radial force was considered as a sum of four components: osmotic {OS} (when a membrane is present or under osmotic stress), electrostatic {ES}, structural {ST} (filament interference, M-lines, etc), and crossbridge {XB}. The forces (or pressures) were assumed to sum to zero at all times and under all conditions. During relaxation, {XB} is absent. {ES} was calculated from known filament dimensions and charge (Millman & Irving, 1988, Biophys. J. **54**:437-447). {ST} was calculated from relaxation data and found to be close to zero over lattice spacings in the normal operating range (d_{10} = 33 - 37 nm), but was large and either expansive or compressive at very small or large spacings, respectively. Crossbridge pressures up to 10^5 N/m^2 were found for small lattice spacings. The stiffness due to crossbridges (defined as the change in pressure per proportional change in lattice spacing [i.e. $\Delta\pi\{D/\Delta D\}$]) is almost three times higher in contracting muscle than in rigor (80 and 30 x 10^4 N/m^2).

Su-Pos56

KINETICS OF MONOMERIC KINESIN HEAD DOMAINS. ((W. Jiang and D.D. Hackney)) Carnegie Mellon Univ., Pittsburgh, PA 15213.

Dimeric kinesin head domains have very tight binding to MTs during ATP hydrolysis and many ATP molecules are hydrolyzed during each diffusional encounter with a MT (D. Hackney, Nature (1995) In Press). Monomeric DKH357, however, has only weak net binding to MTs during ATP hydrolysis ($K_{0.5}$ > 5 μM). When ATP is added to a rigor-like complex of DKH357 with MTs, there is an initial burst of ATP hydrolysis with an apparent rate constant of ~50 /s. Parallel light scattering experiments indicate that net dissociation of DKH357 from the MT also occurs at a similar rate. The magnitude of the burst of ATP hydrolysis, however, is greater than the concentration of DKH357 active sites by ~2 fold. Experiments using pyruvate kinase to trap free ADP indicate that the superstoichiometric component of the burst of ADP production is present as free ADP. These results are consistent with DKH357 hydrolyzing ~2 ATPs on average before net diffusional separation from the MT. Thus the 50 s^{-1} ATPase burst rate does not represent the true rate of ATP hydrolysis, which is faster. Rather it represents termination of the burst process by diffusional separation. The super stoichiometric burst could be due to either hydrolysis of multiple ATP molecules without dissociation of DKH357 from the MT or to dissociation of DKH357 from the MT during each ATPase cycle coupled with a significant probability of recapture of the released DKH357 by the MT before complete diffusional separation can occur.

Su-Pos57

MECHANISM OF MICROTUBULE-MONOMERIC KINESIN HEAD DOMAIN K332 ATPASE ((Y. Z. Ma and E. W. Taylor)) Dept. of Mol. Gen., University of Chicago, Chicago, Il 60637.

K332 was purified from E. Coli strain using plasmid provided by L. Romberg. The mechanism of microtubule-K332 ATPase was fitted to

1 2 3 4 5 6
T+MK—MK(T)—MKT—MKD.P—MKD—MK(D)—MK+D

The rate constants of the steps for monomeric K332 were similar to dimeric K379 in the absence of microtubules. Significant differences were found between MK332 and MK379 complexes. k_{cat} of MK332 (60 s^{-1}) was about twice that of MK379. The binding of K332 to microtubules in the presence of nucleotides was 5 times weaker than of K379. Nucleotide binding to MK332 was weak as measured by the fluorescence enhancement of mant-ATP and mant-ADP. k_{-2} and k_5 was 100 s^{-1} and 300 s^{-1} respectively obtained by extrapolating the concentration dependent curve of rate constants to zero concentration, whereas the rate constants of nucleotide binding to MK379 was less than 1 s^{-1} at very low nucleotide concentration. The rate constant of phosphate burst of MK332 was > 100 s^{-1}. The rate constant of ADP dissociation was 100 s^{-1} (40 s^{-1} for MK379) as determined by measuring the rate of fluorescence decrease of mant-ADP after mixing K332.mant-ADP complex with microtubules in the presence of excess ATP. In the absence of excess ATP, all mant-ADP was released from the MK332.mant-ADP complex, but only 50% of mant-ADP was released from the MK379.mant-ADP complex. The differences between microtubule-monomeric K332 and microtubule-dimeric K379 imply the interaction of the two heads of dimeric K379.

Su-Pos58

KINETIC STUDIES OF MICROTUBULE NCD ATPASE.((E Pechatnikova and E. W. Taylor)) Univ. of Chicago, Chicago, IL 60637.

The ncd motor domain, residues 335-700 was prepared from Bl21 cells using plasmid pH40P provided by R. Vale. The protein is monomeric based on gel filtration and equilibrium ultracentrifugation. Bound nucleotide was removed from Mt-ncd complex by treatment with apyrase. The apparent second order rate constants for mant ATP and mant ADP binding (k^a), the maximum rate of binding step, the phosphate burst, and rate of mant ADP dissociation for reaction of ncd·mant ADP complex with Mt were measured (20° C). The steady state rate is 3 sec^{-1}.

	k^a $M^{-1}s^{-1}$	Max Rate(s^{-1})	Burst(s^{-1})	ADP diss(s^{-1})
mATP	$1.5x10^6$	>250	17-20	
mADP	$4x10^6$	220		4-5(±ATP)

Binding constants of ncd complexes with microtubules decreased in order ATPγS>ATP>ADP>ADP-vanadate. The properties of ncd are similar to a monomreic kinesin except that rate constants for the burst , ADP release and steady state rate are approximately ten times smaller.

Su-Pos59

EQUILIBRIUM AND STRUCTURAL STUDIES OF KINESIN:NUCLEOTIDE INTERMEDIATES. ((S.S.Rosenfeld, J.J. Correia, J.Xing, B.Rener, and H.C.Cheung)) Dept. Neurology, Cell Biology, and Biochemistry, Univ. Alabama at Birmingham, Birmingham, AL 35294 and Dept. Biochemistry, Univ. Mississippi, Jackson, MS 39216

We have examined the interactions of two kinesin constructs--K332 and K413--with nucleotide and microtubules in order to develop a structural model for kinesin-dependent motility. K332 is monomeric, while K413 is largely dimeric at concentrations >5μM. Dimerization of K413 reduces k_{cat} for the microtubule-activated ATPase by nearly 5-fold, suggesting that the rate-limiting step in the enzymatic cycle is coupled to movement of a dimerization segment. Beryllium fluoride and aluminum fluoride form stable ternary complexes with K332:ADP and K413:ADP, mimic the kinesin:ATP state, and *enhance* the microtubule affinity. By contrast, inorganic phosphate binds to K413:ADP with an apparent dissociation constant of 0.8 mM and *reduces* microtubule affinity. Binding of the kinesin constructs to microtubules can be fit to a model in which kinesin:ATP binds in a *strong* state with positive cooperativity. Hydrolysis of ATP to ADP+P_i leads to dissociation of one of the attached heads of dimeric kinesin and converts the second head to a *weak* state. Dissociation of the phosphate then allows the second head to reattach to the microtubule. For both K413:ADP and K332:ADP, sedimentation velocity is not affected by addition of beryllium fluoride. However, fluorescence anisotropy decay studies of native and labelled K413 show significant prolongation in the rotational correlation time by addition of beryllium flouride. These results suggest that the transition from *strong* to *weak* binding is associated with an increase in segmental flexibility of the region connecting the catalytic domain to the α-helical tail of the kinesin molecule.

Su-Pos60

MECHANOCHEMISTRY OF Eg5 ((A. Lockhart and R.A. Cross)) Molecular Motors Group, Marie Curie Research Institute, Oxted, Surrey, England RH8 OTL. (Spon. by C. Bagshaw)

Eg5 like kinesin is a plus end directed microtubule (MT) motor that is homologous to kinesin, but moves ~10 to 20 times more slowly . A kinetic study of Eg5 therefore amounts to a kind of natural mutagenesis experiment, in which kinesin has been mutated to move at a reduced speed, and we can ask how the mechanochemistry of the slower "mutant" differs from that of the "wild type" kinesin. We used the recombinantly expressed protein E437GST (residues 12 to 437 of Eg5 fused to the N-terminus of glutathione S-transferase) which is dimeric and moves MTs *in vitro* at 0.063 (±0.003) μm s^{-1}. In the absence of MTs the basal ATPase of E437GST is slow and the release of the fluorescent analogue methylanthraniloyl ADP (mantADP) is rate limiting (~0.006 s^{-1}). MTs accelerate mantADP release to a maximal rate of 4.94 s^{-1}. Under the same conditions the steady state rate of mantATP turnover is 1.92 s^{-1}, suggesting that mantADP release is rate limiting. In MT pelleting experiments, we found that Mg-ADP induces the weakest bound state of E437GST (K_d>>10 μM), whilst ATPγS and AMPPNP induce stronger binding states (K_d's 7.8 and 0.12 μM, respectively). Eg5 therefore shares the same broad pattern of coupling (ADP induces weak binding, ATP analogues induce strong binding; Crevel *et al* J Mol Biol, in press) and the same rate limiting step (MT-activated ADP release) as kinesin and the reverse directed motor ncd (Lockhart *et al* (1995) FEBS Lett 368, 531-5). Recent evidence suggests that ADP release also corresponds to a tilt of the MT attached kinesin head (Hirose *et al* (1995) Nature 376, 277-9). For Eg5, the above evidence suggests that this same ADP release step is rate limiting, and that it corresponds to a switch from weak to strong binding. This step is around ten fold slower in Eg5 than in kinesin consistent with it limiting the rate of physical stepping of both motors.

Su-Pos61

LOCATION OF THE MICROTUBULE BINDING SITE OF HUMAN KINESIN ((G. Woehlke, R. Case, N. Hom-Booher, J. Kull, E. Sablin, R. Fletterick and R. Vale)) Howard Hughes Medical Institute and Depts. of Pharmacology and Biochemistry, UCSF, San Francisco, CA 94143-0450. (Spon. by R. Vale)

Crystal structures of the motor domains of kinesin and ncd (a kinesin-related motor that moves in opposite direction along a microtubule to kinesin) have recently been solved. We have examined sequence alignments of amino acids of a variety of kinesin-related motors and mapped the positions of highly conserved residues in the three-dimensional structure. The majority of these highly conserved residues appear to comprise elements of the nucleotide binding pocket and many are clustered around the position where the γ-phosphate of ATP would be located (present structure contains bound ADP). However, some conserved stretches of amino acids (including the well conserved HIPYR motif) are located in surface loops. Since these regions are also on the opposite side of nucleotide binding pocket in the motor, they may constitute part of the interface that interacts with the microtubule. A set of solvent exposed amino acids have been mutated to alanine ("alanine scan") and mutant kinesin motors are being expressed in bacteria. Results of microtubule gliding assays, binding studies and ATPase assays of these mutants will be presented. The goal of this work is to define precisely the kinesin-microtubule interface and to understand how this interaction changes during the ATPase cycle.

Su-Pos62

TRANSCRIPTIONAL ELONGATION UNDER LOAD. ((M.D. Wang[1], H. Yin[2], R. Landick[3], J. Gelles[2], and S.M. Block[1])) [1]Dept. Molecular Biology, Princeton Univ., Princeton, NJ 08544; [2]Dept. Biochemistry, Brandeis Univ., Waltham, MA 02254; [3]Dept. Bacteriology, Univ. of Wisconsin, Madison WI 53706.

The transcriptional elongation rates of single molecules of *E. coli* RNA polymerase were measured using a feedback-enhanced optical trapping interferometer. Stalled ternary transcription complexes, consisting of single molecules of RNA polymerase, each associated with a DNA template and RNA transcript, were adsorbed onto the surface of a coverglass inside a flow cell. A polystyrene bead (0.52 μm dia.) was attached to the transcriptionally downstream end of each DNA molecule by a biotin-avidin linkage, so that the bead was tethered to the surface via its connection to the DNA and polymerase. Transcription was started by introducing buffer containing NTPs into the flow cell, after which the bead was trapped and its position monitored. Elongation resulted in the bead being pulled away from the trap center. After allowing bead movement through a short distance, a force-feedback clamp was activated to arrest subsequent displacement: this procedure allows rapid force development in the elastic DNA tether with minimal photodamage to the enzyme. Knowledge of the bead position, applied force, and the DNA force-extension relationship (determined separately, see Wang *et al., Biophys. J.*, this issue) are sufficient to calculate the DNA tether length as a function of time. These quantities will permit computation of the transcriptional elongation rates of polymerase under load, and thereby allow us to establish the force-velocity relationship for this enzyme.

Su-Pos63

STRETCHING DNA WITH OPTICAL TWEEZERS. ((M.D. Wang[1], H. Yin[2], R. Landick[3], J. Gelles[2], and S.M. Block[1])) [1]Dept. Molecular Biology, Princeton Univ., Princeton, NJ 08544; [2]Dept. Biochemistry, Brandeis Univ., Waltham, MA 02254; [3]Dept. Bacteriology, Univ. of Wisconsin, Madison WI 53706. (Spon. by S.M. Block)

A feedback-enhanced optical trapping interferometer was constructed and used to make direct measurements of the force vs. extension (F–x) relationship for single DNA molecules under a variety of ionic conditions. In this apparatus, the position of an optically-trapped bead is measured to sub-nanometer-level accuracy by interferometry. The amplitude of the laser light is servoed by an acousto-optic modulator (AOM) so as to maintain the displacement of the bead at a preset position: under such conditions, the feedback signal to the AOM provides a continuous measure of applied force. One end of a DNA molecule (~1.3 μm contour length) was fixed to a coverglass surface, via its attachment to an RNA polymerase molecule, and the other end to a 0.52 μm dia. polystyrene bead, by a biotin-avidin linkage. The DNA was then stretched by moving the stage piezoelectrically over calibrated distances while the bead was maintained in the trap. In contrast to earlier methods, complete F–x curves could be obtained in under 1 min. Low-force regions of F–x curves ($F < 5$ pN) are well fit by an interpolation formula based on entropic elastic theory (Bustamante, *et al., Science* 265: 1599-1600, 1994). The fits yield a persistence length of ~50 nm in buffers containing either 10 mM Na^+/0 mM Mg^{2+} or 150 mM Na^+/5 mM Mg^{2+}. Buffers containing 10 mM Na^+ and 400 μM spermidine, a trivalent cation promoting DNA condensation, produce a significant reduction in persistence length.

Su-Pos64

VIDEOMICROSCOPIC DETERMINATION OF THE GRAVITY THRESHOLD FOR SWIMMING BEHAVIOR AND MECHANICAL PERFORMANCE IN THE JELLYFISH *AURELIA AURITA* DURING THE SLS-1 AND IML-2 SPACE SHUTTLE MISSIONS. ((F.A. Lattanzio, Jr., D.B. Spangenberg, L. Chiao, C. Philput and R. Schwarte)) Eastern Virginia Medical School, Norfolk, VA 23501

Aurelia aurita polyps and ephyrae were sent on two shuttle missions to determine the effects of micro-gravity (micro-g) on development and behavior. Ephyrae have gravireceptors, structures related in function to the inner ear, which orient the animals while swimming. In the SLS-1 mission, the free swimming ephyrae were videotaped on earth and in space and their swimming patterns analyzed to formulate a statistical model, based on regression analysis, to distinguish between swimming at micro-g and 1 g. This model was used in the IML-2 mission to determine the gravity threshold of ephyrae, which was defined as the point at which >50% of the ephyra switched from micro-g to 1-g swimming behavior. This threshold was determined through the use of the NIZEMI (provided by Dornier/DARA), a slow-rotating programmable centrifuge with videomicroscope. The threshold for ephyrae that were developed on earth and were measured after 2 days at micro-g was between 0.312-0.339 g. Other experiments included swimming pulse acceleration as an indicator of muscle adaptation, the effects of removing the statoliths of gravireceptors on the determination of gravity thresholds and measurements of g-threshold for ephyrae that developed from sessile polyps in space. Supported by NASA grants NAG2353 and NAG 2767.

Su-Pos65

STRUCTURAL CHANGES IN THE HYDRATION SHELLS OF THE "CONTRACTILE" AND REGULATORY PROTEINS, *NOT* MAJOR CONFORMATIONAL CHANGES, ARE RESPONSIBLE FOR MECHANOCHEMICAL TRANSDUCTION IN MUSCLE
(Avraham Oplatka) Weizmann Institute of Science, Rehovot, Israel.
(Spon. by I.Z. Steinberg)

There is no real indication for *tight* binding of the myosin heads to actin in active muscle - on the contrary. Moreover, *free* active myosin fragments can induce tension generation and movement. Conclusions: (1) a *continuous* three-dimensional protein network (is not obligatory but) simply does not exist in active muscle; (2) all models based on the structure of the *rigor* actin-S-1 complex are groundless; (3) rotation of the heads *cannot* stretch any "elastic element" thus generating the "contractile" force; (4) the sliding distance (s.d.) has nothing to do with the head's length; (5) the steric blocking mechanism of muscle regulation, which takes it for *granted* that the heads are *bound* to actin in active muscle, becomes doubtful; (6) mechanochemical transduction occurs while the proteins are at a distance *i.e.*, long-range forces must be involved. Such are the hydration and electrostatic repulsive forces. When these are overcome the proteins can approach each other (without touching) thus witnessing an increasing repulsive force which can be perceived by a transducer. The energy required for this purpose is produced during the force-generating step, in conjunction with the liberation of water molecules from the hydration shells of the proteins (Oplatka, FEBS Lett. *355*, 1. 1994). It is claimed that regulation is also associated with the re-structuring of the hydration shells following the binding of Ca^{2+}. The force and the s.d. should depend on the number, energy and direction of movement of the liberated water molecules. Hence, all factors (muscle type, ionic strength, temperature, osmotic stress, chemical modification etc.) which might determine the size, structure and adhesiveness of the hydration shells of both "contractile" and regulatory proteins should affect the mechanical properties of muscle.

Su-Pos66

CHEMICALLY DRIVEN MOTILITY OF BROWNIAN PARTICLES
((Huan-Xiang Zhou and Yi-der Chen)) Department of Biochemistry, Hong Kong University of Science and Technology and NIDDK, NIH, Bethesda, MD 20892-0520.

It is known that the long-time movement of a Brownian particle is not directionally biased in the presence of a periodic potential, if the potential is *static*. But, if the potential is asymmetric within a period and is randomly or regularly switched on and off (so that the force acting on the particle fluctuates), then a net directional movement of the particle can be achieved. In this report, we demonstrate with a simple model that a Brownian particle can also execute directional movement in a *static* (*non-fluctuating*) periodic potential when coupled with a nonequilibrium chemical reaction. In other words, the free energy of a nonequilibrium chemical reaction can be directly transduced by an enzymatic Brownian particle to do mechanical work. It is found that the direction of movement depends not only on the asymmetry of the potential, but also on the free energy and the kinetic mechanism of the chemical reaction. Thus, in principle, different enzyme molecules could be separated based on their enzyme activities. The formalism is also applicable to biological motors. The results obtained in this study suggest that single biological motors with only one force-generating state can also move continuously on a periodic polymer in the presence of brownian motion.

Su-Pos67

DIRECT OBSERVATION OF POLYMERIZATION-LINKED MOVEMENT OF CHROMOSOME-BOUND MICROTUBULES.
((A.J. Hunt and J.R. McIntosh)) Dept. of Molecular, Cellular, and Developmental Biology, University of Colorado, Boulder, CO 80309

During mitosis kinetochore microtubules elongate and shorten by incorporation or loss of tubulin subunits, principally at their chromosome-bound ends. We have reproduced this phenomenon *in vitro* using an assay in which movement of a labeled microtubule segment is observed as the microtubule loses or gains subunits at its chromosome-bound end.

Chromosomes isolated from cultured CHO cells are bound to coverslips coated with antibody to DNA. Short microtubules, brightly labeled with rhodamine and stabilized by polymerization in the GTP analogue GMPCPP, are allowed to bind to the chromosomes. From these seeds labile microtubules are grown in the presence of GTP and dimly labeled tubulin. After washing with GTP and unlabeled tubulin we observe bright seeds within dimly labeled microtubules that are bound end-on to chromosomes. As a microtubule continues to grow, its labeled portion moves away from the chromosome to which it is bound. Sometimes a microtubule switches to rapid shortening and the bright seed is reeled in toward the chromosome until either there is a transition back to growth or the labile portion is completely depolymerized.

At [tubulin] = 1.0 mg/ml the average speed of movement away from a chromosome was 16 ± 7 nm/s (± S.D., n = 12), which is similar to 17 ± 5 nm/s observed for elongation of free microtubule ends. Movement toward a chromosome proceeds at 107 ± 68 nm/s (n = 6), substantially slower than 565 ± 105 nm/s observed during rapid shortening of free ends. This work was supported by the Office of Naval Research.

Su-Pos68

INTRACELLULAR pH OF VASCULAR SMOOTH MUSCLE MYOCYTES IS LARGELY RESISTANT TO CHANGES IN EXTRACELLULAR pH.

((R.G. WEBSTER W.A. COETZEE L.H.CLAPP)) Cardiovascular Research, Rayne Institute, St. Thomas' Hospital, London, SE1 7EH, UK.

We investigated the effect of changing extracellular pH (pH_o) on intracellular pH (pH_i) in isolated myocytes from guinea-pig aorta and rat main mesenteric artery. The pH-sensitive dye carboxy-SNARF-1/AM was used to measure pH_i in cells perfused with a HEPES-buffered Tyrode's solution (22°C) at pH_o 7.4 (control), 6.4 or 8.0 (test). Changes in pH_i were small and occurred slowly in both cell types, effects were measured 8 min after changing pH_o. Recovery (Rec.) was measured 5 min after return to pH_o 7.4. Calibrated data (±sem) are shown in table (✳ = different from control, p<0.05; paired t-test).

	Aorta			Mesenteric		
pH_o	Control	Test	Rec.	Control	Test	Rec.
6.4	6.92±0.03	6.74±0.06 (5) ✳	67 %	6.58±0.08	6.30±0.13 (10) ✳	31%
8.0	6.89±0.06	6.95±0.08 (8)		6.56±0.07	6.72±0.07 (10) ✳	63%

Na-H exchange inhibitors ethyl-isopropyl amiloride (EIPA) (30 μM, n=5) and HOE 694 (10 μM, n=5) had no effect on the response of aortic myocytes to pH_o 6.4. However, recovery was blocked by EIPA, but not HOE 694. These data suggest that Na-H exchange does not govern the magnitude of the response to changes in pH_o, but might influence recovery. In conclusion, the pH_i of vascular smooth muscle myocytes appears to be largely resistant to changes in pH_o, and this is not due to regulation by Na-H exchange.

Supported by British Heart Foundation

Su-Pos69

ENDOTHELIN MODULATION OF MESENTERIC ARTERIAL SMOOTH MUSCLE MEMBRANE POTENTIAL AND STOC'S.

((C.E. Hill, D. Wu, S.J. Vanner)) GI Diseases Research Unit, Hotel Dieu Hosp. & Queen's Univ., Kingston, ON, Canada.

Endothelin-1 (ET-1) constricts vascular smooth muscle (VSM) by a sequence of events thought to involve Ins-1,4,5-P_3-mediated cytosolic Ca^{2+} increase, activation of Ca^{2+}-sensitive Cl^- channels, and opening of L-type Ca^{2+} channels by the ensuing membrane depolarization (although some VSM hyperpolarize in response to ET-1). Ca^{2+}-activated K^+, or Maxi-K, channel activity may play a role in repolarizing the membrane. We studied the effects of ET-1 on whole-cell current- or voltage-clamped mesenteric arteriole VSM to assess the involvement of Maxi-K channels in the ET-1 response. The membrane potential of freshly dissociated cells is characterized by intermittent spike-like transient hyperpolarizations (TH). ET-1 increased, and iberiotoxin decreased, the frequency of a large-amplitude subpopulation of TH's without affecting the resting membrane potential, suggesting that Maxi-K channels do not play significant roles in setting basal membrane potential but are important in TH generation. Under voltage clamp spontaneous transient outward currents (STOC) of similar frequency were observed. STOC waveforms were analyzed in order to determine the current components responsible for TH.

Su-Pos70

OSCILLATION OF FORCE AFTER LENGTH PERTURBATIONS IN RABBIT DUCTUS ARTERIOSUS.

((T. Shibata and K. Takigiku)) Dept. of Pediatrics, Yokohama City Univ. School of Medicine, Yokohama 236, Japan

We studied mechanical property of the contracted smooth muscle of rabbit ductus arteriosus (DA).
[Method] Rings of DA (diameter:1.2mm, length:1.5mm, n=14) of fetal rabbits at 28 days of gestational age were quickly excised and slipped over 2 tungsten pins in a tissue bath which was perfused by hypoxic Tyrode's solution (35°C) bubbled by a gas mixture of 98% N_2 and 2% CO_2. A pin was connected to a force transducer and the other to a vibrator. After 2 hours' equilibration, the ductus ring was stretched to the length where the DA produced force of 0.1 gm, and the gas mixture was changed to 98% O_2 and 2% CO_2 or the perfusate was changed to high potassium solution (K:65mEq/l). [Result] The DA generated the force ranged from 1 to 2 gm. The trace of the force of DA with intact and damaged endothelium showed irregular, small oscillations in oxygen-induced contracture, but not in high potassium contracture. Marked sinusoidal oscillation in force after step length perturbations (20μm) was observed in the DA with intact or damaged endothelium. Frequencies calculated by Maximum Entropy Method were 4.32×10^{-4} to 8.92×10^{-4} Hz. High potassium contracture, however, did not show any oscillation. [Conclusion] Oxygen-induced contracture force appeared to be developed by cyclic movements of cross-bridges whereas the potassium-induced contracture was not the case. Endothelial function might not affect the oscillatory movement of force.

Su-Pos71

EFFECT OF GASTROSTOMY TUBE FEEDING ON GASTRIC ELECTRICAL RHYTHMS IN ELDERLY PATIENTS.

((Yatian Zhang, S.Mohapatra and H.Levendoglu)) GI Motility Clinic, Division of Gastroenterology, Department of Medicine. The Brookdale Hospital Medical Center, Brooklyn, New York. 11212-3198

Percutaneous Endoscopic Gastrostomy (PEG) is a procedure by which patients who are incapable of oral food intake can be provided with appropriate nutrition. The known unphysiological conditions associated with this procedure include pumping of food into the stomach through the PEG tube, and constraint of the stomach against the anterior abdominal wall. Potential disturbances of gastric electrical activity were investigated by electrogastrography (EGG), which records cutaneous electrical activity. The PEG procedure was applied to a group of 19 patients (mean age 82), whose inability to swallow food arose mainly from cerebral events. The potential changes in EGG activity following PEG were evaluated by comparison with EGG activity during a 1 hour baseline period. The normal 3 cpm activity was present during 48% of the baseline recording, while bradygastria occurred 26% of the time, and tachygastria occurred 24% of the time. There were no statistically significant differences after the PEG procedure, suggesting that the PEG procedure had no lasting effect on the EGG. Food was administered either slowly (infusion rates varying from 25 to 100 ml per hour), or by a 300 ml bolus feeding. There were no statistically significant effects of infusion on the distribution of EGG activity. In contrast, bolus feeding increased bradygastria ($p < .05$); the altered EGG pattern returned to baseline value after one hour. Thus nutrition can be supplied to these elderly patients by continuous infusion via PEG, without altering the baseline gastric electrical activity.

Su-Pos72

SINGLE FIBRE CONTRACTILE PROPERTIES OF HUMAN LEVATOR PALPEBRAE SUPERIORIS, ORBICULARIS OCULI AND VASTUS LATERALIS MUSCLES.

((Sian P. Campbell, Gordon S. Lynch, Bartley R. Lynch, David A. Williams)) Muscle and Cell Physiology Laboratory, Dept. of Physiology, University of Melbourne, Parkville, Victoria 3052, Australia.

Extraocular muscle (EOM) exhibits unique differences in its composition from normal limb skeletal muscle. These differences may be an adaptation to the low-load demands placed on the muscle throughout life or specific developmental characteristics. Thus, it was of interest to examine the physiological contractile properties of an EOM, specifically the levator palpebrae superioris (LPS) and compare them to those of two other muscles, orbicularis oculi muscle (OOM) and vastus lateralis muscle (VLM). The OOM is the antagonist muscle to the LPS, thus undergoing similar load demands but is of a different embryological origin. In contrast, VLM is a representative limb skeletal muscle which is exposed to large changing load demands throughout life.

The EOM and OOMs were collected from consenting patients undergoing operations for various eye related disorders. Vastus lateralis samples were obtained from healthy-male volunteers by percutaneous muscle biopsy. Muscle samples were tied to small capillary tubes and stored in chemical skinning solution. Single chemically skinned fibres were attached to a sensitive force transducer and activated in Ca^{2+}- and Sr^{2+}-buffered solutions. Fibre type determination was made on the basis of the fibre's contractile characteristics and PAGE analysis.

Previously described fibre type classification criteria for single skinned fibres were unable to accurately classify all the EOM and OOM data. Thus, a new classification system was adopted to account for those fibres with marked differences in contractile parameters while incorporating previously described fibre types. The LPS and each of the three regions of the OOM displayed a majority of fibres which most closely correlate to an intermediate histochemical fibre type. The VLM displayed a large cross section of fibre types. These data suggest that the LPS and OOM display similar fibre type characteristics, differing considerably from those of the representative limb skeletal muscle.

Supported by NH&MRC (Australia).

Su-Pos73

CANINE TRACHEAL SMOOTH MUSCLE STIFFNESS DURING STRETCH DEPENDS ON MUSCLE LENGTH AT CONTRACTION ONSET.

S.J. Gunst and M.-F. Wu. Dept. Physiol./Biophysics. Indiana Univ. Sch. of Med., Indianapolis, IN 46202-5120

The effect of isometric muscle length and contraction duration on stiffness and force during slow stretch were measured in canine tracheal smooth muscle strips. Muscles were contracted isometrically at L_o, $0.75L_o$, and $0.50L_o$ using 10^{-5} M ACh. After 5 min, contracted muscles were shortened rapidly to 0.2 L_o and stretched slowly back to their initial length at a rate of $0.2L_o$/min. A 25 micron, 40 Hz oscillation was imposed on the muscle during stretch so that stiffness could be determined. During stretch, both muscle force and the stiffness/force ratio (S/F ratio) were greatest in muscles contracted at the shortest length (0.5 L_o), and lowest in muscles contracted at the longest length (L_o). Another group of muscles were contracted isometrically at $0.6L_o$ and stretched slowly to L_o at different time points during the contraction: 30 s, 1, 5, or 10 min. The S/F ratio during stretch increased progressively with the duration of isometric contraction prior to stretch. However, no effect of contraction time on the S/F ratio was observed if muscles were shortened to $0.2L_o$ prior to being stretched, suggesting that the shortening procedure eliminated the effects of contraction time on muscle stiffness. Results are consistent with the possibility that the cytostructure of muscles contracted at different lengths differs, and that cytostructural changes occur during the plateau phase of isometric contraction which increase muscle stiffness.

Supported by HL29289.

Su-Pos74

MUCOSAL MODULATION OF MYOSIN PHOSPHORYLATION AND CONTRACTION IN AIRWAY SMOOTH MUSCLE. ((C.T. Wong and C.-M. Hai)) Dept of Physiology, Brown University, Providence, RI 02912.

We tested the hypothesis that airway mucosa modulates myosin light chain phosphorylation in airway smooth muscle by comparing bovine tracheal smooth muscle having intact mucosal and epithelial layers (SME) with smooth muscle free of attached layers (SM). At L_o, active stresses induced by 110 mM K^+ and 1 uM carbachol in SME were 34% and 42% lower than the corresponding values in SM. Myosin light chain phosphorylation was similarly lower in SME. When SME and SM were activated by different [carbachol] ranging from 10^{-9} to 10^{-4} M, both active stress and myosin phosphorylation were lower in SME at a given [carbachol]. However, when active stress was plotted against myosin phosphorylation for SME and SM, the two relationships were not significantly different. Addition of L-arginine did not significantly affect stress development by SME. When carbachol-induced active stress was measured in the same SME strip before and after removal of mucosa, stress recovery was time-dependent up to 2 hr. When active stress was measured at different muscle lengths ranging from 0.2 to 1.0 L_o, and then normalized by the maximum stress at L_o in carbachol-activated SME and SM, the two relationships were not significantly different. We conclude that airway mucosa attenuates airway smooth muscle contraction by modulating myosin light chain phosphorylation without altering the length-dependence of active stress development.

Su-Pos75

Differences in nucleotide binding by actomyosin (AM) are major determinants of phasic and tonic properties of smooth muscle.((A.Khromov,A.V.Somlyo and A.P.Somlyo)) Department of Molecular Physiology and Biological Physics,UVA, Charlottesville,Va, 22908.

The kinetics of cross-bridge detachment from rigor by MgATP (0.1-2.5 mM) released by laser flash photolysis of NPE-caged ATP were studied in α-toxin permeabilized tonic (rabbit femoral artery-Rf) and phasic (rabbit bladder-Rb) smooth muscles in the absence of Ca^{2+} ions. Endogenous ADP was removed by treatment of the preparation for 20 min with 18 U/ml of apyrase.The photolysis solution contained 200 U/ml of creatine kinase and 20 mM phosphocreatine.The time course of MgATP-induced tension decay was biphasic (consisting of fast and slow component) in both muscles.The initial fast phase (0.2 s) of relaxation from rigor after photolytic liberation of ATP was modelled with a kinetic scheme including the rate of photolytic release of ATP (~116s^{-1}) and irreversible ATP binding to AM followed by rapid cross-bridge detachment [1,2].The experimentally determined dependencies of the rate of the fast component vs [ATP] were clustered between lines plotted for values of k_{+T} =2x10^4-5x10^4 $M^{-1}s^{-1}$ and 2x10^5-5x10^5 $M^{-1}s^{-1}$ for Rf and Rb,respectively.The significantly lower (~10 times) apparent second order rate constant (k_{+T}) of ATP association with AM ,in conjunction with ~5 fold higher affinity of AM for ADP [3] in Rf, in comparison with Rb, are probably major determinants of the slow mechanical properties of tonic smooth muscle [3,4].Supported by NIH grant HL 48807.[1]Y.E.Goldman et al,J.Physiol,(1984)**354**:577-604.[2]A.V.Somlyo et al.J.Gen. Physiol. (1988),**91**:165-192.[3].A.Fuglsang et al.J Muscle Res.and Cell Motil.(1993),**14**:666-673. [4]A.Khromov et al.Biophys.J.(1995 in press).

Su-Pos76

POLYMERIZATION OF MYOSIN IN CONTRACTING RAT ANOCOCCYGEUS MUSCLE. ((Jun-Qing Xu[1], Jean-Marie Gillis[2] and Roger Craig[1])) [1]Dept. of Cell Biology, U. Mass. Medical School, Worcester, MA 01655 and [2]Dept. de Physiologie, Université Catholique de Louvain, Bruxelles, Belgium.

The state of assembly of myosin in vertebrate smooth muscle *in vivo* is controversial. *In vitro* studies on purified smooth muscle myosin show that it is monomeric (10S) under relaxing conditions and filamentous under contraction conditions. Conventional EM and antibody labelling studies suggest that myosin is filamentous in relaxed as well as contracting muscle and that 10S myosin occurs in only trace amounts. However, birefringence, conventional EM and X-ray diffraction evidence suggests that in certain smooth muscles (rat anococcygeus) *in vivo,* while myosin filaments exist in the relaxed state, their number increases on contraction. We have used rapid freezing followed by freeze-substitution, which provides close to *in vivo* preservation of tissue ultrastructure, to observe directly the numbers of filaments in relaxed and contracting anococcygeus. The results have been compared with those from guinea pig taenia coli, in which other techniques have revealed no change in filament number. In the anococcygeus, after allowing for cell shrinkage on contraction, we find evidence for a 24% increase in the number of myosin filaments observed in transverse sections of contracting muscle compared with relaxed muscle. In the taenia coli we find no change. These results are in qualitative agreement with earlier findings. They provide direct evidence for polymerization of myosin in contracting rat anococcygeus. Supported by NIH grant HL47530.

Su-Pos77

SMOOTH MUSCLE MYOSIN LC_{17} ISOFORM mRNA AND PROTEIN LEVELS IN SMOOTH MUSCLE TISSUES AND CELLS. ((A.A. Korwek, D.P. Meer and T.J. Eddinger)) Biology Department, Marquette University, Milwaukee, WI 53233.

This study was designed to examine smooth muscle myosin light chain 17 (LC_{17a} and LC_{17b}) content and regulation in rabbit single smooth muscle cells. cDNA produced via reverse transcription (RT) from single smooth muscle (SM) cells or SM tissue was utilized in the polymerase chain reaction (PCR) using two oligonucleotide primers from the known sequence of mouse LC_{17b} (nucleotide positions 195-214, and 471-452; Halstones and Gunning, Gene Bank, UO4443). These primers span the alternative splice site which generates the difference between the $LC_{17a\&b}$ isoforms. Isoelectric focusing (IEF) urea glycerol gels were used to separate the two protein isoforms and Western blot analysis identified their positions on these gels. Densitometric analyses of the PCR products corresponding to the mRNA of $LC17_{a\&b}$ were compared to the relative protein levels of $LC_{17a\&b}$ in adjacent tissue samples showing a good correlation for the tissues tested (aorta, carotid, bladder). Previous work has shown these methods to be precise and accurate in determining the relative ratio of the SM myosin heavy chain isoforms. This study confirms that the LC_{17} isoforms may also be examined from single SM cells. Mechanical measurements on single cells will allow possible mechanical correlations with these isoforms to be determined.

Su-Pos78

LENGTH-DEPENDENT ACTOMYOSIN ATPase ACTIVITY IN CHEMICALLY SKINNED CANINE AIRWAY SMOOTH MUSCLE ((**Jizhong Wang** and **Newman L. Stephens**)) Department of Physiology, University of Manitoba, Canada R3E 0W3

It has been shown that the sustained level of smooth muscle regulatory myosin light chain (LC_{20}) phosphorylation is dependent on initial muscle length; the shorter smooth muscle length the lower is the LC_{20} phosphorylation level. We previously reported that actomyosin ATPase activity of smooth muscle in isotonic shortening was greater than that in isometric contraction. The lower LC_{20} phosphorylation and greater actomyosin ATPase activity in isotonic shortening led us to further investigate the length effect on ATPase activity in smooth muscle. We, therefore, measured (1) the time courses of actomyosin ATPase activity during isometric contraction at different initial muscle lengths; and (2) the length-ATPase activity in steady state during a prolonged isometric contraction. We found (1) in isometric contractions, chemically skinned smooth muscle preparations with longer initial muscle length, but less than L_o, tended to have higher ATPase activity. However, the difference at all time points were not statistically significant. (2) When the initial muscle length was shorter than L_o, ATPase activity demonstrated a positive linear dependence on initial length, while ATPase activity tended to be negatively proportional to initial length at lengths greater than L_o. We concluded that the lower level of ATPase activity at length shorter than L_o was due to lower LC_{20} phosphorylation and crossbridge cycling rate. However, when muscle initial length was greater than L_o, the total ATP consumption was determined by a balance between increased ATP consumption by myosin light chain kinase and decreased crossbridge cycling rate. Our data suggested that the effect of the latter had a greater impact than the former in determining the magnitude of energy consumption. The linear dependence of ATPase activity at lengths either less or more than L_o, also implied that ATPase activity of smooth muscle was affected by overlap of thin and thick filaments, *i.e.*, by the number of interacting crossbridges. (Supported by the Resp. Hlth. Natl. Ctr. of Excellence, Canada; J.Wang is the recipient of a studentship from the Medical Research Council of Canada).

Su-Pos79

TYROSINE PHOSPHORYLATION OF PAXILLIN IN SKINNED CANINE TRACHEAL SMOOTH MUSCLE. ((D. Mehta, F.M. Pavalko and S.J. Gunst.)) Dept. Physiology and Biophysics, Indiana Univ, Sch. Med., Indianapolis, IN 46202.

Paxillin, a cytoskeletal protein that may be involved in the attachment of actin filaments to focal adhesion sites, has been shown to be heavily phosphorylated on tyrosine residues during embryonic development, integrin mediated cell adhesion and fibroblast transformation. Our laboratory has shown that tyrosine phosphorylation of paxillin increases during muscarinic contraction of canine tracheal smooth muscle (Pavalko et al, Am J Physiol 1995). The purpose of this study was to determine the Ca^{2+} dependence of the tyrosine phosphorylation of paxillin. Tracheal muscle strips were skinned in 1% Triton and then exposed to increasing concentrations of Ca^{2+} (pCa 9 to pCa 4.0). Paxillin was extracted, electrophoresed and transferred to nitrocellulose. Tyrosine phosphorylation was detected by using anti-phosphotyrosine antibody and the paxillin protein band was confirmed using anti-paxillin antibody. Paxillin was phosphorylated on tyrosine residues at pCa 9.0. Paxillin phosphorylation did not increase when the pCa was increased to 4.0. The results indicate that paxillin phosphorylation can occur in Triton-skinned muscles even at pCa 9.0. Under these conditions, increase in pCa did not stimulate additional paxillin phosphorylation.
Supported by PHS HL 29289 and Am. Heart. Assoc. Fellowship to Mehta.

Su-Pos80

TYROSINE PHOSPHORYLATION OF PAXILLIN IN CA-DEPLETED CANINE TRACHEAL SMOOTH MUSCLE STRIPS DURING STIMULATION WITH ACETYLCHOLINE ((Z.L. Wang, F.M. Palvalko and S.J. Gunst)) Dept Physiol/Biophys, Ind U Sch of Med, Indianapolis, IN 46202

The tyrosine phosphorylation of paxillin has been associated with remodelling of the actin cytoskeleton during embryonic development and during fibroblast adhesion to the ECM. Previously, we have shown that the tyrosine phosphorylation of paxillin increases during isometric tracheal smooth muscle contraction induced by acetylcholine (ACh) (Gunst, S.J., Biophys. J. 68:A277, 1995). In this study we investigated the Ca^{2+}-dependence of ACh-induced paxillin phosphorylation. Muscle strips were depleted of $[Ca^{2+}]_i$ by incubating them in Ca^{2+}-free PSS containing 0.1mM EGTA and repeatedly contracting them with ACh until the contractile response was negligible. Control and Ca^{2+}-depleted muscle strips were stimulated with 10^{-4} M ACh and freeze-clamped after 5 min. ACh stimulation was also studied at different $[CaCl_2]$ (0.05 to 0.5mM). In separate experiments, Ca^{2+}-depleted muscle strips were stimulated with ACh 10^{-7} to 10^{-4} M. Muscle proteins were extracted, separated by SDS-PAGE, and transferred to nitrocellulose. Tyrosine phosphorylation of paxillin was assessed using anti-phosphotyrosine and anti-paxillin Ab, and quantified by densitometry. Tyrosine phosphorylation of paxillin after 10^{-4} M ACh was similar in Ca^{2+}-depleted and control muscle strips. $[CaCl_2]$ did not affect the tyrosine phosphorylation of paxillin in response to ACh. However, paxillin phosphorylation of Ca^{2+}-depleted muscle strips increased when the ACh concentration increased. Results suggest the tyrosine phosphorylation of paxillin may occur through Ca^{2+}-independent pathways in canine tracheal smooth muscle.

Supported by HL29289 and American Lung Assoc.

Su-Pos81

PROBING ACTIN-TITIN INTERACTION WITHIN CARDIAC MYOFIBRIL I-BANDS. ((W.A. Linke, R. Wojciechowski and J.C. Rüegg)) Physiology II, Univ. Heidelberg, Im Neuenheimer Feld 326, D-69120 Heidelberg, Germany.

Single myofibrils or small bundles of up to five myofibrils were isolated from both fresh and glycerinated rat ventricle and were suspended between two fine glass needles under an inverted microscope. By using a sensitive force transducer (~5 nN resolution) and a piezoelectric micromotor, we measured the stiffness of relaxed myofibrils (pH 7.1, room temperature) from the force response to small magnitude, 5 to 50 Hz, sinusoidal oscillations. Mechanical measurements were complemented by immunofluorescence microscopy studies to investigate whether in the I-band of cardiac sarcomeres, titin filaments may associate with the thin filament.

Possible sites of titin-actin interaction are the N1-Z-line region, which at physiological sarcomere lengths (SLs) appears to be stiff (Trombitas *et al., Biophys. J.* **68(2):**A64, 1995), and perhaps the N2-line region (Funatsu *et al., J.Cell Biol.* **120**:711, 1993). To test for the first possibility, the N1-line was labelled using a monoclonal titin antibody (T12) and a fluorophore, to visualize the two closely spaced T12 stripes per sarcomere, symmetrical about the Z-line. We then measured the antibody's translational movement upon myofibril stretch. The T12 position remained stationary with stretch to an SL of ~3 μm, but above that SL, the stripes began to move away from the Z-line. However, when actin filaments were selectively removed by application of gelsolin (0.1 mg/ml), the pattern of translational movement upon stretch was quite different from the control situation: the T12 antibody now began to move away from the Z-line at a much shorter SL of ~2.6 μm. Thus, actin removal had apparently increased the N1-Z-line region elasticity. In accordance with these results, we also found that following depolymerization of actin by gelsolin, the stiffness of relaxed cardiac myofibrils (SL ~2.5 μm) decreased significantly, in average by 30%. This stiffness decrease was not due to elimination of weakly bound cross-bridges upon actin extraction, since caldesmon, an inhibitor of these cross-bridges, did not affect the stiffness of control specimens. Therefore, the observed stiffness decrease after actin removal appears to be a result of changes in I-band titin properties. Preliminary results of experiments aimed to test the possibility of N2-line titin-actin interaction have so far failed to show measurable interactions near the N2-line region. We conclude that it is particularly the N1-Z-line titin region that stiffens by associating with actin filaments, thereby further supporting the high resting tension of cardiac sarcomeres *in vivo*.

Su-Pos82

LENGTH TRACES DURING ISOTONIC SHORTENING ARE LINEAR IN SINGLE MYOCYTE-SIZED SKINNED PREPARATIONS. ((K.S. McDonald, M.R. Wolff and R.L. Moss)) Depts of Physiology and Medicine, Univ of Wisconsin, Madison, WI 53706.

Length traces during isotonic shortening of cardiac muscle have been reported to be curvilinear, possibly due to passive elasticity in parallel or in series with active elements or shortening-induced inactivation of cycling cross-bridges. In this study, we assessed isotonic shortening in skinned single myocyte-sized preparations. Rat hearts were mechanically disrupted and single myocyte-sized fragments were tied into stainless steel troughs attached to a force transducer or position motor. Myocytes (n=6) were adjusted to passive sarcomere length of ~2.30 μm, yielding mean (±S.D.) cell length of 167±24 μm and cell width of 22.8±3.2 μm. Maximal tensions (12°C) were 20.4±8.8 kN/mm² at sarcomere length 2.33±0.11 μm. Shortening velocities, measured over a range of loads using a servo system to clamp force, yielded hyperbolic force-velocity relationships (V_{max}=2.28±0.95 ML/sec). Contrary to previous reports, muscle length traces during isotonic shortening were linear in these preparations (Figure). This observation suggests that curvilinear shortening previously reported for cardiac muscle results from extracellular viscoelastic elements. Thus, this single myocyte preparation allows for direct study of mechanisms regulating cross-bridge cycling during loaded shortening.

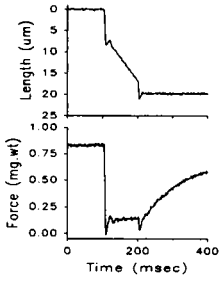

Su-Pos83

KINETICS OF PHOSPHATE RELEASE IN SKINNED CARDIAC MUSCLE STUDIED BY PHOTOLYSIS OF CAGED-PHOSPHATE. ((H. Martin, & R.J. Barsotti)) Bockus Research Institute, The Graduate Hospital, Philadelphia, PA 19146.

To study the involvement of phosphate release in force generation we have examined the transient tension response of Triton-skinned Guinea-pig trabeculae to laser photolysis of caged phosphate (1-(2-nitrophenyl) ethyl phosphate). Incubation of caged-Pi containing solutions with sucrose-sucrose phosphorylase was used to reduce contaminating Pi. In fully activated trabeculae (pCa 4.5, I=200mM, 21° C), photolysis of caged-Pi (5 mM) decreased tension with a time course which exhibited several distinct phases (see Figure). The amplitude of the initial decline in tension scaled with laser energy and was used to estimate [Pi] photolytically produced, based on the steady-state effect of Pi on maximum tension (pCa 4.5). The rate of tension decline varied between 10 and 45 sec^{-1} when photolytically produced [Pi] increased from near zero to 2mM (51 trials on 9 fibers). The relation between the rate of tension decline and [Pi] extrapolated to a value of 16 sec^{-1} at zero Pi and increased with a second order rate constant of 1.4 ± 0.2 X 10^4 M^{-1} sec^{-1}. These results suggest that in cardiac muscle, like rabbit *psoas* muscle, force generation is coupled to phosphate release and that Pi release is too rapid to limit isometric acto-myosin ATPase activity. (Supported by HL 40953 to RJB)

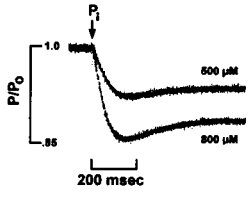

Su-Pos84

THE METHYLAMINE COMPOUND BETAINE AMELIORATES THE DECREASED CALCIUM-SENSITIVITY CAUSED BY OTHOPHOSPHATE (Pi) IN CARDIAC MUSCLE. ((C. Lauder and M.A. Andrews)) Division of Physiology, NY College of Osteopathic Medicine, Old Westbury, NY 11568.

We have previously determined that betaine, a known protein stabilizer increases maximal Ca^{2+}-activated force generation (Fmax) of Triton-skinned cardiac muscle fibers under all conditions tested, without altering Ca^{2+}-sensitivity (*Biophys. J. 66:A302; J. Am. Osteopath. Assoc. 94:760).* Betaine is being used in the present experiments to investigate whether its capacity to stabilize proteins may ameliorate the decrease in Ca^{2+}-sensitivity of the contractile apparatus caused by Pi. Triton-skinned rat cardiac papillary muscle bundles of 150-200 μm diameter were used, and all experiments were conducted at a constant pH of 7.00, at 22° C. Solutions contained (mM): 5 EGTA, 20 imidazole, 2 Mg^{2+}, 5 MgATP, 15 phosphocreatine, appropriate betaine and KH_2PO_4, and 100 u/ml CPK. Total ionic strength was maintained at 200 mM (appropriate $KMeSO_3$ added). Muscle fibers were activated in a step-wise manner through a series of solutions of pCa 8.5 to 4.0 to determine Ca^{2+}-sensitivity of the contractile apparatus. Solutions contained either 0 mM or 20 mM Pi, and either 0 mM or 100 mM betaine. Results indicate that 20 mM Pi decreases the calcium-sensitivity of cardiac muscle, significantly increasing the average Ca50 (the calcium concentration required to reach 50% of Fmax) from 1.9 μM to 3.9 μM, with no alteration of the Hill coefficient. Addition of 100 mM betaine significantly ameliorated the effect of Pi on Ca50, decreasing pCa50 back toward control levels (to Ca50 = 2.6 μM), with no change in the Hill coefficient. Also, as shown previously, 100 mM betaine increased Fmax (here to a mean of 139% of control). In summary, these results provide further evidence for our hypothesis that, at physiological levels, the effects of Pi are, at least in part, related to destabilization of the contractile proteins. Such effects can then be ameliorated by stabilization of the muscle proteins (Support: NYCOMRI).

Su-Pos85

STRUCTURAL AND DYNAMIC RELATIONSHIPS BETWEEN *APO*-AND Ca^{2+}-LOADED CALMODULIN. ((E.L. Mehler & H. Weinstein)), Dept. of Physiol. & Biophys., Mt. Sinai Schl. of Med., CUNY, New York, NY 10029

The solution structure of Ca^{2+}-free calmodulin (CaM) has been determined recently (Zhang, et al., 1995, Nature Str. Biol., **2**, 758-767; Kuboniwa et al., *ibid*, 768-776). The *apo*-structure of CaM clearly exhibits a repositioning of the inner two helices in each domain, thereby blocking and closing the hydrophobic surfaces required for target binding. To study the molecular mechanisms responsible for the structural changes induced by Ca^{2+} binding, molecular dynamics simulations have been carried out to follow the evolution of the *apo*-structure, starting from the *holo*-structure from which the Ca^{2+} were removed. Due to the lack of interaction between the domains, the calculations were carried out on the N-terminal (Tr1) and C-terminal (Tr2) fragments separately. The simulations for Tr1 were started from the crystal structure of fully loaded CaM (Babu, et al., 1988, JMB, **204**, 191-204) but with the Ca^{2+} deleted, and allowed to equilibrate fully (rmsd 1.9Å after 100ps). Subsequently the run was continued to 400ps, but no further change was observed. In the same time the rmsd from the known *apo*-structure diminished from 4.8Å to about 4Å. At 400ps the structure was heated to 500K, the simulation was continued for another 200ps and then various cooling protocols were used to obtain the final *apo*-structure. The optimal structures obtained from these protocols typically showed an rmsd of ≈5Å from the crystal structure, and ≈2.5Å from the *apo*-structure. Superposition of the simulation structure on the *apo*-structure clearly shows that the inner helices had repositioned correctly, to block the hydrophobic binding surface of the domain. The analysis of the dynamic changes due to Ca^{2+} removal indicates the likely functional consequences of the structural changes differentiating the *apo* and *holo* forms.

Su-Pos86

STRUCTURAL DYNAMICS AT A TARGET-BINDING SURFACE OF CALMODULIN ((F. Pitici, E.L. Mehler and H. Weinstein)) Dept. Physiology and Biophysics, Mount Sinai School of Medicine, NY, NY 10029 (Sponsor D. Strahs)

The specific interaction of calmodulin (CaM) with targets is attributed to its ability to form extensive hydrophobic contacts throughout the binding interface. However, in the crystal structure of the uncomplexed CaM [Babu et al., J. Mol. Biol. 204:191, 1988], most residues that are critical for complexation have negligible solvent exposures, and thus apparently low target accessibilities. By means of molecular dynamics (MD) of the uncomplexed Ca^{2+}-loaded C-terminal tryptic fragment of CaM (tr2C), we seek to identify the dynamic mechanisms underlying the observed target-induced conformational changes in the interactive surface of CaM. Simulations are performed using the CHARMM force field with the par19 set of parameters. Atomic fluctuations and correlations between atomic displacements [McCammon, Reports Progr. Phys. 47:1, 1984] are computed: i) from a 1 ns-long MD trajectory of tr2C in a 9 Å water layer; and ii) from the calculated normal modes (NM). To characterize the atomic motions occuring in MD, the atomic correlations are studied for contiguous 100 ps time intervals of the trajectory. The analysis reveals a repetitive pattern of large negative correlations, ranging from -.6 to -.4, that corresponds to the anticorrelated motion of groups of residues: 108-115 (helix F and linker) relative to 142-147 (helix H). By NM analysis it is found that a similar motion corresponds to a low frequency mode of ~3 cm^{-1}. The relationship between this intrinsic mode of motion and the responsivity of tr2C to external perturbations is investigated using sensitivity analysis [Wong et al., J. Phys. Chem. 97:3100, 1993]. Helix F and the linker are found to be the structural elements of tr2C most sensitive to pertubations acting in the plane of the target-binding surface. Their dynamic response to perturbation is in a direction that corresponds to the target-induced conformational changes.

Su-Pos87

CONTRACTILE PROPERTIES OF SKINNED SKELETAL MUSCLE FIBERS CONTAINING SMOOTH MUSCLE MYOSIN REGULATORY LIGHT CHAIN. ((G.M. Diffee, M.L. Greaser and R.L. Moss)) Department of Physiology and Muscle Biology Lab, University of Wisconsin, Madison, WI 53706.

A striking difference between striated muscle and smooth muscle is the role played by the myosin regulatory light chain, which has a key regulatory role in smooth muscle but apparently a modulatory role in striated muscle contraction. In order to determine to what extent the properties of regulation depend on the type of regulatory light chain present we replaced the endogenous regulatory light chain (skRLC) in rabbit skinned psoas fibers with the regulatory light chain from avian smooth muscle (smRLC). We were able to acheive nearly complete exchange of smRLC for skRLC by incubating the fibers in a low ionic strength EDTA solution containing 1 mg/ml smRLC for 30 minutes at 28-30 °C. Following incorporation of smRLC into fibers we found that neither maximal isometric tension (P_o) nor maximal shortening velocity (V_o) were significantly changed from control. However, smRLC incorporation did affect the kinetics of tension development, measured as the rate constant of tension redevelopment (k_r) following mechanical dissociation of cross-bridges by a release and restretch maneuver. We found that k_r at high levels of activation (> 50% of P_o) was reduced following smRLC incorporation while at low activation k_r was increased compared to control, effectively reducing the Ca^{2+} dependence of k_r. These results suggest that Ca^{2+} sensitivity of the rate of transition from non-force to force generating cross-bridge states is determined in part by the properties of the regulatory light chain that is present. In addition, the ability to acheive stoichiometric replacement of skRLC with smRLC in skeletal muscle fibers holds promise for further studies of the roles of RLC and RLC phosphorylation in contraction.

Supported by NIH AR08226 and HL25861

Su-Pos88

MYOSIN REGULATORY LIGHT CHAIN MODULATES THE Ca^{2+} DEPENDENCE OF THE KINETICS OF TENSION DEVELOPMENT IN SKELETAL MUSCLE FIBERS. ((J.R. Patel, G.M. Diffee, and R.L. Moss)) Dept. of Physiology, University of Wisconsin, Madison, WI 53706.

We examined the rate of tension development in bundles of skinned skeletal muscle (rabbit psoas) fibers before and after partial extraction of myosin regulatory light chain (RLC). In control fiber bundles, the rate of tension development was highly dependent on the concentration of activator Ca^{2+} released by UV flash photolysis of DM-nitrophen. There was greater than a two-fold increase in the rate of tension development when the post-flash [Ca^{2+}] was increased from the lowest level tested (generating steady tension that was 42% of maximal tension) to the highest level (generating 97% of maximal tension). This dependence of rate on the level of Ca^{2+} activation was present regardless of whether the fiber bundle was activated from a relaxed or a pre-activated state. However, when 40-70% of the myosin RLC was extracted from the fiber bundles, tension developed at the maximal rate regardless of the concentration of activator Ca^{2+}. Thus, the Ca^{2+} dependence of the rate of tension development was eliminated by partial extraction of myosin RLC. This effect was partially reversed by partial reconstitution of the fibers with RLC. The elimination of the Ca^{2+} dependence of tension development kinetics was specific to the extraction of RLC rather than an artifact of the co-extraction of both RLC and TnC because the rate of tension development was still Ca^{2+} dependent even when nearly 50% of the endogenous TnC was extracted from fiber bundles replete with RLC. These results provide further support for the idea that myosin RLC is a key component in modulating Ca^{2+} sensitive cross-bridge transitions that limit the rate of force development following the photorelease of Ca^{2+} in skeletal muscle fibers.

Supported by NIH AR08226 and HL25861

Su-Pos89

ALTERED MOLECULAR FREE MOBILITY OF PROTEINS DURING ELECTROPHORESIS IN THE PRESENCE OF GLYCEROL: CONDITIONS FOR ENHANCED SEPARATION OF TROPOMYOSIN AND TROPONIN SUBUNITS. ((Erik R. Rennie[1] and Peter J. Reiser[2])) Biophysics Program[1] and Oral Biology[2], The Ohio State University, Columbus, OH 43210.

Most proteins migrate according to their molecular weight (MW) on SDS-PAGE. However, several proteins (e.g., tropomyosin) migrate anomalously in the presence of molar excess SDS. Anomalous protein migration may be due to insufficient binding of SDS or an asymmetric shape of the SDS-protein complex. Glycerol is often added to gels to improve band resolution and we have observed a marked effect of glycerol concentration ([G]) on the relative migration order of myosin heavy chain isoforms. The purpose of this study was to obtain quantitative information on the relative electrophoretic mobility (R_f) of differently-colored standards over a wide MW range at different acrylamide concentrations (%A) and [G]s. We hypothesized that, by increasing [G] in the separating gel, SDS will become displaced and, thus, alter the migration and molecular free mobility (Y_o) of specific proteins, as determined by Ferguson plot analysis extrapolated to 0%A. An alteration in Y_o could reflect an alteration in charge density. We observe a decrease in Y_o with increasing [G] which is consistent with a decrease in charge density and which supports our hypothesis. The R_f values of several myofibrillar proteins, identified with immunoblots, were also determined. Troponin-I and the slow isoform of myosin light chain 1 typically co-migrate on SDS gels. However, under conditions of high [G], these proteins migrate separately. Y_o values of the lower MW proteins were altered to a greater extent, compared to higher MW proteins, with varying [G]. There is a marked retardation of tropomyosin migration from the 35-40 kD region to the region just below α-actinin with high [G] in gels. In summary, inclusion of glycerol in SDS-PAGE alters free electrophoretic mobility of proteins based on shifts in Y_o. This observation is consistent with a change in protein charge density. Therefore, the electrophoretic migration of various myofibrillar proteins (e.g., tropomyosin, troponin-T, troponin-I and myosin light chains) can be manipulated by altering %A and/or [G] to enhance their separation. (Sponsored by NIH grant AR39652).

Su-Pos90

INTERFILAMENT SPACING AND Ca^{2+} SENSITIVITY IN SKINNED RABBIT PSOAS MUSCLE FIBERS. ((Yi-Peng Wang and Franklin Fuchs)) Dept. of Cell Biol. & Physiol., University of Pittsburgh Sch. Med., Pittsburgh, PA 15261.

Moderate osmotic compression of the filament lattice (with 5% Dextran T-500) enhances force generation and Ca^{2+} sensitivity in skinned skeletal and cardiac muscle fibers (Godt and Maughan, 1981; Harrison, et al, 1988). Changes in filament separation with varying sarcomere length may account for length-dependent changes in cardiac Ca^{2+} sensitivity (Wang and Fuchs, 1995). The effect of osmotic compression varies with sarcomere length. With rabbit psoas fibers 5% Dextran has a maximum effect at short sarcomere length (1.8-2.0 μm) and the effect disappears at longer lengths (2.7-2.8 μm). At sarcomere length 2.0 μm 5% Dextran increased maximum force (~ 10%) and Ca^{2+} sensitivity (~ 0.25 pCa units) but both effects were reversed with 10% Dextran. With 15% Dextran there was a marked fall in both force (~ 25%) and Ca^{2+} sensitivity (~ 0.2 pCa units). There appears to be an optimal filament separation at which both force generation and Ca^{2+} sensitivity are greatest. The data are consistent with the hypothesis that changes in Ca^{2+} sensitivity associated with change in myofilament geometry are related to the number of strong-binding cross-bridge interactions. Supported by NIH grant AR10551.

Su-Pos91

EVIDENCE FOR *DYNAMIC* INTERACTION BETWEEN THE TRIGGER SITES IN SKELETAL TnC BY STEADY-STATE FLUORESCENCE & ACRYLAMIDE QUENCHING

((*Venu G. Rao, Hong Su, Joel M. Friedman, Arvind B. Akella, Jag Gulati*)) The Molecular Physiology Laboratory, Albert Einstein Col. of Med., Bronx, NY 10461

To elucidate the Ca-induced trigger mechanism of sTnC, we strategically placed a tryptophan in sites I and II (F26→W for site I variant or F75→W for site II variant). The fluorescence properties were systematically compared for W-mutants with Ca-deficient site I (sTnC-1.26W & sTnC-1.75W) or site II (sTnC-2.26W & sTnC-2.75W). Steady-state fluorescence emissions (relative quantum yields) and acrylamide quenching properties were compared between EGTA and Ca^{2+}. The Ca-effect on quantum yield was blocked for site I & site II mutants. Thus, site I responsiveness is nearly abolished when either site I or site II is Ca-deficient. Similarly, 75W responsiveness was also blocked, with site I or site II Ca-deficiency but the effect of site II Ca-deficiency was much more pronounced. This strongly indicates that the conformational changes in both sites I & II are interdependent and require concomitant Ca-binding in both sites. These effects were further investigated with acrylamide fluorescence quenching of 26W and 75W mutants. Acrylamide quenching results indicated that association of Ca^{2+}-ion greatly enhanced the dynamic (K_{sv}) and static (V) quenching parameters of sTnC.26W & sTnC.75W. These increments in dynamic and static quenching parameters indicate that, with Ca, tryptophan residue in each position becomes highly accessible to solvent. This accessibility was blocked in site I and site II mutants. These results provide the first direct structural evidence that the two trigger sites in skeletal TnC act as a dynamically coupled unit during Ca-activation. The findings also indicate that site II dominates the coupling mechanism. *[Supported by NIAMS/NIH]*

Su-Pos92

SMALL-ANGLE SCATTERING AND MODELING STUDIES OF MYOSIN LIGHT CHAIN KINASE WITH AND WITHOUT Ca^{2+}•CALMODULIN

((J. K. Krueger, Wei Gu, G. A. Olah, N. Bishop, and J. Trewhella)) Los Alamos National Laboratory, Los Alamos, NM 87545. ((Gang Zhi and J. T. Stull)) Department of Physiology, UT Southwestern Medical Center, Dallas TX 75235.

Small-angle X-ray scattering experiments were performed on a truncation mutant of skeletal muscle myosin light chain kinase (MLCKt) with and without bound Ca^{2+}•calmodulin (CaM). MLCKt consists of the catalytic core and the C-terminal regulatory region containing an autoinhibitory sequence and the CaM-binding domain. To aid in interpretation of the scattering data, a molecular model of MLCKt was constructed. The catalytic core was modeled using the known crystal structure of cAMP-dependent protein kinase as a template. The autoinhibitory sequence, located between the catalytic core and the CaM-binding domain, contains specific basic residues previously proposed to bind to the catalytic core. These residues were placed near acidic residues on the surface of the catalytic core which have been proposed to bind to the autoinhibitory sequence in smooth muscle MLCK. The rest of the regulatory region, which includes the CaM-binding domain, was placed along the core similar to the C-terminal sequence of the twitchin kinase crystal structure. Based upon a previous proposal, K579 was allowed to interact with E377 and E421 near the active site. The loop regions were refined using molecular dynamics simulations. The final model was energy minimized using harmonic constraints to the backbone atoms of most secondary structures. A Monte Carlo integration routine was developed to test models of MLCKt complexed with Ca^{2+}•CaM against the scattering data. The models are based on our MLCKt model structure and the NMR structure of CaM complexed with the peptide corresponding to its binding domain from skeletal muscle MLCK. The results of these model calculations, now underway, will provide us with the first insights into the structure of CaM complexed with a functioning protein.

Su-Pos93

ROTATIONAL MOTION OF TROPOMYOSIN ON THE F-ACTIN FILAMENT TITRATED WITH S1.

((I.K. Chandy & R.D. Ludescher)) Department of Food Science, Rutgers-The State University of New Jersey, New Brunswick, NJ 08903-0231.

We have confirmed that the binding of myosin heads (S1) modulates the movement of tropomyosin on the actin filament by using a phosphorescent probe, erythrosin-5-iodoacetamide, covalently attached to the skeletal muscle tropomyosin. Steady state phosphorescence emision anisotropy was used to observe the rotational motion of tropomyosin in a complex with actin and S1 on the micro- to millisecond time scale. The anisotropy of the Tm-actin alone was 0.015. Upon titration with S1 the anisotropy increased to a value of 0.044 at a final S1:actin ratio of 1:1; measurements of the average phosphorescence lifetime demonstrate that the increase is due to a change in the rotational motion of the protein. Binding of S1 thus reduces the rate and/or amplitude of tropomyosin motion on F-actin. These results suggest that Tm can fluctuate between on and off states on F-actin during the lifetime of the probe (260us) and that S1 binding reduces Tm motion by constraining the protein to the on state. (Research supported by the Muscular Dystrophy Association).

Su-Pos94

KINETICS OF THE CALDESMON-MYOSIN INTERACTION.

((B. Leinweber, F.W.M. Lu., and J.M. Chalovich)) East Carolina University School of Medicine; Greenville, N.C. 27858-4354.

The smooth muscle protein, caldesmon binds to both myosin and actin. The role of caldesmon binding to myosin is unclear, but it is possible that caldesmon crosslinks myosin to actin. Two (of many) possibilities for the function of this crosslinking are stabilization of actin-myosin interactions under relaxed conditions and maintenance of force by inhibiting dissociation of actin-myosin as in the latch state. As a guide to determine the possible function of the caldesmon-myosin interaction, we have studied the kinetics of the binding of acrylodan labeled caldesmon to smooth muscle HMM by stopped-flow fluorometry. Acrylodan labeled caldesmon was shown earlier to exhibit a change in fluorescence upon binding to HMM (Mani & Kay (1993) Biochemistry 32:11217-11223). At 15°C and 55 mM ionic strength the observed rate of association was well described by a mono-exponential function. The observed rate increased hyperbolically with increasing [HMM] and reached a maximum value of 285 sec^{-1}. The hyperbolic increase, as well as the observed biexponential dissociation reaction indicated that the reaction consisted of at least two steps, the first step being too fast to observe. The overall equilibrium constant for the reaction was estimated to be 5×10^{-6} M^{-1}. The observed half-life of dissociation was approximately 8 msec. This suggests that the caldesmon-myosin interaction is incapable of maintaining force for prolonged periods of time.

Su-Pos95

RECIPROCAL EFFECTS OF CALDESMON AND MYOSIN S1 ON THE RATE OF BINDING TO ACTIN.

((A. Sen, Y.-d., Chen and J.M. Chalovich)) East Carolina University Medical School, Greenville, N.C. 27858 and NIH, Bethesda, MD 20892.

We had shown earlier that S1 and caldesmon compete for binding to actin. Such competition for binding to a long lattice, such as actin, can occur by several mechanisms including Mosaic Multiple Binding, Pure Competitive Binding and Competitive Binding with Cooperativity. Equilibrium binding experiments have suggested that Mosaic Multiple Binding is the most likely possibility [Chen & Chalovich (1992) Biophys. J. 63: 1063-1072] although the differences between the predicted curves are small. These models could be more clearly distinguished by simultaneously measuring the rate of S1 detachment from actin and the rate of caldesmon binding to actin [Chen & Chalovich (1995) 68: A59]. To make these simultaneous measurements, we have studied the rate of dissociation of fluorescently labeled S1 from actin and the simultaneous rate of association of IANBD labeled caldesmon to actin using stopped-flow fluorescence spectroscopy. IEADANS labeled S1 was particularly well suited for measurement of the detachment of rate of S1 in the presence of caldesmon. Characterization of the fluorescent probes and an analysis of the kinetic data in terms of the possible models for competitive binding of caldesmon and S1 will be presented.

Su-Pos96

LOCALIZATION OF PROTEIN REGIONS INVOLVED IN THE INTERACTION BETWEEN CALPONIN AND MYOSIN.

((P.T. Szymanski and T. Tao)) Muscle Research Group, Boston Biomedical Res. Inst., 20 Staniford St., Boston, MA 02114.

Calponin (CaP) is a thin filament-associated protein that has been suggested to play a role in regulation of smooth muscle contractility. It has previous been shown to interact with actin, tropomyosin and calmodulin. More recently we showed that CaP also interacts with smooth muscle myosin. In the present study we used a combination of co-sedimentation and fluorescence anisotropy assays to localize the regions in myosin and in CaP that are involved in the interaction between these two proteins. Fragments of chicken gizzard myosin and recombinant chicken gizzard αCaP (RαCaP) were generated by proteolytic digestion. We found that intact RαCaP co-sediments with myosin rod, and that RαCaP labeled with the fluorescent label 1,5-IAEDANS interacts with HMM, but not with subfragment-1 of myosin. Our results also show that whereas the 22 kDa N-terminal fragment of RαCaP (residues 7-182) is capable of co-sedimenting with intact smooth muscle myosin, the 13 kDa C-terminal fragment (residues 183-292) is not. These observations indicate that the S2 region of myosin and the region in CaP that contains the actin-binding domain (residues 145-182) are primarily involved in the interaction between calponin and myosin. (Supported by NIH P01-41637 and AHA-13-523-934 to PTS)

Su-Pos97

HEAT TREATMENT MAY AFFECT THE BINDING PROPERTIES OF PURIFIED CALDESMON. ((Shaobin Zhuang, Katsuhide Mabuchi and C.-L. Albert Wang)) Muscle Research Group, Boston Biomedical Research Institute, Boston, MA 02114.

The soluble form of smooth muscle caldesmon (CaD) is extremely sensitive to proteolysis. Because of its apparent heat stability, a widely used purification procedure of CaD involves extensive heat treatment (Bretscher, 1984), during which step most of the proteins in the tissue homogenate, including proteases, precipitate and are thereby easily removed by centrifugation. CaD thus purified exhibits reasonably good capacity to co-sediment with actin, interacts with Ca^{2+}/calmodulin and retains the ability to inhibit actomyosin ATPase activity. Since the secondary structure of CaD undergoes reversible helix-coil transition upon heating, it is generally accepted that thermally unfolded CaD can be re-natured back to its "native" conformation after cooling. On the other hand, heat-purified CaD binds to reconstituted F-actin in a tether-like fashion, whereas length-wise binding is seen in the native thin filament (Mabuchi et al., 1993), suggesting subtle differences exist between the two systems. We have recently been able to isolate, without heat treatment, a batch of full-length, recombinant chicken gizzard CaD over-expressed in insect cells (High 5) using a baculovirus expression system, probably because of the much lower proteolytic activities present in these cells. We found that such unheated CaD binds to F-actin in a length-wise fashion, very much the same as that observed in the native system. This finding may indicate possible existence of an additional, heat-labile, actin-binding site in (the N-terminal region of) CaD, and also suggests that the difference previously observed in the binding modes between the native and the reconstituted systems can be explained without invoking another protein component. Supported by a grant from NIH (P01-AR41637).

Su-Pos98

Ca^{+2} AND Zn^{+2} BINDING PROPERTIES OF RECOMBINANT HUMAN NON-MUSCLE CALCYCLIN. ((J. Kordowska, W. F. Stafford and C.-L. A. Wang)) Muscle Research Group, Boston Biomedical Research Institute, 20 Staniford St., Boston, MA 02114.

Calcyclin (CaCY) is a member of the S100-like, Ca^{2+}-binding protein family. One of its isoforms found in chicken gizzard, named caltropin, was shown to interact with caldesmon (CaD) and decrease its binding to smooth muscle heavy meromyosin. We have PCR-amplified the full-length cDNA of human non-muscle CaCY and subcloned it into an expression vector, pAED4, and purified the overexpressed protein from *E. coli* strain BL21(DE3)pLysS with a yield of 40 mg/l of culture. CaCY, with or without labeling at its single Cys residue, in the presence or absence of divalent metal ions, sedimented as a dimer during ultracentrifugation. Upon binding of Ca^{2+}, CaCY exhibited an about 40% enhancement of the Tyr fluorescence, the apparent binding constant (K_a) being $3.2 \times 10^4\ M^{-1}$. Binding of Zn^{2+} resulted in a greater (75-80%) enhancement in Tyr fluorescence, and the affinity was much higher ($K_a = 6.8 \times 10^6\ M^{-1}$). Saturation occurred at a Zn^{2+}/CaCY ratio of 2:1, suggesting at least two Zn^{2+}-binding sites. In the presence of EGTA/NTA, the Ca^{2+} binding isotherm of CaCY exhibited a midpoint at pCa = 4.4. When CaCY labeled with IANBD was used, the extrinsic fluorescence exhibited a biphasic change. Initially the NBD emission increased with a midpoint (pCa 4.4) identical to that observed for the Tyr fluorescence change; at a higher Ca^{2+} concentration, the NBD fluorescence decreased with a midpoint of pCa = 3.2. This second phase may represent another class of Ca^{2+}-binding site which does not change the Tyr fluorescence. Same experiments performed with added CaD showed a clear left-ward shift of the binding curve, indicating the binding constants for both classes of site are increased. Supported by grants from NIH.

Su-Pos99

CHARACTERIZATION OF CALDESMON PHOSPHORYLATED BY MITOGEN-ACTIVATED PROTEIN KINASE. **((D.B. Foster, T.Y.K. Heinonen, T.S. Tsuruda and A. S. Mak)) Department of Biochemistry, Queen's University, Kingston, Ontario, K7L 3N6.**

Mitogen-Activated Protein (MAP) kinase phosphorylates smooth muscle caldesmon *in vitro* and *in vivo*. However, it has not been established clearly whether MAP kinase phosphorylation of caldesmon might regulate its function. Using intact h-caldesmon (h-CD) and a COOH-terminal fragment of human fibroblast l-caldesmon (CaD39, residues 244-538) expressed in *E. coli*, we have examined the functional consequences of both *in vitro* phosphorylation and Ser-> Asp mutation of MAP kinase consensus sites.

Our data indicate that residues Thr498 and Ser504 of CaD39 (chicken gizzard h-CD residues Thr696 and Ser702) are the predominant phosphorylation sites. Phosphorylation of h-CD and CaD39 reduces their K_a for actin 2 to 3-fold in the presence and absence of tropomyosin. However, phosphorylation of these proteins has little effect, if any, on their ability to inhibit acto-HMM ATPase activity. To simulate phosphorylation at residues Thr498 and Ser504 of CaD39, these residues were mutated to Asp. The mutations had no discernible effect on CaD39-mediated inhibition of acto-HMM ATPase. We conclude that phosphorylation of caldesmon by MAP kinase is unlikely to regulate its function by influencing ATPase activity.

(funded by the Medical Research Council of Canada)

Su-Pos100

IN SITU NEUTRON SCATTERING BY TROPONIN I IN WHOLE TROPONIN ((D. B. Stone[1], P. A. Timmins[2] and R. A. Mendelson[1])) [1]C.V.R.I. and Dept. Biochem. & Biophys., Univ. Calif. San Francisco, CA 94143; [2]Institut Laue-Langevin, 38042 Grenoble Cedex, France.

Small-angle neutron scattering is being used to investigate the R_g of troponin I (TnI) within the reconstituted whole troponin complex. Previous *in situ* studies of TnI by neutron scattering (Olah *et al.*, Biochem. 33: 8233-9, 1994) have utilized the TnC-TnI complex in the presence of 2-3 M urea and Ca^{2+}. Whole Tn, in addition to being a more complete system, is highly soluble without addition of choatropic agents in both the presence and absence of Ca^{2+}. Deuterated (chicken) fast skeletal muscle troponin I, expressed in *E. coli* grown on deuterated algal hydrolysate in D_2O, was purified and combined with recombinant (protonated) fast skeletal muscle troponin C and fast skeletal muscle troponin T. Following renaturation and separation from excess subunits by anion exchange chromatography, the reconstituted whole troponin complex regulated the actin-activated MgATPase of myosin subfragment 1 with a Ca^{2+}-dependence similar to that obtained with native whole rabbit skeletal muscle troponin. The dependence of the activity on the concentration of the reconstituted troponin complex saturated at a troponin:actin ratio close to 1:7, indicating that the reconstituted Tn was fully functional. Scattering from the reconstituted whole troponin complex was carried out on the D11 beamline at ILL using 1 nm wavelength neutrons. Samples were in a 42% D_2O solvent in which protonated troponins C and T are rendered "invisible". Preliminary results indicate that TnI in whole Tn is a highly asymmetric structure whose overall shape is unaltered by Ca^{2+} addition. (Supported by NSF MCB-9404705)

Su-Pos101

THE EFFECTS OF MUTATIONS IN THE N-TERMINAL DOMAIN OF TROPONIN C ON THE CALCIUM SENSITIVITY OF SKINNED RABBIT PSOAS FIBRE SEGMENTS. ((S.A. Virani, L. LeBlanc, T. Borgford, and B.H. Bressler)) Department of Anatomy, University of British Columbia, and Department of Chemistry, Simon Fraser University, Vancouver, B.C., Canada.

In a previous report to the Society, substitutions of the N-cap residue at the C-helix of chicken skeletal troponin C (position 54) were shown, in solution, to decrease the affinity and coopertivity of calcium binding to TnCs low affinity domain (Leblanc L. and Borgford T., *Biophys. J.*, 68, A58 (1995)). In the current study, we have employed a F29W/T54V mutant of chicken TnC to determine the effects of helix destabilization and N-terminal domain attenuation on the calcium sensitivity and cooperativity of skinned single rabbit psoas muscle fiber segments. Force-pCa curves were obtained from single fiber segments following trifluoperazine extraction of TnC and reconstitution with the double TnC mutant at sarcomere lengths of 2.4μm and 3.0μm respectively. Similar data was obtained for the single F29W mutant and for non-substituted control fibers. Our results indicate a significant depression in both calcium sensitivity and cooperativity of fiber segments reconstituted with F29W/T54V at both resting and long sarcomere lengths. No appreciable difference in these parameters was detected between control fibers and those treated with the single F29W mutant. While our earlier findings showed that a similarly destabilizing mutation in the high affinity domain of TnC had no effect on the calcium sensitivity of reconstituted fibers, our current observations suggest that helix stability in the low affinity domain of troponin C plays a critical role in mediating the calcium sensitivity and cooperativity of the contractile apparatus. (Supported by MRC).

Su-Pos102

CHARACTERIZATION OF TROPONIN SUBUNITS FROM FAST AND SLOW MUSCLES OF SALMONID FISH. (D.M. Waddleton, T. Bieger, D.M. Jackman and D.H. Heeley), Dept. Biochemistry, Memorial University, St. John's, NF, Canada A1B 3X9.

The subunits of troponin (Tn) have been examined in the fast and slow swimming muscles of mature salmonid fish. Three fast isoforms of Tn-T (1F, 2F and 3F) and two slow isoforms of Tn-T (1S and 2S) were resolved by SDS PAGE. The Tn-Ts were identified by partial amino acid sequence, reaction with an anti-Tn-T antibody and copurification with whole Tn. Following separation by ion exchange, all Tn-Ts were found to be N-terminally blocked, to contain no cysteine and one tryptophan and to possess molecular masses ranging from 27-30 kDa. Isoforms 1F and 1S had very low solubility in benign solution (pH 7.00). Isoforms 2F and 3F exhibited a stronger interaction than isoform 2S to the matching tropomyosin isoform affinity column. In the case of Tn-I and Tn-C one fast isoform and one slow isoform were resolved by SDS PAGE. In other work, a full length cDNA encoding Tn-I was isolated from Atlantic salmon fry. The sequence (180 amino acids) consists of a conserved region spanning residues 90-180 and a more divergent N-terminal region. We are now investigating whether the sequence corresponds to a mature or immature form of Tn-I.

Su-Pos103

STRUCTURAL ANALYSIS OF SEPARATE TROPOMYOSIN-DEPENDENT AND INDEPENDENT INHIBITORY SEQUENCES IN CALDESMON

((I.D.C. Fraser and S.B.Marston))
NHLI (CM), Imperial College, Dovehouse Street, London SW3 6LY, UK.

Studies were carried out with bacterially expressed C-terminal domain 4 fragments of human caldesmon (CD). H9 (human 726-793 (chicken 669-737)) and H7 (622-767 (566-710)) were both identified as Ca^{2+}-calmodulin regulated inhibitors of the actin-Tm activated ATPase and full inhibition was correlated with one CD bound per 14 actin monomers. A further expressed subfragment H2 (683-767 (626-710)), containing the sequence common to H7 and H9, did not inhibit actin-Tm activation but, conversely, was able to potentiate the actin-Tm activated ATPase rate. Furthermore, addition of H2 reversed the Tm-dependent inhibitory effect of H7, H9 and native CD. These results demonstrate that H2 contains sequence which is essential but not in itself sufficient for CD's Tm-dependent inhibition. Additional sequence at either N-terminus (eg. H7) or C-terminus (eg. H9) is required for inhibitory function. Further subfragments were produced containing the H2 sequence with short extensions of 20 N-terminal amino acids, H14 (663-767 (606-710)), and 12 C-terminal amino acids, H15 (683-779 (626-722)). H14 and H15 were both able to inhibit actin-Tm activated ATPase activity, thus supporting the above hypothesis. In the absence of Tm, H9 had no inhibitory effect whereas H7 and H2, in common with native CD, were inhibitory when added to a high CD:actin ratio. This suggests the presence of a separate Tm-independent inhibitory site in the C-terminus of CD. Further assays carried out with a 5-fold increase in ionic strength demonstrated that the Tm-independent properties of H7 and H2 are salt independent whereas the Tm-dependent effects of H9 and H2 are salt dependent. We propose that domain 4 of CD contains separate Tm/salt-dependent and Tm/salt-independent inhibitory sites. The properties of these two sites can explain most of the anomalous results concerning CD's inhibitory mechanism.

Su-Pos104

MEASUREMENT OF TROPONIN AND CALDESMON BINDING TO TROPOMYOSIN USING A RESONANT MIRROR BIOSENSOR

((Eric J. Hnath, Jennifer S. Olson and George N. Phillips Jr.)) Department of Biochemistry and Cell Biology, Rice University, Houston, TX 77005

A resonant mirror optical biosensor was used to examine the binding of troponin and caldesmon to tropomyosin. Previously published work on caldesmon and troponin binding to tropomyosin simply reported equilibrium binding constants. The use of an optical biosensor allows the measurement of association and dissociation rates in addition to equilibrium binding constants. This biosensor measures optical changes occurring when one biomolecule binds to another that has previously been immobilized to the sensor surface. In most of our experiments tropomyosin was immobilized to the surface. The binding of troponin and TnT subunits to skeletal, smooth, and unacetylated tropomyosins were measured. Binding constants for skeletal and smooth tropomyosin were similar while the affinity of troponin for unacetylated tropomyosin was much weaker. Similar measurements were made of the binding of caldesmon and caldesmon fragments to the three tropomyosins. The binding of caldesmon and fragments was highly dependent on ionic strength. Only whole caldesmon and the C-terminal domain bound with any appreciable specific affinity at 50 mM ionic strength or higher. In contrast to the troponin studies, the affinities were similar for all three tropomyosins. In general the affinities reported here are tighter than those previously determined by florescence studies. We were also able to observe calcium dependent differences in the binding of troponin to tropomyosin. Modulation of caldesmon binding to tropomyosin by calmodulin and calcium was also observed.

This work supported by NIH grants AR32764 and AR41637, the Robert A. Welch Foundation, and the W.M. Keck Foundation.

Su-Pos105

EFFECT OF PREGNANCY AND UTERINE DISTENTION ON CALDESMON (CDM) EXPRESSION IN MYOMETRIAL TISSUES.

((R.A. Word, Sheng-Xi Liu, K.E. Kamm, and V.K. Lin)) Depts. of Ob-Gyn, Physiology, and Urology, Univ of TX Southwestern Medical Ctr, Dallas, TX 75235. (Spon. by R. Victor)

Previously, we reported that the content of CDM is increased 5-fold in myometrium obtained from pregnant (P) women compared with myometrium from nonpregnant (NP) women. In this investigation, we determined the relative contribution of hormonal and mechanical stimuli on pregnancy-induced alterations in expression of high (*h*)- and low (*l*)-molecular weight isoforms of CDM. By immunoblot analysis, *h*CDM was predominant (85-95%) and was increased 4-5-fold in myometrium from P rats compared with ovariectomized rats or ovariectomized rats treated with estradiol, progesterone, or estradiol + progesterone. The content of *l*CDM was similar in all uterine tissues. In myometrium from unilateral P rats, expression of *h*CDM was 1.9-fold greater in the fetal horn compared with the empty horn. Furthermore, the content of *h*CDM increased in the empty horn with experimentally-induced uterine distention. In NP animals treated with progesterone, uterine distention for 10 d resulted in increased expression of *h*CDM (1.8-fold). We used S1-nuclease protection and phosphoimaging analysis to determine the relative amounts of *h*- and *l*-CDM mRNA in myometrial tissues from NP and P women. In both tissues, RNA transcripts for *h*CDM were more abundant than *l*CDM (87 ± 3%, NP; 92.5 ± 1.7%, P). Conversely, >99% of CDM mRNA was *l*CDM in myometrial smooth muscle cells in culture. Whereas the amounts of *l*CDM mRNA were similar in NP and P tissues (85 ± 28 compared with 127 ± 35 cpm/μg total RNA), *h*CDM mRNA levels were increased in myometrium from P women (1766 ± 553 compared with 578 ± 134 cpm/μg RNA). Taken together, we conclude that pregnancy-induced increases in the content of *h*CDM are associated with increased levels of *h*CDM mRNA, and that during pregnancy, expression of *h*CDM in myometrium is regulated by mechano-sensitive transduction pathways.

Su-Pos106

AN ANTIBODY TO SMOOTH MUSCLE TELOKIN RECOGNIZES A PROTEIN AT THE INTERCALATED DISC IN CARDIAC MYOCYTES

((G. C. Scott-Woo, L.G. Anderson, D.L. Severson, M. Ikebe and G.J. Kargacin)) Univ. of Calgary and Case Western Reserve Univ.

Telokin is an 18 kDa acidic protein that is nearly identical in sequence to the C-terminal portion of smooth muscle myosin light chain kinase (MLCK). It is, however, expressed independently, and, in some cases, to a greater extent than MLCK. Analysis of the telokin gene, mRNA and protein structure indicate that telokin is structurally similar to the immunoglobulin domain of cell adhesion molecules and plasma membrane receptors and that its expression is hormonally sensitive. The function of telokin, however, is largely unknown. We have used antibodies specific to the telokin portion of MLCK (LKH3) and the non-telokin portion of MLCK (LKH18) to compare the localization of MLCK and telokin in freshly isolated cardiac myocytes. LKH18 labeling indicated the presence of MLCK in the myocytes but showed no obvious specific localization. The telokin antibody (LKH3) specifically labeled the intercalated disc. LKH3 labeling was intracellular and was more highly localized than that seen with anti-vinculin or anti-A-CAM. The protein labeled with LKH3 was found in isolated intercalated disc preparations and was reduced in myocytes after short term culture (24 - 48 h). These results indicate that telokin or a telokin-related protein functions as a regulatory and/or structural element at the intercalated disc. (supported by HSFA and AHFMR)

Su-Pos107

NEBULIN FRAGMENT ALTERS RIGOR BINDING OF MYOSIN SUBFRAGMENT-1 TO ACTIN.

((D.D. Root, J. Wright and K. Wang)) Dept. of Chemistry and Biochemistry, University of Texas at Austin, TX 78712.

Nebulin is a giant protein of the skeletal muscle sarcomere which coextends with actin along the entire length of a thin filament. Nebulin is composed primarily of 20-30 recurring motifs called superrepeats. The bacterially-expressed human nebulin fragment NA3 corresponds to one superrepeat that has been localized by immuno-electron microscopy to the overlap region between thin and thick filaments. NA3 binds to both actin and S1 with submicromolar dissociation constants. These binding results are supported by zero-length EDC crosslinking of NA3 to actin and to S1. Fluorescence of F-actin labeled with pyrene on C374 is quenched by as much as 80% by rigor myosin subfragment-1 (S1) binding to actin even after subsequent addition of NA3. Since NA3 has little effect on pyrene actin fluorescence in the absence of S1, the data indicate that S1 still interacts with actin after the addition of nebulin fragment. Fluorescence resonance energy transfer efficiencies between a donor fluorophore on C707 of S1 and an acceptor fluorophore on C374 of actin are greatly enhanced by the addition of NA3. Calculations based on these data estimate that the distance between C707 on S1 and C374 on actin decreases from ~45 Å to ~20 Å upon the addition of NA3, thereby revealing a substantial reorientation of S1 in the rigor acto-S1 complex. Crosslinking patterns of rigor acto-S1 by EDC are altered by the addition of nebulin fragments such that the ratio of the 260 kDa to 175/185 kDa bands increases several fold. The morphology of S1 decorated F-actin is also significantly affected by the addition of nebulin fragment. These data, taken together, suggest a substantial reorientation of the myosin head on actin in the presence of nebulin.

Su-Pos108

CROSS-LINKING STUDIES OF THE INTERACTION OF NEBULIN FRAGMENTS, ACTIN AND MYOSIN SUBFRAGMENT 1.

((Oleg Andreev and Kuan Wang)) Dept. of Chemistry and Biochemistry. University of Texas, Austin, TX 78712.

Nebulin is a giant actin binding protein consisting of nearly 200 tandem repeats of 35 residue sequence modules. These modules are thought to be actin binding domains along the length of nebulin. To explore the interaction of F-actin with nebulin, a 7-module human nebulin fragment (NA4), localized in overlap region of thick and thin filaments, was cross-linked to actin with 1-ethyl-3-(3-dimethylaminopropyl)-carbodiimide (EDC). NA4 was mixed with F-actin at different molar ratios and cross-linked with 50 mM EDC for 1 hr at 20°C in 50 mM KCl, 1 mM $CaCl_2$, 0.5 mM $MgCl_2$, 10 mM Tris-HCl, pH 7.5. Cross-linked complexes containing both actin and NA4 were identified by labeling NA4 or actin with fluorescent dyes. At low molar ratio of NA4 to actin, at least 4 cross-linked complexes of NA4 and actin were observed. It is likely that these four complexes resulted from cross-linking of 1 NA4 to 1, 2, 3 and 4 actins. In contrast, cross-linking at a molar excess of NA4 produced only the 1:1 complex of NA4 and actin. A similar reduction of higher complexes of NA4 and actin was observed when myosin subfragment 1 (S1) was added at low molar ratio of NA4 to actin under rigor conditions. Interestingly, NA4 also inhibited the cross-linking of the central domain of S1 (50 KDa) to actin as evidenced by a preferential reduction of 185 and 265 KDa complexes. The production of 175 KDa complex (S1 cross-linked to actin via C-terminal domain) was not affected by NA4. Our data support the notion that NA4 contains one strong and several weak actin binding sites. The binding of NA4 through the weak sites to F-actin is inhibited by S1 or by excess of NA4 fragments.

Su-Pos109

SEQUENCE MOTIFS AND AFFINITY PROFILES OF TANDEM REPEATS AND TERMINAL SH3 OF HUMAN FETAL NEBULIN. ((K. Wang, M. Knipfer, Q.-Q. Huang, A. van Heerden, G. Gutierrez, X. Quian* and H. Stedman*)) Dept. of Chem and Biochem, Univ. of Texas, Austin, TX 78712; Dept. of Anatomy, Univ. of Penn. Philadelphia, PA 19104*

Analysis of deduced protein sequence of ~5500 residues of human fetal skeletal muscle nebulin reveals structural motifs that are informative for the understanding its design principles of this modular, multifunctional protein ruler in the thin filament of skeletal muscle sarcomeres. The bulk of the sequence is constructed of ~150 tandem copies of ~35-residue modules that can be classified into seven types. The majority of these modules form 20 superrepeats, with each superrepeat containing a seven-module set (one of each type in the same order). These superrepeats are further divided into five segments, with each segment containing adjacent, highly homologous superrepeats. A single repeat region of seven nebulin modules and a Src homology domain (SH3) are found at the C-terminus of nebulin. The interaction of actin with fragments of repeating modules or the C-terminal SH3 supports its role as a giant actin-binding cofilament of the composite thin filament. The binding of tropomyosin, troponin and calmodulin to nebulin fragments suggests the possibile formation of a composite regulatory complex per nebulin superrepeat. The modular construction, superrepeat structure and segmental organization of nebulin sequence appear to encode thin filament length, periodicity, insertion and sarcomere proportion in the resting muscle.

Su-Pos110

ROLE OF PROTEIN KINASE A (PKA) AND PROTEIN KINASE C (PKC) PHOSPHORYLATION OF TROPONIN I IN CARDIAC MUSCLE. ((A. Malhotra, A. Nakouzi, J. Bowman and P.M. Buttrick)) Montefiore Medical Center and Albert Einstein College of Medicine, Bronx, N.Y.

Phosphorylation of TnI (inhibitory subunit of troponin) has been postulated to regulate the cardiac contractile apparatus. To evaluate the role of the protein kinase A (PKA) or protein kinase C (PKC) induced phosphorylation mutant TnI constructs were generated by site-directed mutagenesis and bacterially expressed using the pGEX vector system. In mutant 1 (MI) putative PKA target sites were altered (ser 22 / ser 23 to ala) and in mutant 2 (M2) putative PKC target site was altered (thr 143 to ala). Genetically engineered regulatory protein TnI and its mutants were expressed and purified by affinity column chromatography. PKA dependent phosphorylation was ~95% reduced in mutant 1 and unchanged in mutant 2 and PKC dependent phosphorylation was ~90% reduced in mutant 2 relative to the wild type construct. Ca^{+2} Mg^{+2} ATPase of reconstituted actomyosin was not changed by M1 or M2 in the absence of exogenous PKA or PKC. Ca^{+2} sensitivity was diminished when cTnI was phosphorylated by PKC. However, Ca^{2+} sensitivity was minimally lost when M2 was treated with PKC suggesting thr 143 is critically involved in the regulatory function. By recapitulating sarcomeric function *in vitro*, these mutants, in combination with conventional myofibrillar ATPase analyses could provide insight into mechanisms of dysfunction in pathologic states.

Su-Pos111

BINDING OF MYOSIN LIGHT CHAIN KINASE TO MICROFILAMENT BUNDLES IN LIVING SMOOTH MUSCLE CELLS. ((P.-J. Lin, K. Luby-Phelps, and J. T. Stull)) Department of Physiology, UT Southwestern Medical Center, Dallas, TX 75235. (Spon. by A. Zot)

Myosin light chain kinase (MLCK) binds tightly to myofibrils in smooth muscle. Association of MLCK to microfilament bundles in living smooth muscle cells was examined by microinjection of fluorescently-labeled MLCKs. Full-length (amino acids 1-1147) and truncated (amino acids 656-1004) rabbit smooth muscle MLCK was expressed in Sf9 cells. The truncated MLCK contains the catalytic core and calmodulin-binding domain but lacks N- and C- termini that bind to purified actin and myosin, respectively. Purified MLCKs labeled with Cy3 showed Ca^{2+}/calmodulin-dependent activity. The Cy3-MLCKs were co-microinjected with FITC-dextran (10 kDa) into bovine tracheal smooth muscle cells in primary culture. Fluorescence microscopy and ratio imaging to FITC-dextran showed that full-length MLCK was localized mainly to microfilament bundles, while truncated MLCK was diffusely distributed in the cytoplasm, apparently due to the lost of its ability to bind to microfilament bundles. The mobility of full-length MLCK in the resting bovine tracheal smooth muscle cells was determined by fluorescence recovery after photobleaching (FRAP). The full-length MLCK was effectively immobile with a diffusion coefficient (1.7×10^{-10} cm^2/sec) 140-fold less than FITC-dextran (2.35×10^{-8} cm^2/sec). These results indicate that MLCK N- and/or C-termini are necessary for MLCK binding to the contractile apparatus. This experimental approach with additional mutant MLCKs will provide insights into the cellular regulation of MLCK mobility in living cells.

Su-Pos112

GTPγS-INDUCED PHOSPHORYLATION OF THE 130-kDa SUBUNIT OF MYOSIN LIGHT CHAIN PHOSPHATASE IN PERMEABILIZED SMOOTH MUSCLE. ((L. Trinkle-Mulcahy, K. Ichikawa*, S.U. Mooers, S.R. Narayan, M.J. Siegman, D.J. Hartshorne* and T.M. Butler)) Thomas Jefferson Univ., Phila. PA 19107 and * Univ. of Arizona, Tucson, AZ 85721.

We have recently shown that thiophosphorylation of the 130-kDa subunit is associated with a marked decrease in myosin light chain (MyLC) phosphatase activity in permeabilized smooth muscle (JBC 270:18191, 1995). Since GTPγS has been shown to decrease phosphatase activity (Kitazawa *et al.* PNAS 88: 9307, 1991), we determined whether there is an increase in the phosphorylation of this subunit coincident with the GTPγS-induced increase in calcium sensitivity of MyLC phosphorylation (MyLCP) and force. Permeabilized (α-toxin) rabbit portal veins were incubated in pCa 6, ATP (0.5 mM), phosphocreatine (20 mM) and caged γ^{33}P-ATP (0.06 mM, 0.7 mCi/ml). Muscles were treated with GTPγS (300 μM) for 10 sec prior to the photolytic release of ^{33}P-ATP and frozen 45 sec later. Control muscles were treated similarly, except for the omission of GTPγS. Extracted proteins were subjected to SDS PAGE, and those which showed a significant increase in ^{33}P with GTPγS include MyLC and a doublet at about 130 kDa. The larger and smaller proteins in the doublet react with antibodies to MyLC kinase and the 130-kDa subunit of MyLC phosphatase, respectively. The inhibitory effect of GTPγS on MyLC phosphatase activity may be mediated by phosphorylation of the phosphatase. (Supported by HL50586 to TMB; HL20984, HL23615 to DJH)

Su-Pos113

BINDING OF KINASE-RELATED PROTEIN TO UNPHOSPHORYLATED SMOOTH MUSCLE MYOSIN. ((D.L. Silver[1], A.V. Vorotnikov[2], D.M. Watterson[3], V.P. Shirinsky[2], and J.R. Sellers[1])) [1] NHLBI, NIH, Bethesda, MD 20892, [2] Laboratory of Molecular Endocrinology, Inst. Exp. Cardiol., Russian Cardiology Res. Centre, Moscow 121552, Russia, [3] Dept. Mol. Pharmacol., Northwestern Univ., Chicago, IL

Kinase-related protein (KRP), also known as telokin, is an independently expressed protein product derived from a gene within the gene for myosin light chain kinase (MLCK). KRP binds to unphosphorylated smooth muscle myosin filaments and stabilizes them against ATP-depolymerization *in vitro*. By cosedimentation assays KRP bound unphosphorylated myosin with a stoichiometry of 1 mol/mol and an affinity of 7 μM. KRP protected myosin against papain digestion, suggesting it binds at the S1-S2 junction of myosin and may prevent myosin from assuming a folded 10S conformation. Both PK-A and MAP kinase transferred 1 mol phosphate/mol KRP as determined by a shift in isoelectric focussing. We could find no significant effect *in vitro* of KRP phosphorylation by either kinase to myosin binding or stabilization in the presence of ATP. Preliminary results suggest that deletion of 10-20 amino acids in the amino terminus and 7 amino acids in the carboxyl terminus did not prevent bacterially expressed KRP's from binding to myosin.

Su-Pos114

WORTMANNIN INHIBITION OF CONTRACTION AND OXYGEN CONSUMPTION (JO_2) IN INTACT VASCULAR SMOOTH MUSCLE. ((C. J. Wingard, and R. A. Murphy)) Department of Molecular Physiology and Biological Physics, Box 449, University of Virginia Health Sciences Center, Charlottesville, VA 22908.

Our aim was to block MRLC phosphorylation using inhibitors of myosin light chain kinase (MLCK) without affecting intracellular [Ca^{2+}] or other events associated with activation. This allows partitioning of the energetic cost for phosphorylation and activation from total JO_2. The MLCK inhibitor, wortmannin (Wort), was an effective inhibitor of stress, MRLC phosphorylation and JO_2 in K^+-induced contractions in intact swine carotid media rings. In unstimulated rings JO_2 fell during incubation with 10μM Wort. for 60 min from 63.3 (± 5.4) to 49.3 (± 12.9). When K^+-depolarized, JO_2 fell from 115.6 (± 11.1) to 61.3 (± 9.2) nmols O_2 min^{-1} g^{-1}, MRLC phosphorylation fell from 29.3% (± 3.6) to 3.8% (± 0.8), and active stress was reduced from 1.732 (± 0.148) to 0.006 (± 0.034) x 10^5N m^{-2}. Increases in JO_2 seen with the onset of stimulation in Wort.-treated rings was between 9 - 19 nmols O_2 min^{-1} g^{-1}. This may reflect the energy derived from oxidative metabolism necessary for activation processes other than MRLC phosphorylation. This rate was ~12% of the steady-state JO_2 for a K^+-induced contraction. After inhibition of a K^+-contraction additional stimulation with 30μM histamine led to a small transient contraction and transient rise in MRLC phosphorylation to 11.0% (± 1.1), while steady-state JO_2 remained unchanged: K^+109mM + 10μM Wort: 59.9 (± 8.9), K^+109mM + 30μM histamine + 10μM Wort: 57.8 (± 10.0) nmols O_2 min^{-1} g^{-1}. The non-MRLC phosphorylation dependent JO_2 was equivalent to the J_{ATP} of aerobic glycolysis used to support lactate production under similar stimulus conditions: 42.0 (± 8.0) nmols lactate min^{-1} g^{-1} (Wingard *et.al., J. Physiol.*,1995, 481.1: 111-117), supporting the hypothesis that MRLC phosphorylation was the significant fraction of the energtics of activation. Supported by AHA VA Affiliate Grant in Aid to CJW and NIH grant PO1HL19242 to RAM.

Su-Pos115

EFFECT OF PKA DEPENDENT PHOSPHORYLATION OF CARDIAC TROPONIN I ON ITS INTERACTION WITH N- AND C-TERMINAL DOMAINS OF CARDIAC TROPONIN C. ((M. Chandra[1], B-S. Pan[2] and R. J. Solaro[1])) [1]University of Illinois at Chicago, College of Medicine, Chicago, IL 60612. [2]Merck & Co. Inc., West point, PA 19846.

To investigate the effect of protein kinase A(PKA) dependent phosphorylation of the N terminal region of cardiac troponin I(cTnI) on its interaction with cardiac troponin C(cTnC), we have generated a cTnI mutant containing a Cys at position 5(S5C, C81I, C98S) as well as N- and C- terminal domains of cTnC containing residues 1-89 and 90-161, respectively. cTnI was selectively labeled at Cys 5 with the fluorescent probe IAANS. A decrease in fluorescence intensity was associated with the binding of cTnI to cTnC in EGTA, Ca^{2+} or Mg^{2+} suggesting that the interaction between N terminal segment of cTnI(amino acid residues around Cys 5) and cTnC is metal independent. The decrease in fluorescence intensity of the IAANS probe was similar whether or not the C- terminal domain of cTnC was present as an isolated fragment or as part of the intact cTnC. On the other hand, the N- terminal domain of cTnC alone did not induce any changes in fluorescence intensity of the probe under any conditions. Fluorescence intensities of PKA phosphorylated cTnI showed significant differences when compared to unphosphorylated cTnI under all conditions. This is attributed to the phosphorylation induced conformational changes around the N terminal segment of cTnI. These observations are consistent with an antiparallel mode of interaction between cTnI and cTnC. Our study also indicates that PKA dependent phosphorylation affects the interaction of cTnI with cTnC.

CARDIAC CALCIUM HOMEOSTASIS

Su-Pos116

CHRONIC DOXORUBICIN DECREASES CRC mRNA ABUNDANCE EARLIER AND GREATER THAN OTHER MUSCLE-SPECIFIC AND NON-MUSCLE mRNA TRANSCRIPTS. ((D.A. Dodd, M. Summar, R.J. Boucek, Jr., J.B. Atkinson, and S.Fleischer)) Vanderbilt University Medical Center, Nashville, TN 37232

Doxorubicin (dox) causes a cardiomyopathy (CM), and in children may also impair heart growth. Calcium release channel (CRC) abundance correlates with severity of the CM, and CRC mRNA abundance decreases markedly during onset of the CM in a chronic rabbit model. We used this rabbit model to compare relative abundance of other muscle-specific and non-muscle mRNA transcripts during onset of the CM. Three rabbit litters received either dox 1 mg/kg/dose IV twice weekly (T, n=11) for 10, 12, or 14 doses, respectively, or normal saline (C, n=11). Total RNA was isolated either 4 days, 4 weeks, or 10 weeks after completion of therapy, and Northern blots were performed. Transcripts evaluated were for sarcoplasmic reticulum (SR) [CRC, calcium pump protein (CPP)], muscle-specific [myosin (MHC)], and non-muscle [cyclophyllin] proteins. After 10 doses, CRC and other transcripts were increased at all time periods (150% T vs. C). After 12 doses, abundance was lower for CRC (40% T vs. C), than other transcripts (80-100% T vs. C) at 4 days. CRC abundance remained low at 4 weeks (40% T vs. C) and approached normal at 10 weeks (90% T vs. C). Other transcripts gradually rose at 4 weeks (90-110% T vs. C), and 10 weeks (100-140% T vs. C) to levels above control. After 14 doses, while CRC mRNA was not detectable at 4 days and 4 weeks, other transcripts were decreased to a lesser degree (10-30% T vs. C) at 4 days, and (30-60% T vs. C) at 4 weeks. At 10 weeks, other transcripts recovered (90-120% T vs. C), while CRC only partially recovered (60% T vs. C). Morphologically, the microscopy score was consistent with very early CM changes. Thus, 1) prior to onset of CM (10 doses), dox increases abundance of mRNA transcripts, 2) with onset of the CM (12-14 doses), CRC mRNA abundance is depressed earlier and to a greater extent than other transcripts, and 3) this pattern is distinct from that described for stress-induced CM.

Su-Pos117

Ca^{2+} AND NITRIC OXIDE (NO) SIGNALING IN INTACT ENDOTHELIAL CELLS FROM RABBIT AORTIC OR PULMONIC VALVES ((L. Li and C. van Breemen)) Department of Pharmacology & Therapeutics, The University of British Columbia, Vancouver, BC V6T 1Z3, Canada

The concentration of cytoplasmic Ca^{2+} ($[Ca^{2+}]_i$) in intact endothelial cells from rabbit aortic or pulmonic valves was measured by using digital imaging microscopy. Upon stimulation with agonist, $[Ca^{2+}]_i$ increases. Correspondingly, parellel NO measurement using a porphyrinic NO microsensor demonstrated an increase in NO release. The agonist-induced sustained $[Ca^{2+}]_i$ increase was greatly reduced by SK&F 96365, a blocker of receptor-operated channel (ROC) blocker, and Ni^+, a potent Ca^{2+} entry blocker. The inhibitor of endoplasmic reticulum (ER) Ca^{2+}-ATPase also induced an increase in $[Ca^{2+}]_i$, which was not blocked by SK&F 96365, but by Ni^+. Divalent cation influx measured as Mn^{2+} quenching of fura-2 fluorescence was enhanced by agonist, but not by Ca^{2+} ER-ATPase inhibitor. These data suggest an increased Ca^{2+} entry through ROC upon agonist stimulation. Depletion of ER does not signal an increased Ca^{2+} entry. The results can be best explained by a "Superficial Buffer Barrier" (SBB) hypothesis where inhibition of Ca^{2+} reuptake into the ER disrupts the function of ER as a Ca^{2+}entry buffer barrier, thus increasing the effectiveness of Ca^{2+}leak in raising $[Ca^{2+}]_i$.

Su-Pos118

PROTEIN KINASE C-REGULATED ADP-RIBOSYL CYCLASE ACTIVITY IN CARDIAC SARCOPLASMIC RETICULUM ((L. G. Mészáros[1] and G. Varadi[2])) [1]Department of Physiology and Endocrinology, Medical College of Georgia, Augusta, Georgia, 30912 and [2]Institute of Molecular Pharmacology and Biophysics, University of Cincinnati, Cincinnati, OH 45267. (Spon. by Yasuo Mori)

The lymphocyte surface antigen CD38 has been shown to be expressed in a number of mammalian tissues and to catalyze the formation of both ADP-ribose (ADPR) and cyclic ADP-ribose (cADPR) from NAD. We found that a CD38 monoclonal antibody (OKT-10) is capable of (i) recognizing a cardiac sarcoplasmic reticulum (SR)-bound 29 kD protein in Western blots and (ii) inhibiting (by about 50%) the SR-bound ADP-ribosyl cyclase activity assessed by measuring the formation of the fluorescent NGD product cyclic GDP-ribose (cGDPR). The SR ADP-ribosyl cyclase activity was reduced in the presence of ATP, which effect was further potentiated (up to 60% inhibition) by the protein kinase C (PKC) activator phorbol myristate acetate (PMA). Inhibitors of PKC (chelerythrine and staurosporine) prevented the inhibitory action of ATP *plus* PMA. These results indicate that an SR-bound CD38-like protein with PKC-regulated ADP-ribosyl cyclase activity is expressed in heart muscle. For the first time, an intracellular cADPR forming enzyme is identified in a mammalian tissue.

Su-Pos119

CALCIUM-DEPENDENT INACTIVATION IN HUMAN CARDIAC CALCIUM CHANNELS: IS INACTIVATION DEPENDENT UPON INTERNAL CALCIUM? ((William J. Crumb Jr., Theresa P. Roca, John D. Pigott, and Craig W. Clarkson)) Tulane University School of Medicine, New Orleans, LA.

Inactivation of the L-type cardiac calcium current in many cell types consists of voltage-dependent and calcium-dependent components. The calcium-dependent component of inactivation has been attributed to Ca ions acting on a site on the cytoplasmic side of the channel. We studied the time course of inactivation of the calcium current recorded from isolated human atrial myocytes using the whole-cell patch clamp technique. Inactivation was assessed using a two-pulse protocol. Calcium channel inactivation could be described by the sum of two exponentials. Modulation of internal [Ca] produced effects on inactivation kinetics inconsistent with an internal site for Ca modulation of inactivation. For instance, high buffering of internal calcium ([10mM EGTA & 20mM BAPTA]$_i$, [1.8mM Ca]$_o$) was without significant effect on the time course of inactivation (τ_1 37.1 ± 8.7 ms and τ_2=282.7 ± 68.4 ms vs τ_1=31.3 ± 7.9 ms and τ_2=253.3 ± 27.8ms in the absence of BAPTA, n=5-8). When using Na as the charge carrier, increasing [Ca]$_i$ from 11nM to 1μM was without significant effect on time course of current inactivation (τ_1=57.5 ± 7.4 ms τ_2=1059 ± 138.3 ms vs τ_1=78.2 ± 50.9ms τ_2=1082.8 ± 36.6ms, respectively, n=6). In contrast to internal Ca, the addition of Ca to the external solution produced marked effects on the time course of inactivation. With 1.8mM Ba as the charge carrier, the fast and slow components of inactivation development were 140.2 ± 45.7ms and 964.8 ± 212.4 ms, respectively (n=7). The addition of 100 nM to 1 μM [Ca]$_o$ produced up to a five-fold decrease in the time constants of inactivation, with the time constants after addition of 100nM Ca (τ_1=34.1 ± 18.8ms τ_2=266.5 ± 94.06ms) being virtually identical to that observed when Ca (1.8 mM) is the charge carrier. In contrast to previous reports, these results suggest that inactivation of the L-type calcium channel in human heart can be modulated by submicromolar concentrations of Ca acting at a site within the pore or on the external surface of the channel.

Su-Pos120

DYNAMIC CHANGES IN AUTOFLUORESCENCE OF CARDIAC MUSCLE CAUSED BY HALOTHANE REQUIRE CONTINUOUS CORRECTION OF FURA-2 SIGNALS.
((DE Wingrove, MF Patterson, & FJ Julian)) Dept. of Anesthesia, Brigham & Women's Hospital, Boston, MA 02115.

Inhalation anesthetics cause an increase in the autofluorescence of heart muscle that is almost entirely due to a rise in NADH. This fluorescence has an excitation peak at 355nm and emits strongly at 510nm thus overlapping most of the fura-2 fluorescence spectrum. Prior efforts to correct the fura-2 signal for NADH fluorescence have focused on first performing the anesthetic exposure to the muscle in the absence of dye to obtain the autofluorescence signal, and then to the dye-loaded muscle to obtain the combined fura-2 and autofluorescence signal. We have examined this technique in preparations of rat right ventricular trabeculae mounted to a force transducer and using a PTI microfluorimeter. These trabeculae are then loaded with the salt form of fura-2 using a micropipette and iontophoretic apparatus. Observations of trabeculae not loaded with dye indicated that the autofluorecence at 510nm emission can change by 25% or more over the course of the 2-3 hours it takes to perform these experiments despite efforts to keep the sample well oxygenated. With halothane exposure the autofluorescence increases quickly to a peak value and then gradually decreases thereafter. Efforts to circumvent this problem using the alternative dye fura-red have not been successful since fura-red does not load easily into these preparations and has a very low quantum efficiency. We have therefore made use of the fact that NADH has its peak emission at a wavelength of 455nm whereas the fura-2 fluorescence intensity is relatively low at 455nm. Monitoring the fluorescence emission simultaneously at both 510nm and 450nm (while alternately exciting at 345nm and 380nm) allows continuous separation of the NADH signal from the fura-2 signal and thus more accurate fura-2 measurements under conditions of continuously changing autofluorescence. Supported by NIH GM48078.

Su-Pos121

MEASUREMENT OF INTRACELLULAR CALCIUM TRANSIENTS (ICT's) IN RAT TRABECULAE WITH IONTOPHORETICALLY INJECTED FURA-2 DYE.
((MF Patterson & FJ Julian)) Department of Anesthesia, Brigham & Women's Hospital, Boston, MA 02115.

The use of acetoxymethyl esters (AM) of Ca^{2+}-sensitive dyes in cardiac muscle is complicated by loading into subcellular organelles such as mitochondria. We have used a slightly modified version of the technique used by Backx & ter Keurs (Am. J. Physiol. 264: H1098, 1993) to iontophoretically load the pentapotassium salt of Fura-2 into rat cardiac trabeculae. In these experiments we simultaneously measured twitch tension and the ICT in response to various external $[Ca^{2+}]$. The ratio (R) of emission at 510nm in response to excitation at 345nm to that at 380nm was taken as an indication of $[Ca^{2+}]_i$. The sensitivity of the tension to changes in $[Ca^{2+}]_o$ from 0.5mM to 4 mM is consistent with previous reports in the literature. We found that the peak R value increased with increasing $[Ca^{2+}]_o$, in contrast to tension which plateaued or decreased at 4 mM $[Ca^{2+}]_o$. Thus, while the peak of the ICT continued to increase, spontaneous activity in response to calcium overload of the preparation could be responsible for suppressing tension production in response to stimulation.. Interestingly, the declining phase of the ICT is characterized by a "relaxation calcium transient" (RCT) similar to that reported previously for skeletal muscle and which coincides with a clear increase in the rate of relaxation of twitch force. We suggest that the absence of this feature in most reports is due to extra mounting compliance and internal motion. Supported by NIH GM48078

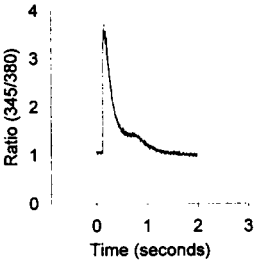

Su-Pos122

ANGIOTENSIN II-SENSITIVE PERIPHERAL CARDIAC NEURONS AFFECT CARDIODYNAMICS VIA AT_1 RECEPTORS.
((M. Horackova and J.A. Armour)) Department of Physiology and Biophysics, Dalhousie University, Halifax, NS B3H 4H7 Canada.

To determine whether angiotensin II-sensitive cardiac neurons exist in intrathoracic extracardiac (stellate and middle cervical) and intrinsic cardiac ganglia and whether such neurons possess AT_1 or AT_2 receptors experiments were performed on anesthetized dogs and also on long-term cultures of adult guinea-pig ventricular cardiomyocytes with or without intrathoracic neurons. In 10 dogs cardiac augmentation was induced when angiotensin II (100 μM) was administered into limited loci within acutely decentralized stellate or middle cervical ganglia which were neurally connected to the heart or into the regional artery (12 dogs). In accord with that, angiotensin II increased the beating frequency of adult cardiomyocytes cocultured with adult extrinsic or intrinsic cardiac neurons but not that of noninnervated cardiomyocytes. Intrinsic cardiac neuronal activity was enhanced by angiotensin II in the presence of timolol *in situ* and *in vitro* even though *in situ* cardiac effects were eliminated. Angiotensin II-induced effects were blocked by losartan (a selective AT_1 receptor antagonist), not PD-123319 (a selective AT_2 receptor antagonist) in both models. It is concluded that 1) angiotensin II-sensitive neurons exist in intrathoracic extracardiac and intrinsic cardiac ganglia; 2) these neurons possess AT_1 receptors; 3) angiotensin II-sensitive neurons act directly to enhance cardiomyocyte function.

Su-Pos123

DISSOCIATION BETWEEN THE POSITIVE INOTROPIC AND ALKALINIZING EFFECTS OF ANGIOTENSIN II (AngII) IN CAT MYOCARDIUM.
((A. Mattiazzi, M. Vila-Petroff, G. Pérez, B. Alvarez, MC. Camilión de Hurtado and H.E. Cingolani)). Centro de Investigaciones Cardiovasculares, La Plata, Argentina.

It has been suggested that the predominant mechanism of the positive inotropic effect of AngII is an increase in Ca^{2+} myofilament sensitivity mediated by intracellular alkalosis due to Na^+/H^+ activation (J Physiol 480, 203-215, 1994). We reexamined the issue in 11 cat papillary muscles contracting isometrically (0.2 Hz, 30°C) loaded with the fluorescent dye BCECF-AM for simultaneous measurement of intracellular pH (pH_i) and contractility. Evidence will be presented showing that the increase in developed tension (DT) elicited by AngII is not related to its alkalinizing effect: 1) In HEPES buffer the positive inotropic effect of AngII (0.5μM) peaked at 9.7 ± 0.8 min (240 ± 57% above control) without significant changes in pH_i (n=4). The increase in pH_i became significant (0.05 ± 0.01 pH units) only after 16 min of exposure to the drug, when the positive inotropic effect of AngII was already fading. After 30 min of exposure to AngII, pH_i increased 0.10 ± 0.03 pH units whereas DT declined to 167 ± 37% above control. 2) In bicarbonate buffer the AngII-induced positive inotropic effect peaked at 8.7 ± 0.7 min (216 ± 49% of control) and declined to 108 ± 32% above control after 30 min, without significant pH_i changes (n=7). Conclusions: 1) In HEPES buffer we detected a temporal dissociation between the positive inotropic and the alkalinizing effect of AngII. 2) In bicarbonate, the positive inotropic effect of AngII was evident even in the absence of detectable pH_i changes. 3) AngII would modify a bicarbonate-dependent mechanism which offsets the alkalinizing action of Na^+/H^+ activation.

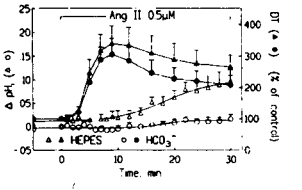

Su-Pos124

TRANSMURAL INTRACELLULAR pH (pH_i) MEASUREMENTS IN ARTERIALLY PERFUSED VENTRICULAR MYOCARDIUM: A NOVEL CONFOCAL FLUORESCENT MICROSCOPY METHOD.
((B.J. Muller-Borer, H. Yang, D.R. Sandiford, J.J. Lemasters, W.E. Cascio)) The University of North Carolina, Chapel Hill, NC 27599. (Spon. by J.D. Cortese)

In order to study the effect of CO_2 production, diffusion and accumulation on physiologic processes in ventricular myocardium, confocal fluorescent microscopy was used to measure transmural pH_i in isolated arterially perfused right ventricular rabbit papillary muscles. Confocal images were acquired from the surface and deeper intramural layers (500 µm) of cylindrical muscles (radius 0.5±0.1 mm, n=3) suspended in a gaseous atmosphere (PCO_2=38 mmHg) and perfused with oxygenated Tyrode's solution (PCO_2=35 mmHg, pH_e=7.4). Cells were loaded with carboxy-SNARF-1 AM (10 µmol/L) and contraction was inhibited with diacetyl monoxime (20 mmol/L). A K2S-BIO epifluorescent microscope with a Leitz SW 50x/1.00NA objective and cooled CCD camera were used to acquire confocal images (acquisition time <30s) using single excitation (546 nm), dual emission (620 nm, 585 nm) techniques. During normal arterial perfusion the intensity of emitted light collected at 620 nm and 585 nm decreased as a function of depth, yet the ratio remained constant confirming the homogeneity of transmural pH_i. Increasing the CO_2 content of the perfusate (PCO_2=213 mmHg, pH_e=6.6) and the surrounding atmosphere (PCO_2=234 mmHg) decreased the intensity ratio (620nm/585nm) uniformly at the surface and intramural layers again confirming the homogeneity of transmural pH_i. We conclude that this fluorescent ratiometric technique offers a valid method to measure transmural pH_i and study the effects of CO_2 diffusion and accumulation in arterially perfused ventricular myocardium.

Su-Pos125

EFFECTS OF ANOXIA AND REOXYGENATION ON CYTOSOLIC $[CA^{2+}]$, $[NA^+]$, AND PH IN GUINEA-PIG VENTRICULAR MYOCYTES.
((L. Ralenkotter, T.J. Delcamp, & R.W. Hadley.)) Dept. of Pharmacology, University of Kentucky College of Medicine, Lexington, KY 40536.

Alterations in ionic homeostasis during anoxia and reoxygenation were investigated in single guinea-pig ventricular myocytes. Cytosolic $[Ca^{2+}]$ was measured with indo-1 AM or fluo-3 AM, $[Na^+]$ was measured with SBFI-AM, and pH was measured with BCECF-AM. Preliminary experiments indicated that photobleaching and intracellular compartmentation were minor with every indicator except fluo-3. The use of fluo-3 was further plagued by artifacts associated with extensive changes in cell shape. BCECF measurements showed that intracellular acidification was an early event in anoxia, with pH reaching a new plateau value approximately at the onset of rigor contracture. This observation is in agreement with the idea that most of the acidosis can be attributed to anaerobic glycolysis, as the production of protons and ATP seems to cease at the same time. SBFI measurements showed that a substantial rise in $[Na^+]$ was also an early event in anoxia, beginning at approximately the same time as acidification. However, $[Na^+]$ continued to rise after rigor began, and showed no signs of approaching a new steady-state level. However, indo-1 measurements demonstrated that changes in cytosolic $[Ca^{2+}]$ was a late and variable event in anoxia. $[Ca^{2+}]$ was most affected by reoxygenation, when cells often demonstrated a marked increase, sometimes reaching micromolar concentrations. This spike in $[Ca^{2+}]$ inevitably preceded hypercontracture.

Su-Pos126

INTRAMITOCHONDRIAL [Ca^{2+}] AND MEMBRANE POTENTIAL: EFFECTS OF ANOXIA. ((T.J. Delcamp & R.W. Hadley.)) Dept. of Pharmacology, University of Kentucky College of Medicine, Lexington, KY 40536.

An ultraviolet-compatible confocal microscope was used to make quantitative measurements of mitochondrial [Ca^{2+}] and membrane potential in single guinea-pig ventricular myocytes. The indicators TMRE and indo-1 AM were used to measure potential and [Ca^{2+}], respectively. Confocal images obtained with TMRE revealed a punctuate pattern of fluorescence, with fluorescence bands stretched along the long axis of the cell, and divided by z-lines. These "bright spots" were identified as mitochondria, because of the insensitivity of the fluorescence to digitonin, while either valinomycin or the protonophore FCCP could quench the fluorescence. It was not possible to resolve all the mitochondria in a plane, as some mitochondria were obviously only partially in the focal plane. However, deliberately focusing on particular mitochondria allowed exceptional resolution, as the total mitochondrial membrane potential was calculated to be -190 mV. It was also demonstrated that indo-1 and confocal microscopy could produce superior measurements of both cytosolic and mitochondrial [Ca^{2+}]. Studies of the effects of anoxia on mitochondria revealed that reoxygenation-induced hypercontracture was often preceded by a rise in mitochondrial [Ca^{2+}], and a collapse of the mitochondrial membrane potential.

Su-Pos127

INTRA-SR FREE Ca IN RAT CARDIAC MICROSOMES ((T.R. Shannon & D.M. Bers)) Loyola Univ. Chicago, Maywood, IL 60153.

We studied the free SR Ca concentration ($[Ca]_{SR}$) in isolated rat cardiac microsomes during Ca transport by the SR Ca pump. Rat ventricular tissue was homogenized with a Polytron in the presence of 25 μM mag-fura-2 tetrapotassium salt. Homogenates were subsequently centrifuged at low speed to sediment unbroken membranes and mitochondria. The SR enriched microsomes were suspended in BAPTA buffer with free [Ca] = 100 nM, pH 7.2. Fluorescence of the entrapped vesicular dye was measured at 340/380 nm excitation wavelengths and 497 nm emission in a cuvette with constant stirring. Oligomycin (4 μM) and 20 μM ruthenium red were also present to inhibit residual mitochondrial uptake and to block SR Ca-release channels. MgATP addition (3 mM) caused a rise in fluorescence which leveled off within 10 min. Raising extravesicular Ca to 230 nM caused little or no additional increase in steady state intravesicular fluorescence. Caffeine (5 mM) with high extravesicular Ca (1 μM) caused a rapid decline in fluorescence due SR Ca efflux through the previously blocked SR Ca-release channels. The dye was subsequently calibrated by equilibration of the vesicular lumen with known free [Ca]'s in the extravesicular solution through the open release channels. The data indicate that the mag-fura is very nearly saturated by the lumenal free [Ca], meaning that the $[Ca_{SR}] \geq 1$ mM when extravesicular [Ca] = 100 nM. This [Ca] is higher than some published $[Ca]_{SR}$ values for intact SR or endoplasmic reticulum (50-600 μM) in a variety of cell types.

Su-Pos128

CYCLIC ADP-RIBOSE DOES NOT MODULATE INTERNAL CALCIUM RELEASE IN RAT VENTRICULAR MYOCYTES. ((Xiaoqing Guo and Peter L. Becker)) Dept. of Physiology, Emory University School of Medicine, Atlanta, GA.

Cyclic ADP-ribose (cADPr) has been demonstrated to modulate Ca^{2+}-induced Ca^{2+}-release (CICR) from internal stores in sea urchin eggs. It has been suggested that cADPr may also play such a role in cardiac tissue as well (Meszaros et al, *Nature* 364:76, 1993), although this hypothesis has been challenged (Sitsapesan et al, *Circ. Res.* 75:596, 1994). The purpose of this study was to examine the ability of cADPr to regulate sarcoplasmic reticulum (SR) calcium release in an intact cardiac cell preparation. Isolated rat ventricular myocytes loaded with the calcium-sensitive dye fluo-3 were studied under voltage clamp using the whole-cell ruptured-patch technique. Cells were also loaded with 1 to 100 μM caged-cADPr (Aarhus et al, *J. Biol. Chem.* 270:7745, 1995) and 0.6 μM calmodulin via the patch pipette. The effect of cADP-ribose on SR calcium release was assessed by comparison of the fluo-3 fluorescence change triggered by voltage-dependent inward calcium current before and after flash photolysis of the caged cADPr. Flash photolysis of caged cADPr did not result directly in SR Ca^{2+} release, nor did it alter the amount of Ca^{2+} released from the SR in response to inward calcium current (n=21). In contrast, under similar conditions, extracellular application of appropriate concentrations of caffeine (1-2.5 mM) produced both effects (n=6). Thus, cADPr does not seem to exert any significant effect on the cardiac SR Ca^{2+}-release during excitation-contraction coupling. In conclusion, it is unlikely that cADPr serves as a physiological modulator or trigger of SR calcium release in rat ventricular myocytes.

Su-Pos129

VOLTAGE- AND CA^{2+}-DEPENDENT INACTIVATION OF L-TYPE CALCIUM CURRENT IN HUMAN ATRIAL CELLS ((H. Sun, N. Leblanc, and S. Nattel)) Montreal Heart Institute, 5000 Bélanger St., Montreal (Quebec) H1T 1C8, Canada

Inactivation of L-type calcium current ($I_{Ca(L)}$) plays a major role in action potential repolarization and intracellular Ca^{2+} homeostasis in cardiac myocytes; however, little is known about mechanisms of $I_{Ca(L)}$ inactivation in human cardiac tissue. This study was designed to address this issue by simultaneously recording $I_{Ca(L)}$ and intracellular Ca^{2+} concentration ($[Ca^{2+}]_i$) with indo-1. The inactivation curve of $I_{Ca(L)}$ in 1 mM external Ca^{2+} exhibited a U-shaped voltage dependence with maximal inactivation (90 ± 4% for 0.5 s prepulse) occurring at +10 mV. Putative voltage-dependent inactivation, studied with Na^+ as the charge carrier, increased as a monotonic function of prepulse amplitude with 50% inactivation occurring at -25 mV. While voltage-dependent inactivation developed very slowly (50% of inactivation at 2.3 s after the onset of depolarization), the Ca^{2+}-dependent component of inactivation reached its maximum within 10 ms and began to decline for longer depolarizations (>1s). Intracellular dialysis with 10 mM EGTA did not affect the voltage-dependent process, but significantly slowed the onset of Ca^{2+}-dependent inactivation and accelerated its decay. The time course of $I_{Ca(L)}$ decay during a voltage step was biexponential and appeared to be closely related to variations in $[Ca^{2+}]_i$, except for the first 50 ms of depolarization where > 50% of $I_{Ca(L)}$ decay occurred before the onset of the Ca^{2+} signal. Suppression of SR Ca^{2+} release by ryanodine increased τ_{fast} (10.7 ± 0.9 ms vs. 43.2 ±3.1 ms) but did not affect τ_{slow}. Increasing external Ca^{2+} from 1 to 5 mM reduced both τ_{fast} and τ_{slow}. These results suggest that: (1) the Ca^{2+}-dependent mechanism plays a determinant role in the inactivation of $I_{Ca(L)}$ in human atrial cells under physiological conditions; (2) SR Ca^{2+} release influences the time course of $I_{Ca(L)}$ decay; and (3) Ca^{2+}-dependent inactivation results from a local accumulation of Ca^{2+} ions and the subsequent binding of Ca^{2+} to an inactivation site near the inner mouth of the Ca^{2+} channel pore.

Su-Pos130

REST EFFECTS ON SPONTANEOUS OSCILLATION FREQUENCY IN RAT CARDIAC MYOCYTES. ((S.J. Cook, J.P. Chamunorwa & S.C. O'Neill)) Veterinary Preclinical Sciences, The University of Liverpool, PO Box 147, Liverpool, L69 3BX, U.K.

In rat ventricular muscle a period of rest leads to an increase in the force of contraction: post-rest potentiation. In cardiac muscle from many other species the opposite is true; post rest decay takes place. Post-rest decay is thought to be due to the fall of intracellular sodium that takes place during the rest. This, acting via Na/Ca exchange reduces the intracellular calcium concentration and depletes the sarcoplasmic reticulum (s.r.). In spite of this, force of contraction in rat muscle remains potentiated over long rest periods, possibly due to the relatively high intracellular sodium concentration ($[Na^+]_i$) in this species. We have found in single myocytes isolated from rat ventricle a rest period often leads to development of spontaneous oscillations of intracellular calcium, indicating overload of the s.r. In 11/13 cells the frequency of these oscillations fell as the duration of the rest increased. To ascertain whether changes in $[Na^+]_i$ are involved, we have measured $[Na^+]_i$ using SBFI. In all cells the reduction in frequency of oscillations takes place during the fall in $[Na^+]_i$. We would suggest the following explanation: as $[Na^+]_i$ falls, the net rate of entry of Ca into the cell is likely to be falling. This would limit the availability of calcium to the s.r. pump requiring more time to fill the s.r. to the point that produces spontaneous release. This effect of rest in rat cells would not require a fall in s.r. content.
Supported by The Wellcome Trust, J.P.C. is a Fellow of The Beit Trust

Su-Pos131

ULTRA-SLOW INACTIVATION OF THE CARDIAC L-TYPE Ca^{2+} CURRENT APPEARS TO BE TEMPERATURE-INDEPENDENT
((Stephen O. McMorn, Simon M. Harrison and Mark R. Boyett))
Department of Physiology, University of Leeds, Leeds LS2 9JT, UK

In rat ventricular myocytes, increasing stimulation rate from 0.5 to 3 Hz for 30 s produces a reversible decrease of the L-type Ca^{2+} current (i_{Ca}) resulting from incomplete recovery from Ca^{2+}- and voltage-dependent inactivation. The whole cell patch clamp technique was used to investigate the effect of temperature on the different forms of inactivation. At 37°C, the first i_{Ca} at 3 Hz was reduced by 9 ± 1 % (mean ± SEM, n=5) compared to control i_{Ca} at 0.5 Hz as a result of incomplete recovery from Ca^{2+}- and fast voltage-dependent forms of inactivation. This was followed by a further progressive 21 ± 2 % decrease of i_{Ca} over the next 30 s resulting from incomplete recovery from ultra-slow voltage-dependent inactivation (Boyett *et al.*, 1994, *Pflügers Archiv*, **428**, 39-50). At 22°C, the first beat at 3 Hz led to a 38 ± 7 % (n=5) decrease of i_{Ca} which was significantly different from that at 37°C ($P<0.05$). This was followed by a further progressive decrease of 26 ± 4 %, which was not significantly different from that at 37°C ($P=0.29$). This shows that the progressive decrease of i_{Ca} (resulting from ultra-slow inactivation) was not significantly affected by temperature. The majority of the effect of temperature on the rate-dependent decrease was therefore due to the initial decrease of i_{Ca} during the first beat at 3 Hz. *Supported by the BHF*

Su-Pos132

INDIRECT REGULATION OF THE CALCIUM CURRENT IN FERRET VENTRICULAR MYOCYTES BY THE 4-AP SENSITIVE TRANSIENT OUTWARD CURRENT. ((Nick C. Janvier & Mark R. Boyett)) Department of Physiology, University of Leeds, Leeds LS2 9JT, U.K.

We have used the action potential clamp technique to investigate the role of the transient outward current (i_{to}) in determining the shape and magnitude of the Ca^{2+} current (i_{Ca}) in ferret ventricular myocytes. After buffering intracellular Ca^{2+} with BAPTA-AM a standard control action potential (panel A, filled circle) was used as the voltage clamp command waveform. Application of 20 μM nifedipine, to block i_{Ca}, caused a shift in the compensation current that flowed during the action potential clamp. This shift in current represents i_{Ca} that flows during the control action potential; a typical example is shown in panel B (filled circle). In 5 cells peak i_{Ca} was -0.76±0.1 nA (mean±SEM). The protocol was repeated using a standard action potential recorded after i_{to} had been blocked by 3 mM 4-AP (panel A, open circle). The resulting i_{Ca} had a peak of -0.37±0.04 nA (n=11) that occurred *later* in the action potential (panel B, open circle). In 6 cells, in which intracellular Ca^{2+} was not buffered, the time to peak of contraction was slowed by 9 % when the "4-AP action potential" was used as the voltage-clamp waveform instead of the control.

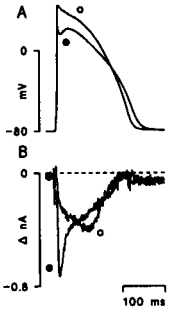

Su-Pos133

L-TYPE Ca^{2+} CURRENTS IN CONTROL AND PHOSPHOLAMBAN-TRANSFECTED C2C12 CELLS ((J. Heiny, H. Masaki, C. Tilgmann*, J. M. Harrer, E. G. Kranias, A. Yatani)) University of Cincinnati, Cincinnati, OH, and *Orion-Farmos Pharmaceuticals, Helsinki, Finland

Ca^{2+} influx through the L-type Ca^{2+} channel (CaCh) regulates cardiac contraction. In addition, phospholamban (PLB) has been shown to be an important regulator of the heart's response to β-adrenergic agonists and ablation of PLB results in significant alterations in Ca^{2+}-homeostasis and contractility (Luo et al., Circ. Res. 75: 401-409, 1994). It is not presently clear whether this effect of PLB occurred solely via its actions at the SR level, or whether other mechanisms at the sarcolemmal CaCh level were involved. To address this, we examined the effects of PLB on CaCh activity. We stably transfected PLB into a murine fast-twitch skeletal muscle cell line (C2C12), which expresses endogenous CaCh activity but has no endogenous PLB. CaCh properties were studied by measuring macroscopic and single CaCh currents using the patch-clamp method. The macroscopic CaCh currents measured from both C2C12 and PLB-transfected (C5/7) cells after 3-4 days in culture are typical skeletal-type CaCh currents (high-threshold and slow activation). Macroscopic CaCh current density increased throughout days 4-8 in both cell lines, and were not significantly different between C2C12 and C5/7 cells. Single CaCh activity was increased by the DHP agonist BayK 8644 in both cell lines, and single-channel conductance and mean open time of CaCh are indistinguishable between the two cell lines. These data show that PLB did not modify the skeletal CaCh and suggest that the effects of PLB on cardiac contractility occur independent from any effect on CaChs. Alternatively, it is also possible that PLB effects are specific for the cardiac isoform of the L-type Ca^{2+} channel.

Su-Pos134

COMPENSATORY MECHANISMS IN PHOSPHOLAMBAN KNOCK-OUT MOUSE HEARTS. ((G. Chu, W. Luo, M.A. Matlib, W.E. Sweet, D.G. Ferguson, G.P. Boivin, J.P. Slack, C.S. Moravec, I.L. Grupp, E.G. Kranias)) University of Cincinnati, Cincinnati, OH 45267. (Spon. by M.A. Matlib)

Phospholamban (PLB) ablation has been shown to be associated with increases in the affinity of the sarcoplasmic reticulum (SR) Ca^{2+}-ATPase for Ca^{2+} and positive inotropy in the mouse heart. To determine whether these alterations are due to the loss of PLB alone or whether they reflect compensatory responses, hearts from PLB knockout (PLB-KO) and wild-type (WT) mice were characterized in parallel. There were no morphological abnormalities observed in the cardiac tissue of KLB-KO mice at the histological and ultrastructural levels. Examination of the gene expression levels of SR Ca^{2+}-ATPase, calsequestrin, Na/Ca exchanger, α-myosin heavy chain, β-myosin heavy chain, α-cardiac actin and α-skeletal actin revealed no significant alterations. However, the ryanodine receptor levels were significantly decreased (25%) upon ablation of PLB, probably in an attempt to regulate the release of Ca^{2+} from SR, which had a higher diastolic Ca-content compared to WT hearts (16.0 ±2.2 *vs* 8.6±1.0 mmol Ca/kg dry wt). Furthermore, the active form of pyruvate dehydrogenase (PDH) was increased (2.2-fold) in PLB-KO hearts and the increased PDH activity was associated with augmentation of myocardial oxygen consumption in PLB-KO compared to WT hearts (228±25 *vs* 140±6 μl O_2/min/g). However, the activity levels of creatine kinase, cytochrome c oxidase and succinate-cytochrome c reductase were similar between PLB-KO and WT hearts. These findings indicate that ablation of PLB is associated with increased diastolic Ca-content and down-regulation of the ryanodine receptor in SR and elevation of energy production by the mitochondria to accommodate for the enhanced myocardial contractility in the PLB-KO hearts.

Su-Pos135

EFFECTS OF β-ADRENERGIC STIMULATION ON TWITCH CONTRACTION OF ISOLATED VENTRICULAR MYOCARDIUM OF PHOSPHOLAMBAN KNOCKOUT MICE. ((Pan, B.-S., Kranias, E., Shen, Y.-T., and Johnson, R.G, Jr.)) Merck Res. Labs. West Point, PA 19486 and Univ. Cincinnati, Cincinnati, OH 45267.

To determine if phospholamban-deficient ventricular myocardium retains responsiveness to β-adrenergic stimulation, the effects of (-) isoproterenol (Iso) on isometric twitch contraction of right ventricle strips from wild type (WT) and phospholamban knockout (KO) mice (129/Srz strain) were characterized. The strips were paced at 20/min (37°C) in the presence of 50 μM lidocaine which prevented Iso-induced arrhythmias. In the absence of Iso, the time to peak tension (TPT) and time to half relaxation ($TR_{1/2}$) in KO ventricle were considerably shorter than in WT ventricle. Addition of 1 μM Iso to WT ventricles shortened TPT and $TR_{1/2}$ and increased the peak force by 35 ± 10% (mean±SEM). However, even with maximal Iso stimulation, TPT and $TR_{1/2}$ in WT ventricles were still significantly longer than in KO ventricles not stimulated by Iso. Addition of 1 μM Iso to KO ventricles induced an increase (41 ± 4%) of the peak force, which was accompanied by small, but significant, decreases of TPT and $TR_{1/2}$. The data support the concept that phospholamban plays a pivotal role in regulating the rate of contraction and relaxation. More importantly, they indicate that the inotropic and lusitropic effects of β-agonists are partially mediated by phospholamban-independent mechanisms, which may include phosphorylation of sarcolemmal Ca^{2+}-channels and TnI.

	WT (n=5)		KO (n=7)	
	basal	+ 1 μM Iso	basal	+ 1 μM Iso
TPT (ms)	56.9±0.7	43.9±0.8*	39.3±0.5	35.0±1.3*
$TR_{1/2}$ (ms)	32.4±1.2	22.9±0.6*	17.4±0.8	16.1±0.6*

{Values are mean +/- SEM. *P < 0.01 vs basal (paired t-test,)} Supported in part by NIH HL26057.

Su-Pos136

EFFECTS OF β-ADRENOCEPTOR ACTIVATION ON SARCOPLASMIC RETICULUM LOAD IN ISOLATED GUINEA-PIG CARDIOMYOCYTES : ASSESSMENT BY RAPID COOLING CONTRACTURE. ((D. Tweedie, S.E. Harding and K.T. MacLeod)) Cardiac Medicine, National Heart & Lung Institute, Imperial College, Dovehouse Street, London, SW3 6LY, U.K.

Ca was released from the sarcoplasmic reticulum (SR) of guinea-pig myocytes by quickly cooling the cell from 22 to 1°C. The maximum amplitude (AMP) of the contracture caused by the rapid cooling (RCC), was used as an index of the amount of releasable SR Ca. To determine SR load at least 3 RCCs were performed on each cell, measurements were made under control conditions and in the presence of isoproterenol (ISO) prior to and during aftercontractions. Data are expressed as mean±SEM, n=9. Compared with control, ISO (0.1-3nM) increased the AMP of both the twitch and the RCC (+23±8% and +24±9%, respectively). Prior to the occurrence of aftercontractions, ISO also reduced the time-to-peak (TTP) contraction (-26±4%) and time-to-50 & 90% relaxation (R50 & R90) of contraction (-22±12% and -30±10%, respectively). During aftercontractions both twitches and RCCs exhibited an elevated AMP when compared with control (34±12% and 25±10%, respectively). TTP contraction was reduced by 40±3%. Due to the occurrence of aftercontractions there was a slowing of the R50 & R90. These studies indicate that in the guinea-pig, β-adrenoceptor activation elevates SR load by 20-25%, however, in cells prior to and during aftercontractions there is no difference in RCC AMP and hence SR load.

Su-Pos137

EFFECTS OF ACTION POTENTIAL DURATION ON CONTRACTION CHARACTERISTICS IN ISOLATED GUINEA-PIG CARDIOMYOCYTES. ((D. Tweedie, C.M.N Terracciano, S.E. Harding and K.T. MacLeod)) Cardiac Medicine, National Heart & Lung Institute, Imperial College, Dovehouse Street, London, SW3 6LY, U.K.

Guinea-pig myocytes were current-clamped (IC), action potential (AP), twitch and Indo-1 flourescence ratio (IF) were measured (0.5Hz, 22°C). Cells were subjected to action potential voltage-clamping (APVc) protocols of different action potential durations (APD). Once twitch characteristics had stabilized with one APD the voltage waveform duration was changed. Data are expressed as mean±S.E.M, n=7-11. Changing from IC to APVc of short duration decreased twitch and IF amplitude (by 76±3% and 45±4%, respectively). When the same cells were changed to an APVc of longer APD the amplitudes of the twitch and IF signal increased in a duration-dependent manner (from -76±3% to 13±17% and -45±4% to 8±9% of control, at 210 and 1200ms APD, respectively). Increasing APD had no significant effects on the time course of the twitch, but had marked effects on the IF signal. Time-to-peak IF signal showed marked prolongation during APVc with longer APD, (from -49±7 to -0.8±8 to 15±14% of control, for 210, 720 & 1200ms APDs, respectively). Time-to-50 & 90% decay (R50 & R90) was prolonged from -37±18% to 7±13% of control R50 and -29±16 to 5±15% of control R90, with APDs of 210 and 1200ms, respectively. The findings of this study suggest APD may have an important role in determining SR load and function in myocytes.

Su-Pos138

RYANODINE BINDING TO A SMALL FRACTION OF AVAILABLE STIES REDUCES CONTRACTILITY IN INTACT HEART ((QiYi Wu and Joseph J. Feher)) Medical College of Virginia, Richmond, VA 23298 (Spon. by G. Ford)

Low concentrations of ryanodine (RY) lock the SR Ca^{2+} release channel in a sub-conducting state. In intact tissue, exposure to RY depletes SR stores due to the persistent opening of the channel. Persistent opening of only a very small fraction of the SR channels could cause depletion of the entire SR store. To determine the sensitivity of the heart to opening of the SR channel, we perfused isolated rat hearts for 5 min with 10, 40, 80 or 160 nM RY followed by 20 min reperfusion without RY. After a transient increase in left ventricular developed pressure (LVDP), LVDP declined progressively to 76±2, 51±2, 33±2, and 29±1 per cent of equilibration pressure, respectively. End-diastolic pressure (EDP) increased from 4±1 mmHg to 13±1 mmHg after 160 nM RY perfusion. In vitro incubation of homogenates with ^{3}H-RY showed that the maximal RY binding could reach 0.7 pmol/mg in 1 M KCl. Perfusion with 80 nM ^{3}H-RY decreased LVDP 32±2 per cent of equilibration pressure and increased EDP to 9±1 mmHg, but only 0.048 ± .004 pmol/mg ^{3}H-RY remained in the heart after reperfusion. Perfusion of the heart with low [Ca^{2+}] (0.2 mM) before, during and after exposure to ^{3}H-RY reduced RY binding to 0.033 ± .004 pmol/mg. The mechanical deficit with low [Ca^{2+}] perfusion suggests that perfusion with low [Ca^{2+}] did not prevent binding of ryanodine to its receptor in the intact heart. These results show that occupancy of only a few of the available RY receptors can nearly maximally reduce the mechanical performance in the intact rat heart.

Su-Pos139

THE 16,16-dimethyl-15-Dehydroprostaglandin B_1, INHIBITS THE ACTIVITY AND THERMAL STABILITY OF THE Ca^{2+}-ATPases FROM CARDIAC SARCOLEMMA AND SARCOPLASMIC RETICULUM. ((Alicia Ortega and Rocio Alvarez)) Depto. de Bioquímica, Facultad de Medicina UNAM, México.

The 16,16-dimethyl-15-dehydro-prostaglandin B_1 (PGB_1)*, a monomer that gave origin to a family of oligomers termed Calciphor, drugs which represent a therapeutic approach to treating tissue injury and protect the cell against the deleterious effects of ischemia, has been found to have by itself an important inhibitory effect on membrane calcium transport enzymes. The Ca^{2+}-ATPases from cardiac sarcolemma and sarcoplasmic reticulum are very important in maintaining low calcium levels in the muscle cells. As the oligomers (PGB_1), can be an effective therapeutic agent for ischemic and reperfution injury such as stroke, myocardial infarct and shock, we undertaking this study to investigate if the monomer of Calciphor has by itself an interaction with these Ca^{2+}-ATPases. We found that the (PGB_1), inhibits both Ca^{2+}-ATPases and decreased their thermal stability by about 5 °C at a 120μM concentration, it possess an mixed inhibition which is competitive with ATP but also has an important not competitive inhibition with calcium. We discus these results in terms of its possible mode of action at the cellular level and the (PGB_1)/ Ca^{2+}-ATPases interaction.

*Source of samples: mono-(PGB_1) was prepared by Dr. George L. Nelson, Dept. of Chemistry, St. Joseph University. PA. and obtained through Dr. Thomas M. Devlin and Dr. Salvador Uribe.

MOLECULAR RECOGNITION AND BINDING I

Su-Pos140

STRUCTURE AND DYNAMICS OF CALMODULIN IN SOLUTION. ((W. Wriggers[1], K. Schulten[1], E. L. Mehler[2], and H. Weinstein[2])) Beckman Institute[1], UIUC, Urbana, IL 61801, Mount Sinai School of Medicine[2], CUNY, New York, NY 10029.

To characterize the dynamic behavior of calmodulin (CaM) in a solvent environment, we are carrying out molecular dynamics (MD) simulations of the Ca^{2+}-loaded structure. The crystal structure of CaM (Babu et al., *JMB* (1988) 204:191) was placed in a solvent sphere of radius 44Å , and 6 Cl^- and 22 Na^+ ions were included to neutralize the system and model a 150mM salt concentration. The total number of atoms is 32,867. After 600ps of simulation, the central tethering helix, which has been shown to undergo large conformational changes upon binding to target proteins, bends slightly over its length. The major structural change is a reorientation of the two Ca^{2+}-binding domains with respect to each other and a movement of helix A (residues 7-19) towards the C-terminal domain. This rearrangement of the structure brings the domains to a more favorable position for target binding, poised to achieve the orientation observed in the CaM-myosin-light-chain-kinase complex (Ikura et al., *Science* (1992) 256:632).

Su-Pos141

CALMODULIN -TARGET RECOGNITION MECHANISMS : DIFFERENTIAL KINETIC ROLES OF CALMODULIN SUBSITES. ((P.M. Bayley, W.A. Findlay and S.R.Martin)) Nat.Inst. Medical Research, Mill Hill, London, NW71AA.

The calcium dependent interaction of calmodulin (CaM) with synthetic peptides derived from M13, the target sequence of skeletal muscle myosin light chain kinase, shows affinities ca. $K_a \sim 10^9\ M^{-1}$ for peptides of n>17 residues. We have investigated the interaction of the N-terminal peptide of M13 (WF10, n=10) with wild-type *Drosophila* calmodulin, and its N- and C-terminal domains, TR1C/TR2C, using CD, and fluorescence. WF10 binds typically with $K_a \sim 10^6\ M^{-1}$ to both WT and TR2C in the presence of Ca. Calcium titration shows that WF10 selectively enhances the affinity of 2 Ca sites, which can be assigned to the calmodulin C-domain. Stopped flow fluorescence shows that the EGTA- or Quin-2-induced dissociation of the complex Ca_4.CaM.WF10 (or Ca_2.TR2C.WF10) proceeds by a slow step where the rate of WF10 dissociation decreases with increasing [WF10], suggesting a relaxation mechanism. For CaM, this involves the reversible dissociation of the peptide from an intermediate kinetic species. The corresponding n=18 peptides behave similarly, consistent with a general mechanism for dissociation of the peptide (P) via an intermediate species Ca_2.CaM.P, where the N-terminal sequence of P interacts with a subsite of calmodulin comprising residues of the C-domain. These results indicate a possible differential kinetic role for the two domains in the interactions of calmodulin with the sk-MLCK target sequence, with the C-domain being of greater importance, reflecting its known higher calcium affinity.

Su-Pos142

ROLE OF BETA-SHEET INTERACTIONS IN CALMODULIN STRUCTURE AND FUNCTION ((J.P. Browne, S.R. Martin and P.M. Bayley)) National Institute for Medical Research, Mill Hill, London, NW7 1AA. (Spon: D.B.Kell)

A highly conserved structural motif in EF-hand Ca binding proteins is a short β-sheet linking two binding sites via residues in the calcium binding loop sequence. The resulting structure frequently forms an independent 2-site domain. This β-sheet appears likely to have a significant role in site-site interactions, co-operativity of Ca binding, structural stability of the domain, and target sequence recognition. Site-directed mutants have been made of the conserved hydrophobic residues in position 8 of each of the four binding sites of *Drosophila* calmodulin. Compared to wild type CaM, which shows substantial Ca-dependent changes in the Tyr-138 fluorescence and near-UV CD properties, the CaM mutant V136G shows perturbation of the properties of Tyr-138, but these are less affected by addition of Ca. The far-UV CD spectrum of apo-V136G is significantly less intense than apo-WT-CaM, and the Ca-dependent increase in far-UV CD is again less for the mutant than for WT-CaM. The addition of a spectroscopically silent 18-residue peptide derived from M13, (the target sequence of sk-MLCK) results in a large increase in α-helix, so that the spectra of the CaM-peptide complexes are closely similar for V136G and WT-CaM. Near-UV CD and fluorescence properties of the V136G-peptide complex are also similar to those of the WT complex. Thus mutation in the β-sheet structure of calmodulin site IV has highly significant secondary and tertiary conformational effects but these can be largely eliminated on binding a suitable target peptide.

Su-Pos143

REAL TIME ANALYSIS OF THE INTERACTION BETWEEN NEURONAL NITRIC OXIDE SYNTHASE (NOS-I) AND CALMODULIN USING SURFACE PLASMON RESONANCE ((M. Zoche[#], M. Bienert[+], M. Beyermann[+] and K.-W. Koch[#])) [#]Institut für Biologische Informationsverarbeitung, Forschungszentrum Jülich, D-52425 Jülich, Germany [+]Forschungsinstitut für Molekulare Pharmakologie, D-10315 Berlin, Germany

Kinetic measurements of the calcium-dependent interaction between Calmodulin (CaM) and a synthetic oligopeptide were performed using a biosensor method based on surface plasmon resonance (SPR). The synthetic oligopeptide represents the CaM - binding domain in the rat brain NOS-I (residues 725-750, $KRRAIGFKKLAEAVKFSAKLMGQAMA\text{-}NH_2$, Bredt et al. (1991) Nature 351, 714). The peptide was immobilized to the biosensor chip by the ligand thiol method via an additional amino-terminal cysteine residue. The SPR measurements for the binding of CaM were performed at 5 μl/min in 10 mM HEPES, pH 7.4, 150 mM NaCl, 3.4 mM EDTA, 5 mM $CaCl_2$ and various concentrations of CaM (6 - 900 nM). We detected a calcium-dependent binding of CaM to the NOS-I-oligopeptide on the sensor chip. The association-rate constant (k_{ass}) and the dissociation rate constant (k_{diss}) were 1.22×10^5 ($\pm4.5\times10^4$) $M^{-1}s^{-1}$ and 6.94×10^{-4} ($\pm1.1\times10^{-5}$) s^{-1}, respectively. The ratio k_{diss}/k_{ass} reveals a dissociation constant (K_D) of 5.7×10^{-9} M. Real time analysis using SPR will be a useful tool for studying nitric oxide synthase function at the molecular level.

Su-Pos144

CALMODULIN DEPENDENT PROTEIN KINASE II STRUCTURE AND INTERACTIONS WITH TA-CALMODULIN. ((K.Török and E.P. Morris)) *Department of Physiological Sciences, University of Newcastle NE2 4HH and Department of Biochemistry, Imperial College, London SW7, UK.*

TA-calmodulin (Török & Trentham, Biochemistry (1994) 33, 12807-20) was used to study the mechanism of calmodulin dependent protein kinase II (CaMKII) by fluorescence stopped-flow in 100 μM $CaCl_2$ at ionic strength 150 mM, pH 7.0 and 21°C. CaMKII was purified from rat forebrains to homogeneity. Fluorescence changes occurred on association of CaMKII with TA-calmodulin in a MgATP-dependent manner: a lag of several 100 ms was followed by a slow fluorescence decrease (~ 0.1 s^{-1}) only in the presence of MgATP. Association of the calmodulin binding peptide αCaMKII(294-309) (Ac-NARRKLKGAILTTMLA-amide) with TA-calmodulin also occurred with a 30% decrease of fluorescence, independent of MgATP. TA-calmodulin is a suitable probe for the detailed studies of CaMKII mechanism. These are in progress.

High quality negatively stained images of purified CaMKII were obtained. Single particle analysis revealed a six-fold symmetric inner core of ~ 12 nm diameter with 12 projections extending to a 25 nm outer diameter suggesting that the main species of oligomeric CaMKII is a dodecamer.

Su-Pos145

HOW DOES THE CALMODULIN:TARGET INTERFACE AFFECT CA2+ AFFINITY OF CALMODULIN COMPLEXES? ((S. Mirzoeva, S. Weigand)) Mol.Pharm.&Biol.Chem., Northwestern University Medical Center, Chicago, IL 60610.
(Spon. by D.M.Watterson)

Calmodulin (CaM) is a eucaryotic intracellular Ca2+ modulated protein. The enhancement of Ca2+ binding affinity of CaM in the presence of CaM binding structures is well documented although the structural basis of this enhancement is not known. We are using a charge perturbation mutagenesis approach in combination with functional and structural analyses to investigate the contribution of specific residues in the CaM:target structure interface to Ca2+ affinity of CaM complexes. We are investigating the Ca2+ binding properties of charge reversal mutant CaMs in the presence or absence of a CaM binding structure such as the model peptide RS20, which is based upon the CaM binding segment of sm/nm MLCK. The structures of CaM and the charge reversal mutant E84K CaM in complex with RS20 are being solved to high resolution by X-ray crystallography. These studies should provide insight into the molecular basis for modulation of CaM affinity for Ca2+ upon the complex formation. Supported in part by NIH grants GM30861 and T32- GM08320.

Su-Pos146

EFFECTS OF MUTATING THE AMINO ACID AT THE -Z POSITION OF A SINGLE Ca^{2+} BINDING SITE MODEL "EF-HAND" PROTEIN. Qi Li, Georgianna Guzman, Todd Miller, Alan Mandveno and James D. Potter. University of Miami School of Medicine, Miami, FL 33101

The cDNA for the wild type Carp parvalbumin B (PVWT) whose crystal structure is known, has been synthesized and expressed in bacteria in our lab. We have chosen parvalbumin as a model since it is a simple Ca^{2+} binding protein, with two Ca^{2+} binding sites, that is very well characterized in terms of its biochemical and biophysical properties. In order to create single Ca^{2+} binding site proteins we have made two mutants that do not bind Ca^{2+} at either the CD (PVEF) or the EF (PVCD) Ca^{2+} binding sites, in which the PHE at position 102 and ASP at positions 51 or 90, respectively, have been replaced with a unique TRP and ALA in order to introduce a fluorescent probe and to inactivate either of the two Ca^{2+} binding sites. Utilizing the flow dialysis method, we demonstrated that both PVCD and PVEF bind only one Ca^{2+} with similar affinity constants relative to the parent mutant, PV_{F102W} (K_{Ca}=3.0 ± 1.5 x 10^7 M^{-1}). The Ca^{2+} affinity of these proteins, determined from the Ca^{2+} dependence of the change in TRP fluorescence are also similar to those obtained with flow dialysis. Using our model Ca^{2+} binding protein. PVEF, which is ideally suited for structural investigations, we prepared two new mutants ($PVEF_{E101D}$ and $PVEF_{E101Q}$) in which the GLU at position 101 was replaced with an ASP or GLN, respectively, to test the effects of mutating the amino acid at the -Z position of this site on its affinity and selectivity for Ca^{2+} and Mg^{2+}. Our data indicate that $PVEF_{E101D}$ has a 100-fold lower binding affinity for Ca^{2+}, but 6-fold higher affinity for Mg^{2+} relative to the model protein (PVEF). The resultant affinity for Ca^{2+} and Mg^{2+} are nearly the same (~ 10^5 M^{-1}). Together with the data for $PVEF_{E101Q}$, the importance of the -Z coordinating carboxylate in determining Ca^{2+}/Mg^{2+} affinity and selectivity will be discussed.

Su-Pos147

PURIFICATION OF CARDIAC CALRETICULIN: EVIDENCE FOR BOUND ATP ((S.E. Cala and L.R. Jones)) Wayne State University School of Medicine, Cardiology Research Division, 421 East Canfield, Detroit, MI 48201 and Indiana University School of Medicine, Krannert Institute of Cardiology, 1111 West 10th Street, Indianapolis, IN 46202

Calreticulin (CRT) is a lumenal ER and SR Ca^{2+}-binding protein that appears to have multiple functions including inhibition of DNA binding by steroid receptors, protein chaperoning, and involvement in hormone-activated Ca^{2+} mobilization. We have purified CRT from canine cardiac SR vesicles using conventional chromatography, producing a single protein band of M_r ~ 60,000. CRT identity was verified by sequencing of the N-terminus and of tryptic fragments. Using affinity-purified rabbit antibodies raised to the intact protein, relative levels of CRT in several membrane samples were determined. CRT co-purified with specific SR protein markers, being highly enriched in free SR vesicles, but was also present in junctional SR. Analysis of purified CRT for endogenous phosphate using a colorimetric method, showed that CRT contained stoichiometric amounts of phosphate. CRT tryptic peptides were separated by reverse-phase chromatography, and phosphate analysis of peptide fractions revealed a single peak of bound phosphate. Sequence analysis of this fraction revealed a single CRT peptide having a sequence that conforms to known ATP-binding sites. These data suggest that purified CRT preparations may contain bound ATP.

Su-Pos148

EFFECTS OF pH AND Ca2+ ON HETERO-DIMER AND HETERO-TETRAMER FORMATION BY CHROMOGRANIN A AND CHROMOGRANIN B. ((Seung Hyun Yoo[‡] and Marc S. Lewis[§])) [‡]NIDCD and [§]NCRR, NIH, Bethesda, MD 20892

The two major proteins of the secretory vesicles of neuroendocrine cells, chromogranin A (CGA) and chromogranin B (CGB), have been shown to undergo pH- and Ca^{2+}-dependent conformational changes and aggregation, and have been suggested to play essential roles during secretory vesicle biogenesis in the trans-Golgi network. CGA has been shown to exist primarily in a tetrameric state at pH 5.5 and primarily in a dimeric state at pH 7.5, and CGB has been shown to exist in a monomeric state at both pH 5.5 and pH 7.5. Using purified CGA and CGB, it recently has been shown that CGA interacts with CGB at pH 5.5. In expanding this investigation, we have studied the temperature dependence of the pH-dependent interaction of CGA and CGB by analytical ultracentrifugation, and found that two molecules of CGA bound to two molecules of CGB at pH 5.5 with ΔG° values of -31.8 to -47.1 kcal/mol in the absence and presence of Ca^{2+} and one molecule of CGA bound to one molecule of CGB at pH 7.5 with ΔG° values of -11.7 to -12.0 kcal/mol in the absence of Ca^{2+}. The magnitude of ΔG° values increased with increasing temperatures at both pH values. However, in the case of pH 5.5 the presence of Ca^{2+} (0.1 mM) decreased the values for ΔH° and ΔS° whereas in the absence of Ca^{2+} the values increased with increasing temperatures, suggesting that the heterotetrameric interaction becomes more ordered in the presence of Ca^{2+}. The heterodimer and heterotetramer formation properties of chromogranins A and B appear to reflect their important roles in the secretory vesicle.

Su-Pos149

CHIRAL RECOGNITION IN DYNAMIC ENERGY TRANSFER PHENOMENA BETWEEN LANTHANIDE SUBSTITUTED COD (III) PARVALBUMIN AND CHIRAL WERNER-TYPE COMPLEXES. ((James P. Bolender, Xiong Sun, and W.DeW. Horrocks, Jr.)) Department of Chemistry, The Pennsylvania State University, University Park, PA. 16802

Lanthanide substitution (Tb^{3+} or Eu^{3+}) in the calcium binding protein Cod (III) Parvalbumin has shown that the CD and EF sites are very similar, and unresolvable via most lanthanide luminescence measurements. The addition of a quencher species allows for resolution of the two sites via site-specific energy transfer phenomena. This study explores the chiral recognition and discrimination phenomena observed in the dynamic energy transfer between the two lanthanide substituted binding sites and chiral Werner-type complexes. The Λ and Δ enantiomers of $Co(en)_3^{3+}$, $Co(chxn)_3^{3+}$, and $Co[(Me_3N)_2sar]^{5+}$ (sar = sarcophagine) are used as chiral probes of dynamic energy transfer. The site specificity of these complexes is on the order of 4-to-1 (k_q^{CD} versus k_q^{EF}) [k_q = quenching rate constant], and the enantioselectivity of the CD binding site is on the order of 2-to-1 (k_q^{Δ}(CD) versus k_q^{Λ}(CD)). These chiral interactions are further explored by Monte Carlo molecular mechanics simulations. This work is supported by N.I.H. grant GM-23599 to W.D.H.

Su-Pos150

EFFECTS OF LEUCINE 89 SUBSTITUTIONS ON STRUCTURE AND REACTIVITY OF SPERM WHALE MYOGLOBIN

(Y. Dou, M. Tenous, M. Siebert, D. Leventhal, J. S. Olson, M. Ikeda-Saito) Dept. of Physiol./Biophys., Case Western Reserve Univ. Sch. of Med., Cleveland, OH 44106-4970; Dept. of Biochem./Cell Biol., Rice Univ., Houston, TX 77251-1892

Effects of electrostatic environments of the proximal heme pocket on the reactivity and structure of myoglobin have been studied by replacing Leu89 by a set of charged and polar residues including Asp, Glu, Lys, Arg, Asn and Gln. The mutations did not cause significant changes in the autoxidation rate, and the CO and O_2 affinities. ^{1}H-NMR of the cyanomet forms of the mutants indicated the slightly altered proximal histidine imidazole orientation which would correspond to the modest changes (less than 2 ~ 3 fold) in the azide and cyanide affinities. The polarity of the proximal heme pocket appears to have much effect on the ligand affinity of myoglobin than that of the distal pocket.

Supported by NIH GM51588, GM35649 and HL47020.

Su-Pos151

THE BASIS OF THE FAILURE OF THE MONOD MODEL IN THE HEMOGLOBIN SYSTEM.

((Jo M. Holt, Yingwen Huang, Alexandra Klinger, Laurent Kiger, Gary K. Ackers and Michael L. Johnson*)) Dept. of Biochemistry & Molecular Biophysics, Washington Univ. School of Medicine, St. Louis, MO 63110 and *Dept. of Pharmacology and Internal Medicine, Univ. of Virginia School of Medicine, Charlottesville, VA 22908 (Sponsored by David P. Cistola)

Cooperative binding and release of oxygen by hemoglobin is based on the ability of the molecule to assume either of two quaternary structures, R or T. In the classic Monod model the proportion between R and T forms is predicted exclusively by the number of ligands bound, regardless of their configuration among the four sites. However, studies of the last decade have shown that cooperativity properties of the intermediates depend strongly on site configuration, according to a symmetry rule (Ackers et al., Science 255, 54-63, 1992; Holt and Ackers, FASEB J. 9, 210-218, 1995). These properties cannot be adequately described by classical theories such as the concerted (MWC) or sequential (KNF) models (Ackers, Biophys. Chem. 37, 371-382, 1990), even though their equations provide good fits to oxygen-binding isotherms. The basis of the failure of these widely-used models as well as the limitations on usage of the Hill coefficient in quantitating cooperativity will be discussed.

Su-Pos152

THREE-DIMENSIONAL SOLUTION STRUCTURE OF APO-S100B DETERMINED BY MULTIDIMENSIONAL NMR SPECTROSCOPY.

((A.C. Drohat[a], J.C. Amburgey[a], F. Abildgaard[b], Mary M. Starich[c], D.J. Weber[a])) [a]Dept. of Biol. Chem., Univ. of MD Sch. of Med., Balt. MD 21201, [b]NMRFAM, Univ. of WI, Madison, WI 53706, [c]HHMI and Dept. of Chem. and Biochem., Univ. of MD Balt. Co., Balt., MD 21228

S100b($\beta\beta$), a 21 KDa homodimer of two non-covalently-joined S100β subunits, is an acidic Ca^{2+}-binding protein found predominantly in the mammalian brain and is thought to be involved in Alzheimers disease and Down's syndrome. The sequence-specific backbone and side chain ^{1}H, ^{13}C, and ^{15}N resonance assignments and secondary structure of S100β has recently been determined (J.C. Amburgey, F. Abildgaard, M.R. Starich, S. Shah, D.C. Hilt, and D.J. Weber., *J. Bio. NMR*, in press). The three-dimensional solution structure of apo-S100b($\beta\beta$) has been determined using data from 2D NOESY, 3D ^{13}C-edited NOESY, 4D ^{15}N,^{13}C- and ^{13}C,^{13}C-edited NOESY, and isotope-filtered NOESY NMR experiments. Each S100β subunit contains two helix-loop-helix (HLH) Ca^{2+}-binding domains known as EF-hands. The HLH comprising helices III and IV is typical, and that of helices I and II is atypical having two extra residues in the Ca^{2+}-binding loop. The HLH domains are brought together by a short two-stranded β-sheet and hydrophobic interactions between helices II and IV. Helix I is positioned nearly parallel to II and IV with hydrophobic interactions to each, whereas helix III is oriented perpendicular to heleces II and IV and on the opposite side of helix I.

Su-Pos153

INVESTIGATION OF PROTEIN-PROTEIN INTERACTIONS OF *trp* SUPER-REPRESSOR MUTANTS.

((Shyam S Vangala*, Kathleen S Martin^{+}, Ross J Reedstrom$^{\#}$, and Catherine A Royer*)) * - School of Pharmacy and $^{\#}$ - Program in Cell and Molecular Biology, The University of Wisconsin, Madison. $^{+}$ - School of Pharmacy, Butler University, Indianapolis, Indiana.

The *trp* repressor (TR) regulates synthesis of tryptophan (L-trp). Wild type (WT) apo TR (TR in absence of L-trp) has been shown to oligomerize to form large aggregates which are destabilized in the presence of L-trp (holo TR). In this study protein-protein interactions for super repressor mutants EK13, EK18 and EK49 TR in the presence and absence of L-trp were studied using fluorescence anisotropy titrations and lifetime measurements. Oligomerization profiles for apo and holo EK18 TR show the same destabilization effect of L-trp as seen for WT TR but higher protein-protein affinities. In addition the holo EK18 TR oligomerization profile indicates specific dimer-dimer association, forming stable tetramers at higher concentrations of TR. This observation indicates that there is change in mode of oligomerization between apo and holo forms of EK18 TR. We postulate that this specific interaction is also true for WT holo TR but occurs at higher concentrations. For EK13 TR the oligomerization profiles of both apo and holo EK13 are similar in the concentration range studied. A similar observation has been previously made for super repressor AV77 TR. Since AV77 TR has been shown to be more folded than WT TR, it was hypothesized that this lack of effect of L-trp indicates that both apo and holo AV77 TR oligomerize in a manner similar to holo WT TR. This may also be true for EK13 TR.

The above studies indicate that protein-protein interactions play an important role in the regulation of L-trp synthesis. Any change in protein-protein interactions might effect the other equilibrium steps not only due to changes in concentration of available TR but also by affecting the interaction of TR with L-trp and operator DNA.

Su-Pos154

MAPPING PEPTIDE-PROTEIN INTERACTIONS USING SITE DIRECTED SPIN-LABELING: THE BINDING OF PROTEIN KINASE C SUBSTRATES TO CALMODULIN.

((Z. Qin, S. L. Wertz, and D. S. Cafiso)). Department of Chemistry and Biophysics Program, University of Virginia, Charlottesville, VA 22901.

Neuromodulin (NM) and the myristoylated alanine rich C-kinase substrate (MARCKS) are proteins that may act as PKC-regulated Calmodulin (CaM) buffers in the nervous system. However, there is evidence that these proteins interact quite differently with CaM. To study the binding of these proteins to CaM, a series of spin-labeled peptides based on the PKC and CaM binding domains of MARCKS and NM were synthesized and derivatized with proxyl nitroxides. EPR spectroscopy was then to investigate the CaM bound structure of the 25 residue MARCKS peptide and the 17 residue NM derived peptide to CaM. The EPR spectra these peptides exhibit dramatic changes when they are bound to CaM, particularly when residues in the central portion of the peptide are labeled. Power saturation EPR spectroscopy shows that an 18 residue stretch of the MARCKS peptide is completely buried within the CaM binding pocket. This data is consistent with a helical configuration for this segment of MARCKS when bound to CaM and is consistent with the crystal and NMR structures of myosin light chain kinase (MLCK)-CaM complexes. In contrast, the NM derived peptide shows a binding pattern which is quite different than the binding motif for MLCK. This peptide is also helical when bound to CaM, but it does not reside in the binding pocket normally occupied by high-affinity CaM substrates.

Su-Pos155

SEQUENCE-SPECIFIC ASSIGNMENTS AND SECONDARY STRUCTURE DETERMINATION OF A TOXIN FROM *PANDINUS IMPERATOR* (PiTX-Kα) USING NMR SPECTROSCOPY.

((T. Tenenholz†, R.S. Rogowski*, J.C. Amburgey†, J.C. Collins, T.A. Gustafson*, M.P. Blaustein*, and D.J. Weber†)) Depts. of Biological Chemistry† and Physiology*, Univ. of MD Sch. of Med., Balto., MD 21201. (Spon. by M.E. Kirtley).

PiTX-Kα, a 35 residue peptide, is a member of the Charybdotoxin (CTX) family of scorpion toxins, which can be used to characterize potassium ion channels. It irreversibly blocks the rapidly inactivating (A-type) potassium channel, but does not block the large conductance Ca(II)-dependant (maxi-K) or delayed rectifier potassium channels. In order to understand the specificity of PiTX-Kα, structural studies were performed using 2-dimensional NMR spectroscopy. To this end, a PiTX-Kα fusion protein was prepared in *E.Coli* containing an overexpression plasmid under the control of a T7 promoter. Milligram quantities of fully functional PiTX-Kα were purified (>99%) after proteolytic cleavage of the fusion protein with enterokinase. Two-dimensional NOESY, DQF-COSY, TOCSY, and ROESY NMR experiments were then used to determine the sequence-specific backbone and sidechain proton assignments and secondary structure of PiTX-Kα. These studies showed that PiTX-Kα has an α-helix (residues 8-19) and two β-strands (βI: 22-25; βII: 29-33) connected with a type I turn to form a small antiparallel β-sheet, similar to other members of the CTX family. The tertiary structure of PiTX-Kα will also be discussed.

Su-Pos156

3-D RECONSTRUCTION OF THE CLP-AP PROTEASE FROM *E.coli*.((E. Kocsis*, M. Kessel*, M. Maurizi+, B.L. Trus#*and A.C. Steven*)) LSBR-NIAMS*, LCB-NCI+, CBEL-DCRT#, NIH, Bethesda, MD 20892 (Spon. by H. Pant)

ClpAP is an energy-dependent multi-component protease of *E. coli*. Its proteolytic component, ClpP, has 14 21-kDa subunits arranged in two seven-fold rings, and its ATP-hydrolyzing component, ClpA, is a two-tiered hexameric ring of 84-kDa subunits. In proteolytically active complexes, either one or two ClpA hexamers are axially stacked with a single ClpP 14-mer, with a consequent mismatch between their respective symmetries (1). To explore their three-dimensional structure in greater detail, we have reconstructed density maps combining end-view projections of ClpP and ClpA with side-view projections of the complex. The reconstructions were carried out using a simple backprojection algorithm (2), and exploited the respective rotational symmetries of ClpP and ClpA. We also performed a similar analysis with a mutant form of ClpP in which the essential catalytic residue, Ser_{111} is replaced by Ala. The reconstruction reveals a cavity ~37Å in diameter in the center of ClpP. This cavity is occluded in ClpP-Ser-Al, which is otherwise indistinguishable from wild-type ClpP. We infer that cleavage of the propeptides, and probably also proteolysis of other substrates, takes place in this chamber. The reconstructions also indicate that the axial channels which are suspected to exist at the poles of the ClpP heptamers to allow entry of substrates into this chamber must be very narrow, as in the 20S proteasome [3].The ClpA reconstruction shows structural distinctions between the two tiers, thus providing supporting evidence for the inference that they represent separate domains, each with an ATP binding site [1].

1. M. Kessel et al, J. Mol. Biol. **250**:587, 1995
2. M. Radermacher, in: Electron Tomography, ed. J. Frank. Plenum Press, pp:97-100, 1992
3. J. Lowe et al., Science **268**:253, 1995

Su-Pos157

CRYO-ELECTRON MICROSCOPY OF THE ENERGY-DEPENDENT CLP-AP PROTEASE ((F. Beuron*, E. Kocsis*, M. Kessel*, M. Maurizi+, A. C. Steven* and F. P. Booy*)) LSBR-NIAMS*, LCB-NCI+, NIH, Bethesda MD 20892

ClpAP, an energy-dependent protease of *E. coli*, consists of a proteolytic component, ClpP, and an ATP-hydrolyzing component, ClpA. The ClpP molecule is composed of 14 subunits, each ~ 21 kDa, arranged in two seven-fold rings. ClpA is a hexameric ring of 84-kDa subunits. As determined by negative staining electron microscopy, active ClpAP complexes contain either one or two ClpA molecules, axially aligned with a single ClpP 14-mer [1]. We have used cryo-electron microscopy to further investigate the structures of both components and their complexes. As in negative stain, frozen hydrated ClpP molecules are frequently observed in top view, in which they display a strong sevenfold symmetry. Averaged images calculated to a resolution of ~ 20 Å show seven globular units (each presumably the co-projection of two ClpP subunits) arranged around a central low-density region of 35 - 40 Å in diameter. In frozen hydrated preparations of ClpA, top views were appreciably more common and side views less common, than in negative stain. The top views show the 6-fold symmetry of ClpA clearly. In addition, virtually all molecules - which presumably represent a variety of orientations - have low-density centers. These regions are considerably smaller than the corresponding feature of ClpP and suggest that ClpA also has a (smaller) central cavity. Preliminary observations of ClpAP complexes confirm the morphology presented in negative stain (six parallel striations) but with superior structural preservation, to judge by their lower curvature. Such data offer good prospects for more detailed characterization of the interactions between ClpA and ClpP, and the structural basis of the mismatch between their respective rotational symmetries.

1. M. Kessel et al, J. Mol. Biol. **250**: 587, 1995

Su-Pos158

THREE-DIMENSIONAL MAPS OF DIFFUSE X-RAY SCATTERING FROM STAPHYLOCOCCAL NUCLEASE. ((M.E. Wall, S.M. Gruner)) Department of Physics, Princeton University, Princeton, NJ 08544 ((S. Ealick)) Division of Biological Sciences, Cornell University, Ithaca, NY 14853. (Spon. by M.E. Wall).

We have obtained measurements of diffuse x-ray scattering from crystals of *Staphylococcal* nuclease by generating three-dimensional maps of diffuse intensity in reciprocal space. The three-dimensionality of the maps has allowed characterization of their degree of internal symmetry: the symmetry exhibited by the maps is consistent with the predictions of the $P4_1$ space group of the unit cell. Different crystals grown under identical conditions yield diffuse maps which differ by as little as 20% in a resolution shell spanning 4.1 Å – 3.6 Å, showing that measurements of diffuse scattering are reproducible. Simulations show that the diffuse scattering in *Staph.* nuclease is modelled well by a map of the calculated structure factor of the unit cell, which is consistent with both a liquid-like motions model [Caspar *et. al.*, Nature **332** (1988) 659] and a crystalline normal modes model [Glover *et. al.*, Acta Cryst **B47** (1991) 960] of the fluctuations. Significant differences are observed between three-dimensional diffuse scattering maps obtained from *Staph.* nuclease crystals with and without Ca^{++} and the substrate analog pdTp (thymidine-3′,5′-diphosphate) bound. These changes are interpreted as the observation of a change in the dynamics of *Staph.* nuclease upon binding of Ca^{++} and pdTp.

Su-Pos159

PROTEASOME-ACTIVATOR COMPLEXES STUDIED BY ELECTRON MICROSCOPY: ROLE OF MODULATOR PROTEIN.
((George Adams[1], George N. DeMartino[2], Edward P. Gogol[1])) [1]Division of Cell Biology and Biophysics, University of Missouri-Kansas City, [2]Department of Physiology, University of Texas Southwestern Medical Center, Dallas, TX

The proteasome is a large multisubunit complex which has several different proteolytic activities. This enzyme complex has been isolated in two distinguishable forms, the simplest of which is a 20S cylindrical particle that has a limited range of peptidase activity. A larger 26S form, with additional components at the ends of the 20S core, exhibits a wider range of proteolytic activity, including the degradation of ubiquitinated proteins. We have attempted to reconstitute the 26S form by combining the isolated 20S with a 700kDa protein (PA700) that endows the resulting assembly with the activities of the 26S form. Though complexes resembling the isolated 26S are visible in these mixtures, the number of larger complexes increases dramatically by including an additional component, a purified "modulator" protein (250kDa) that stimulates the proteolytic properties of the 20S-PA700 complex. Using electron microscopy and image analysis, we have examined assemblies reconstituted from purified and well-characterized components. This work is an attempt to define the role of the modulator protein in the complex, specifically to determine whether it is a structural component or a catalyst of 20S-PA700 particles.

Su-Pos160

SOLUTION STRUCTURE OF A FIBRINOGEN Aα-LIKE PEPTIDE BOUND TO THROMBIN (S195A). ((Muriel C. Maurer, Cathy C. Lester, Elsie E. DiBella, Harold A. Scheraga)) Baker Laboratory of Chemistry, Cornell University, Ithaca, NY 14853-1301. (Spon. by Barbara Baird)

Fibrinopeptide A is released when the R16-G17 peptide bond of the fibrinogen Aα chain is cleaved by thrombin. A number of bleeding disorders, in which hydrolysis of this bond is impaired, have been found to result from single amino acid substitutions in the Aα chain. To allow for structural determination of bound fibrinogen Aα-like peptides on *both* sides of the R16-G17 cleavage site, a mutant of thrombin was prepared with the active site serine converted to an alanine (S195A). The mutant is overexpressed in *E. coli* as prethrombin-2 (S195A), folded, purified, and activated to thrombin (S195A). Results from 1D-line broadening NMR and 2D-transferred NOESY experiments indicate that the fibrinogen Aα-like peptide (D^7FLAEGGGVRGPRV^{20}) binds but is not cleaved upon interaction with thrombin (S195A). The N-terminal portion of bound fibrinogen Aα (7-20) undergoes chain reversal allowing F8 to be directed towards the R16-G17 cleavage site, and the C-terminal portion G^{17}PRV^{20} forms a type-II β-turn. Transferred ROESY experiments suggest that the NMR data are dominated by direct magnetization transfer effects between protons on the bound peptide.

Su-Pos161

Structural Energetics of Thrombomodulin Binding to Thrombin. Alessandro Vindigni and Enrico Di Cera. Dept Biochem & Mol Biophys, Washington Univ Med School, St. Louis, MO 63110.

Thrombomodulin enhances the specificity of thrombin toward the anticoagulant protein C. It binds to an extended surface on thrombin comprising the fibrinogen binding loop and the heparin binding site. Binding to the fibrinogen binding loop involves EGF repeats and both polar and hydrophobic interactions. Binding to the heparin binding site is mediated by the chondroitin sulfate moiety and should exclusively involve electrostatic components. Binding of thrombomodulin to thrombin is characterized by a ΔC_P=–0.8±0.2 kcal/mol/K and a Γ=$-\partial \ln K_d/\partial \ln[salt]$=–5.2±0.1, independent of the allosteric state of the enzyme. The value of ΔC_P is comparable to that observed for the binding of the hirudin fragment 55-65 to the fibrinogen binding loop, while the value of Γ is nearly the same as that observed in the thrombin-heparin interaction. These findings suggest that the fibrinogen binding loop contributes to recognition mostly through hydrophobic interactions, while the heparin binding site contributes through electrostatic interactions. This conclusion is supported by studies on the properties of site-directed mutants of thrombin and fragments of thrombomodulin that target specifically the fibrinogen binding loop.

Su-Pos162

CYTOCHROME P450 RECOGNITION SITES FOR NADPH CYTOCHROME P450 REDUCTASE ((Renke Dai, Richard C. Robinson and Fred K. Friedman)) Laboratory of Molecular Carcinogenesis, National Cancer Institute, NIH, Bethesda, MD 20892

Cytochrome P450 mediated substrate oxidation requires its functional interaction with NADPH cytochrome P450 reductase, which transfers two electrons to the P450 during the catalytic cycle. Although previous studies have identified a number of P450 amino acids that contribute to this interaction, the residues which comprise a surface recognition site for reductase are unknown. In order to identify the interactive surface regions on P450, we utilized a sequence alignment between P450cam and rat P450 2B1 in conjunction with the known structure of P450cam, to generate a model for P450 2B1. Peptides corresponding to predicted reductase binding regions were synthesized and evaluated for their ability to disrupt the P450-reductase interaction as measured by inhibition of reductase-mediated benzphetamine demethylation by P450 2B1. The most potent inhibitors were surface simulatory peptides which combined regions that are spatially proximate but distant in primary sequence. Peptides derived from a combination of the C- and L-helices, and the L-helix and heme binding region, were particularly effective inhibitors. These results indicate that these predicted surface regions include recognition sites for reductase.

Su-Pos163

MUTAGENESIS AND HETERONUCLEAR NMR STUDIES OF THE ROLE OF GLU-57 IN THE MECHANISM OF THE MUT T ENZYME. ((J. Lin, C. Abeygunawardana, D.N. Frick, M.J. Bessman, and A.S. Mildvan)) Johns Hopkins Med. Sch., Baltimore, MD 21205 and Univ., Baltimore, MD 21218

The Mut T enzyme catalyzes the unusual hydrolysis of nucleoside triphosphates (NTP) by substitution at the β-P, yielding NMP and pyrophosphate. Mut T requires two divalent cations, forming an E-M^{2+}-NTP-M^{2+} complex. Mutation of the conserved Glu-57 to Gln (E57Q) results in a $\geq 10^5$-fold loss in activity. The solution structure of the E57Q mutant, based on comparison of ^1H-^{15}N NOESY HSQC spectra, and Hα, and Hβ chemical shifts with those of wild type, differs only near E57. The dissociation constants (K_D) of the E-Mg^{2+} and E-Mn^{2+} complexes are increased 3.3- and 3.5-fold in the E57Q mutant, while the K_D of E-dGTP is unaltered from wild type. The enhanced paramagnetic effect of E-Mn^{2+} on $1/T_1$ of ^1H_2O is halved in the E57Q mutant indicating an altered metal-binding site. Thus E57 is probably a ligand to the enzyme-bound metal. ^1H-^{15}N HSQC titration of E57Q with $MnCl_2$ shows selective broadening of the side chain NH signals of Q57 and the backbone NH signals of K39, E53, E56 and Q57, indicating proximity of bound Mn^{2+} to these residues. ^1H-^{15}N HSQC titrations with $MgCl_2$ and Mg^{2+}NTP show mutual tightening of binding of Mg^{2+} and Mg^{2+}NTP to the wild type enzyme. This synergy is decreased ~10-fold in the E57Q mutant. This weakened interaction between E-Mg^{2+} and Mg^{2+}NTP may be responsible for the large decrease in activity of the E57Q mutant.

Su-Pos164

^{13}C-NMR RELAXATION STUDIES OF BACKBONE AND SIDE-CHAIN MOTION OF THE CATALYTIC TYROSINE RESIDUE (Y14) IN KETOSTEROID ISOMERASE (KSI). ((Q. Zhao, C. Abeygunawardana, and A.S. Mildvan)) Johns Hopkins Medical School, Baltimore,MD 21205

KSI (27 kDa) catalyzes the isomerization of Δ^5- to Δ^4-3-ketosteroids using Y14 as a general acid to donate a H-bond to the 3-oxo group of the substrate. The dynamics of Y14 in free and steroid-bound KSI were studied by ^1H-detected ^{13}C T_1, T_2, and NOE measurements, at 500 and 600 MHz, of $^{13}C\alpha$ and $^{13}C\varepsilon$ labeled Y14 in the Y55F/Y88F double mutant of KSI in which Y14 is the only Tyr. Using the model-free formalism (Lipari and Szabo, JACS 104, 4546, 4559), a time constant for overall rotation (τ_m) of 18 nsec was found, consistent with fluorescence anisotropy decay rates (Wu et al. Biochem. 33, 7415) and Stokes Law. The order parameter (S^2) of the side-chain Cε of Y14, which measures the restriction of its high frequency (nsec to psec) motion, increased from 0.74 to 0.86 on binding the steroid 19-nortestosterone hemisuccinate. In contrast, S^2 of the backbone Cα of Y14 decreased from 0.82 to 0.76 on steroid binding. Hence the decreased amplitude of high frequency side-chain motion of Y14 is partially compensated by an increased amplitude of backbone motion. Lower frequency (msec to μsec) backbone and side-chain motions of Y14, at rates comparable to k_{cat} (1.2×10^4 s^{-1}), detected by exchange contributions to T_2, were unaltered by steroid binding. Thus, the concept of "freezing at reaction centers on enzymes" (FARCE) applies only to high frequency side-chain motions of Y14. Slower motions, unaltered by ligand binding, permit efficient catalysis to proceed.

Su-Pos165

SOLUTION SECONDARY STRUCTURE AND ACTIVE SITE RESIDUES OF 4-OXALOCROTONATE TAUTOMERASE (4-OT) BASED ON HETERONUCLEAR NMR. ((C. Abeygunawardana, J.T. Stivers, C.P. Whitman, and A.S. Mildvan)) Johns Hopkins School of Medicine, Baltimore, MD 21205 and University of Texas, Austin, TX 78712

4-OT, a 41 kDa homohexamer with 62 residues per subunit, catalyzes the isomerization of unsaturated α-keto acids using Pro-1 as a general base (Stivers et al., Biochem., in press). We report backbone and side-chain ^1H, ^{15}N, and ^{13}C NMR assignments and the secondary structure based on CT-HNCA, HNCACB, HCCH-TOCSY, and $^1H^{15}N$ NOESY-HSQC and other spectra. The secondary structure consists of an α-helix (res.13-30), two β-strands (β1, 2-8; β2, 39-45), a β-hairpin (50-57), two loops (9-12; 34-38), and two turns (30-33; 47-50). The β1 strand is *antiparallel* to another β1 strand from an adjacent monomer forming a subunit interface, and is *parallel* to the β2 strand of the same subunit, based on cross strand NOEs seen in the ^{15}N edited NOESY spectrum of 4-OT containing only two ^{15}N labeled subunits/hexamer. Phe-50 is in the active site, based on transferred NOEs to the bound partial substrate 2-oxo-1,6-hexanedioate. Affinity labeling of Pro-1 with the substrate analog 3-Br-pyruvate alters the amide ^{15}N and NH chemical shifts of residues 35-38 in the second loop, Arg-39, and residues 51-54 in the β-hairpin, indicating that these regions change in conformation when substrate binds. Accordingly, flexibility of these regions is indicated by weak αN NOEs and fast NH exchange.

Su-Pos166

X-ray-Diffraction Studies of a Recombinant Bovine Odorant Binding Protein. (G. Bains, H. Monaco, and L. M. Amzel) Department of Biophysics and Biophysical Chemistry, Johns Hopkins University School of Medicine, Baltimore, MD 21205. (Sponsored by L. M. Amzel).

The recombinant bovine odorant binding protein (OBP) has been crystallized under conditions similar to those used to crystallize nonrecombinant OBP (78% ammonium sulfate, 50 mM Tris, pH 8.5). Attempts to solve the structure of OBP using isomorphous replacement have proved difficult as bovine OBP contains no cysteine or methionine residues. To resolve this, a mutant has been engineered in which serine 95 has been replaced by a cysteine. This mutant has been cocrystallized with 1 mM ethyl mercury chloride under the same conditions as those used for recombinant OBP and these crystals diffract out to 3.2 Å resolution as compared with the recombinant wild-type crystals which diffract out to 2.8 Å. A comparison of the diffraction data from the mutant with that of the wild-type indicates that the S95C mutant crystallizes in the same space group as the wild-type ($P2_12_12_1$) with identical unit cell parameters. Diffraction data have been collected on the derivatized S95C mutant. This data will provide a significant improvement to the current phase model for the structure of OBP.

Su-Pos167

INITIAL NMR ANALYSIS OF CONTIGUOUS SH3-SH2 DOMAINS FROM PP60C-SRC. ((Lisa Gentile, Marco Tessari[†], Geerten Vuister[†] and Linda Nicholson)) Section of Biochem., Molec. & Cell Biol., Cornell U., Ithaca, NY 14853, [†]Bijvoet Center for Biomolec. Res., Utrecht U., Padualaan, 3584 Netherlands (Spon. by Quentin H. Gibson)

A model protein comprised of the Src-homology (SH) domains SH3 and SH2 derived from chicken $pp60^{c\text{-}src}$ (Src) is being employed to elucidate the inter- and intramolecular interactions involved in phosphopeptide binding. The SH3 and SH2 domains are modular regulatory components that are also found in numerous other proteins involved in the control of cell growth and differentiation. Structures of isolated SH2 and SH3 domains from a number of proteins, including Src, have been determined using X-ray crystallography or solution NMR. The only structure determination for contiguous SH3-SH2 domains reported is the X-ray structure of the combined SH3-SH2 domains from *Lck*, a member of the Src tyrosine kinase family. Our goal is to investigate the structure and dynamics of the Src SH3-SH2 fragment in solution to address functional questions regarding the role of the SH3 domain in phosphopeptide binding to the SH2 domain. A growing body of evidence indicates that binding of phosphorylated Tyr-527 of the C-terminal tail to the SH2 domain inhibits the intrinsic tyrosine kinase activity of Src, providing an intramolecular switching mechanism. Functional studies have shown that the SH3 domain is essential in regulation of this SH2-phosphopeptide interaction. However, the recent X-ray analysis of the SH3-SH2 domains from *Lck* both in the presence and absence of a phosphopeptide ligand show very few intramolecular interdomain interactions. A solution NMR analysis allows elucidation of structural and dynamic details in an environment free of crystal packing forces. The SH3-SH2 fragment from Src has been over-expressed and isotopically labeled in *E. coli*, and preliminary structural and dynamics results will be presented.

Su-Pos168

INTERACTIONS BETWEEN NFκB AND ITS INHIBITOR iκB ((T. Li, L. O. Narhi, J. Wen, J. Philo, K. Sitney, J.-I. Inuoe, T. Yamamoto, and T. Arakawa)) Protein Chemistry Department, Amgen Inc., 1840 DeHavilland Dr., Thousand Oaks, CA 91320. (Spon. by J. Philo)

The N-terminal portion (318 amino acids) of mouse NFκB (p65) and its complex with iκB (MAD3) (317 amino acids) have been purified to homogeneity. The molecular ratio of NFκB to iκB within the complex has been determined to be 2 to 1 by light scattering and SDS-gel electrophoresis. Protein secondary structure of NFκB (p65) determined by FTIR spectroscopy is in good agreement with those of p50 crystal structure in the p50/DNA complex (Ghosh, et al., Nature, **373**, 303). FTIR spectrum of the NFκB/ikB complex indicate that its secondary structures are composed of 17% α-helix, 39% β-strand, 18% irregular structures and 26% β-turns and loops. By comparing to FTIR data for NFκB alone, it is concluded that iκB (MAD3) in the complex contains 35% α-helix, 27% β-strand, 22% irregular structures and 16% β-turns and loops. Consistent results have also been obtained by CD analysis of a shorter form of iκB (pp40) and the NFκB/ikB complex. The thermostabilities of NFκB, iκB and their complex have been investigated by employing CD spectroscopy. The CD results indicate that the thermal stability of iκB is enhanced upon the formation of the NFκB/iκB complex.

Su-Pos169

S100β INHIBITION OF PKCα AND PKM PHOSPHORYLATION OF A SYNTHETIC PEPTIDE DERIVED FROM p53. ((Paul T. Wilder, and David J. Weber)) Department of Biological Chemistry, University of Maryland School of Medicine, Baltimore, MD 21201.

S100β is a Ca^{2+} binding protein of the S100 family which is involved in both intra- and extra-cellular signalling. S100β is known to be overexpressed in patients with Alzheimer's disease, Downs Syndrome, and AIDS-related dementia. Furthermore, it inhibits the phosphorylation of severeal biologically relevant proteins including MARCKs, GFAP, GAP, τ, and p53 by binding the phosphorylation site on the substrate. In this study, the effects that S100β has on a synthetic peptide derived from human p53 (residues 367-388) were examined. It was found that the phosphorylation of the p53 peptide was inhibited in a dose-dependent manner by S100β under conditions when both Ca^{2+} ion binding sites of S100β are saturated. The Ca^{2+}-dependence of the inhibition was examined using a trypsin cleaved form of PKCα (PKM) which lacks the regulatory domain that makes PKCα dependent on Ca^{2+} and phospholipids. Thus, in asssays with PKM, the S100β-dependent inhibition of phosphorylation of the p53 peptide was determined to be dependent on Ca^{2+} ion concentration. The kinetic parameters for phosporylation in these systems will be presented.

Su-Pos170

THE TRYPTOPHAN FLUORESCENCE OF *TETRACARBIDIUM CONOPHORUM* AGGLUTININ II AND ITS USE IN THE STUDY OF THE BINDING INTERACTION WITH A BIANTENNARY GLYCOPEPTIDE. ((M.P.Brown[1], D.Toptygin[1], K.B.Lee[1], T.Animashaun[2],R.C.Hughes[2],Y.C.Lee[1] and L.Brand[1])) [1]The Johns Hopkins University, Baltimore,MD 21218, [2]National Institute for Medical Research,Mill Hill, London,UK.

The plant lectin *Tetracarbidium conophorum* agglutinin II is useful in the separation of glycoproteins and glycopeptides in a structurally specific manner (Animashaun,T.A., Togun,R.A. & Hughes,R.C. (1994) *Glycoconj.J.* **11**, 299-303). We have characterized the steady-state and time-resolved fluorescence of the tryptophan residues of this lectin and have found that the absorbance and excitation spectra are typical for tryptophan containing proteins. The peak of the emission spectrum when excited at 295nm is 347nm. The fluorescence decay is described by four decay times with the following values: τ_1= 7.33ns, α_1=0.22, τ_2 = 2.70ns, α_2 = 0.27, τ_3 = 0.93ns, α_3 = 0.36, τ_4 = 0.18ns, α_4 = 0.16. The decay associated spectra of τ_1, τ_2, τ_3 and τ_4 peak at 350nm, 338nm, 338nm, and 330nm, respectively. We show that addition of a biantennary glycopeptide to the lectin results in a quench and an 8nm blue shift of the emission spectrum. The effect is saturable, and an

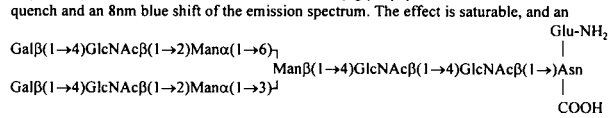

approximate association constant of 1.78(+/-0.07)x$10^5 M^{-1}$ with an assumed 1:1stoichiometry was determined. The steady-state anisotropy of the lectin increases from 0.08 to 0.1 at saturating glycopeptide concentrations. (Supported by NIH Grant GM11632)

Su-Pos171

INHIBITION OF INTRINSIC COAGULATION PROTEASE BY CHONDROITIN SULFATE E. EFFECT OF IONIC STRENGTH AND OSMOTIC STRESS. ((M.P. McGee and H. Teuschler)) Bowman Gray School of Medicine, Wake Forest University, Winston-Salem, NC 27157. (Spon. by R.L. Wykle)

The generation of coagulation FXa (activated factor X) via the intrinsic pathway protease complex (factors IXa/VIIIa) is specifically inhibited by CSE (chondroitin 4-6 disulfate). The purpose of the present study is to examine the role of electrostatic and "hydration" forces on the inhibitory interaction. Inhibition is measured as the normalized difference in the initial rate of factor Xa generation by IXa/VIIIa complexes, in reaction mixtures with and without CSE (average Mw=80000). Ionic strength of solutions is controlled with NaCl. Osmotic stress is induced with polyethylene glycol (Mw=6000). Results show that inhibition, I, is inversely correlated to ionic strength. The log of I decreases with the square root of salt concentration. Slope of regression lines is -4 and -6 for reactions at 25 and 35 °C respectively. Osmotic stress, $\Delta\pi$=0.3 atm., decrease K_I (concentration of CSE resulting in 1/2 maximal inhibition) by approximately 4 fold. Results are interpreted to indicate that inhibition of intrinsic protease by CSE involves electrostatic interactions and transfer of hydration water to bulk solution. Assuming that the observed effect of salt reflects electrostatic forces exclusively, the slope $\lg I/[NaCl]^{1/2}$= -6, is consistent with either 1 and 6 or 2 and 3 opposite sign charges. The volume of water transferred calculated from the slope ln $K_I/\Delta\pi$ is 10841 mol of H_2O per mol CSE bound.

Su-Pos172

CYSTATIN C: SPECTROSCOPIC STUDIES OF PROTEIN STRUCTURE. ((S.L.BARKER, A.G.SZABO)) DEPARTMENT OF CHEMISTRY AND BIOCHEMISTRY, UNIVERSITY OF WINDSOR, WINDSOR, ONTARIO, CANADA N9B 3P4

Unscheduled proteolytic activity of lysosomal proteinases is restricted in part by a series of inhibitors, known as cystatins, which are present both in the cytoplasm and in the extracellular fluid. Cystatin C has been expressed in an *E.coli* TRP auxotroph and purified. The TRP104 residue has been used in fluorescence studies to examine and characterize the properties of the spectroscopic signal in terms of secondary protein structure, electrostatic charge, hydrophobicity, and hydrogen bonding. As well, the interaction of cystatin C with cathepsin B and papain has been examined spectroscopically. Analogues of tryptophan with distinct spectroscopic properties were incorporated and used to analyze the importance of different residues in the binding interaction and the importance of residues on the active site. Uncovering novel information on mammalian proteinases and their complexes with inhibitors will aid in rational design of new specific bioactive proteinase inhibitors with ultimate therapeutic benefit.

Su-Pos173

BIOPHYSICAL STUDIES OF A TMV COAT PROTEIN MUTANT THAT ELICITS A HYPERSENSITIVE RESPONSE IN N. SYLVESTRIS" (J. Toedt, B.Diep, E.J. Anderson, C. Keating, L. Caromile, M. Escobar, E. Anderson, T. Pittman, E. Braswell, T.M. Schuster) University of Connecticut, Molecular and Cell Biology Department and National Analytical Ultracentrifugation Facility (Z.F. Taraporewala and J.N. Culver) University of Maryland, Department of Plant Biology

Several mutational studies have shown that the coat protein of TMV is an elicitor of a hypersensitivity response (HR), a plant response which limits of the infection. (Culver, et. al., 1994, *J. Mol. Biol.* **242**:130-138) Since the wild type virus does not elicit a HR, a study has been undertaken to determine what biophysical alterations are caused by the single amino acid mutations that allow the tobacco plant to respond to the invading virus. Sedimentation velocity measurements of the coat protein, TMVP, have been made at 20 C and 4 C over a wide range of concentrations (5.0mg/ml-0.016mg/ml) for both wild type and mutant 46 (arg to gly), through the use of near and far-uv absorption in the Beckman X^I A analytical ultracentrifuge. Measurements were carried out in 0.1 ionic strength pH 7.0 orthophosphate buffer to examine any possible changes in size, shape, or aggregation. Velocity data were analyzed using the DC/DT software package of Dr. Walter Stafford (*Anal Biochem*, 1991, **203**:295) and the results are compared as $S_{20,w}$ values. Similar $S_{20,w}$ values are seen at 20°C for the wild type and mutant, agreeing with known wild type values for the "20S" and "4S" aggregates(*Protein Science* 1993, 2:1, p. 150). However differences were seen in the ratio of "20S" and "4S" concentrations. Additionally, a concentration dependent increase in S value for the "4S" species of the mutant was found at 4 C in the range of 1.25mg/ml to 5.0mg/ml

Additional analysis of TMVP structure was done using circular dichroism (CD) measurements over a similar concentration range as was used for velocity sedimentation analysis at 20 C and 4°C failed to reveal any differences in secondary structure between the mutant and the wild type virus coat protein. Further analysis was done using virus reconstitution experiments (Schuster, et. al., 1980, *Biophys. J.*, **10**:313). TMV wild type RNA was combined with each protein type and the *invitro* self-assembly was followed spectroscopically at a temperature of 20°C. These conditions allowed for an understanding of kinetic differences in the formation of virus due to the single mutation In addition, since it is known that the "20S" species is required for nucleation of reconstitution and that "20S protein does not form at 4°C, the experiments with protein equilibrated at 4°C allow for conclusions about the relative lag times involved in the formation of "20S" for the mutant and wild type coat protein. "Supported by REU grants from the NSF, and by NSF Grant *BIR* - 9318373

Su-Pos174

A GENERAL SOLID PHASE METHOD FOR CROSSLINKING PROTEINS: A PEANUT AGGLUTININ - HEMOGLOBIN COMPLEX ((J. S. Brunzelle, L. Lapsys, F. Uddin, A. Akrivos, S. Kondubhotla and K. W. Olsen)) Dept. of Chemistry, Loyola University, 6525 N. Sheridan Rd., Chicago, IL 60626

The ability to make covalently linked complexes of proteins that do not normally interact is a practical goal for the formation of multienzyme complexes for industrial and medical use. Using affinity chromatography to form a solid phase, additional proteins can be linked by alternating cycles of crosslinking reagent and protein. As an example, peanut agglutinin (PNA) was bound to a lactose affinity matrix and then activated using dimethylsuberimidate (DMS). After washing the column with buffer to remove the excess DMS, hemoglobin (HbA) was added at pH8.5. After reaction and washing to remove excess HbA, the PNA-HbA complex was eluted by adding lactose. SDS-PAGE and UV/Vis spectroscopy demonstrated the presence of the PNA-HbA complex, as well as large amounts of crosslinked PNA. A much cleaner product was obtained by using sulfosuccinimidyl-4-(p-maleimidophenyl)butyrate (S-SMPB), a heterofunctional reagent that reacts with lysine and cysteine. Since PNA has no cysteine, there was no PNA-PNA crosslinking with S-SMPB.

Su-Pos175

THERMODYNAMICS OF OVOMUCOID THIRD DOMAINS BINDING TO PORCINE PANCREATIC ELASTASE. ((Brian M. Baker and Kenneth P. Murphy)) Department of Biochemistry, University of Iowa, Iowa City, IA 52242 (Spon. by C. Swenson)

Elucidation of the contributions of fundamental interactions to protein energetics remains a long-standing goal in protein chemistry. An understanding of these contributions and their context dependence is necessary. Detailed calorimetric studies of protein-protein interactions where the structures of the initial and final states are known can help to address this problem. We have begun to investigate the binding of turkey ovomucoid third domain (OMTKY3), a potent serine protease inhibitor, to porcine pancreatic elastase using isothermal titration calorimetry and structural energetics calculations. Calculations predict a positive intrinsic $\Delta H°$ of 7 ± 13 kJ/mol (25°C), an intrinsic ΔC_p of -1.4 ± 0.1 kJ/(K mol), and an intrinsic $\Delta S°$ of 200 ± 30 J/(mol K), corresponding to an intrinsic equilibrium constant of 1×10^9 at 25°C. Experiments performed thus far support these calculations, as well as indicate that protons are released upon OMTKY3 binding. A likely candidate for the source of this proton linkage is the imidazole side chain of His-57 in the protease active site. The observed ΔH of binding in pH 7 imidazole buffer is -3.9 ± 1.3 kJ/mol. Using the published association constant of 4.1×10^{10} (1), this corresponds to a $\Delta S°$ of 190 ± 21 J/(K mol). The ΔC_p upon binding has been measured as -1.1 ± 0.1 kJ/(K mol).

1. Bigler, T. L., *et al.*, Prot. Sci, **2**, 786, 1993.

Funded by the Roy J. Carver Charitable Trust

FOLDING AND SELF-ASSEMBLY I

Su-Pos176

THERMODYNAMIC STABILITY OF SYNTHETIC HEME PROTEINS ((B. R. Gibney, F. Rabanal, P. L. Dutton)) Johnson Research Foundation, University of Pennsylvania, Philadelphia, PA 19104

Heme proteins serve a wide variety of functions in the biological milieux. They are involved in ligand transport, dioxygen activation, electron transfer, energy conversion, signal transduction and gene regulation. Our approach to the study of natural redox enzymes is to design and synthesize minimal structures that test the assembly of the component peptides with the incorporation of a particular chosen cofactor. A further goal is to generate in protein structures simplified working versions of complex native enzymes, molecular maquettes. This report focuses on the thermodynamic parameters of unfolding of a series of site modified versions of our prototype[1] four helix bundle heme peptide, H10H24, toward the goal of designing control of heme peptide catalytic properties. The peptides presented modify the orientation of the helix dipoles and make site modifications, both local and distant to the hemes. The heme binding properties and redox potentials of each peptide were ascertained using optical spectroscopy and redox potentiometry. The stability of the apo- and holopeptides was investigated via guanidinium salt and thermal denaturation using circular dichroism spectroscopy. A wide range of stabilities, $[Gdn{\cdot}HCl]_{1/2}$ at 50°C between 2.9 and 5.3M for apopeptides and up to 6.7M for holopeptides, were determined. There is an interplay between global peptide stability, heme binding constants and redox potential helping build a basis to design heme peptides with catalytic properties.

(1) Robertson, D. E.; Farid, R. S.; Moser, C. C.; Urbauer, J. L.; Mulholland, S. E.; Pidikiti, R.; Lear, J. D.; Wand, A. J.; DeGrado, W. F.; Dutton, P. L. (1994) Nature 368, 425-32.

Su-Pos177

INTRODUCTION OF FUNCTIONAL PROPERTIES OF BOVINE HEMOGLOBIN INTO HUMAN HEMOGLOBIN WITH FIVE AMINO ACID SUBSTITUTIONS. ((C. Fronticelli[#], M.T. Sanna[#], F. Huang[#], M. Karavitis[#] and W. Brinigar[°])) [#]Dept. Biol. Chem. Univ. of Maryland, Med. Sch. Baltimore, MD. [°]Dept. of Chemistry. Temple Univ.* Philadelphia, PA.

Bovine Hb (HbBv) has a low oxygen affinity and is regulated by Cl^- rather than by 2,3-DPG. It has been proposed (Fronticelli, Biophys. Chem. 37:141,1990) that these properties are due to the particular amino acids composition of the A and E helices of bovine β-subunits . To investigate the validity of this proposal two mutant human hemoglobins were constructed: β(V1M+H2deleted+T4I+P5A)=PB4 and β(V1M+H2deleted+T4I+P5A+A76K)=PB5. With the exception of Ile at position 4, all the residues changed are the ones found in HbBv at the corresponding positions. In the absence of Cl^-, PB4, PB5 and HBv all have the same oxygen affinity, 3 fold lower that HbA. Addition of Cl^- lowers the oxygen affinity of PB5 and HbBv, but has no effect on the O_2 affinity of PB4. Thus the substitutions in PB4 are sufficient to introduce in HbA the intrinsic low O_2 affinity of HbBv, but they also abolish the Cl- sensitivity of HbA. The additional substitution of A76K reintroduces Cl^- sensitivity in PB5. Crystallographic analysis suggests the presence of an oxygen linked Cl^- binding site between βK8, βK76 and βH77. Computational analyses support this proposition.

Su-Pos178

STABILIZATION OF COMPACT STRUCTURES OF APOMYOGLOBIN AT LOW pH AND LOW Cl^- BY NEUTRAL SOLUTES: THE EFFECT OF WATER ON PROTEIN FOLDING. (M.F.Colombo, S.R.Marão, IBILCE-UNESP, S.J.Rio Preto, SP, BRAZIL)

The role of macromolecular hydration on the energetics of folding / unfolding processes of apomyoglobin (apoMb) induced by acidic pH has been investigated by the osmotic stress method. In this work, we followed the unfolding process of apoMb, induced by acidic pH titration, by far-UV circular dicroism in the presence of sucrose, glucose and sorbitol and at Cl^- only from HCl. We found that these solutes stabilize the protein against denaturation. Comparison of our proton titration isotherms, obtained at different solute concentrations, with the isotherms obtained at different Cl^- concentrations, reveal a mechanism of solute stabilization distinct from that observed with Cl^-. While increased concentrations of chloride favor the transition of the Native (N) to the Molten Globule (MG) state at pH above ≈ 4 and from the Denatured (D) to the MG at pHs below ≈ 4 (Y.Goto, A.L.Fink, *J.Mol.Biol.* (1990) **214**, 803), increased concentrations of the neutral solutes promote the stabilization of N against MG acid denaturation and stabilization of MG against further acid denaturation to the D state. In order to determine a possible mechanism for the observed stabilization of the compact states, we carried out experiments of re-folding of apoMb at pH 2.4 by titrating neutral solutes. These data, analyzed in terms of the dependence of the apparent equilibrium constant for refolding on solute activity and on water activity, show a linear decrease of the free energy change for folding with decreasing water chemical potential and, a non-linear dependence of the free energy with solute chemical potential. These results indicate that the mechanism of stabilization of apo-Mb against pH denaturation by neutral solutes has its origin on the energetics of protein solvation, where lower water activities favor the more compact and less hydrated protein conformations.

Supported by FAPESP and CNPq

Su-Pos179

ASSEMBLY OF EARTHWORM HEMOGLOBIN: ROLE OF SUBUNIT EQUILIBRIA, NON-GLOBIN CHAINS AND VALENCE OF THE HEME IRON. ((H. Zhu, D.W Ownby, and A.F. Riggs)) Department of Zoology, University of Texas, Austin, TX 78712.

The extracellular hemoglobin of the earthworm *Lumbricus terrestris* has four major kinds of O_2-binding chains: *a*, *b* and *c* (forming a disulfide-linked trimer), and chain *d*, together with non-heme, non-globin structural chains, or "linkers." Light-scattering techniques have been used to show that the ferrous CO-saturated *abc* trimer and chain *d* form a tight $(abcd)_4$ complex of 285 kDa at neutral pH. Assembly of the full-sized 4-MDa molecule requires the addition of two linkers per $(abcd)_4$ and is accelerated by calcium. Oxidation of the $(abcd)_4$ complex with ferricyanide causes complete dissociation to the dimers, $(abc)_2$ and $(d)_2$, but addition of CN^- maintains the $(abcd)_4$ complex. The ferrous CO-saturated *abc* trimer and met (ferric) chain *d* also associate to form $(abcd)_4$, but the met *abc* trimer and ferrous CO-saturated chain *d* do not. These results show that interactions between the *abc* trimer and chain *d* depend strongly on both the ligand and the valence state of the heme iron. Oxidation of the intact Hb results in a drop in molecular mass from 4.1 MDa to 3.6 MDa after storage at 4°C for only one day. Addition of CN^- prevents this drop. These experiments indicate that oxidation causes the Hb to shed subunits and explain the wide variations in the molecular mass of *L. terrestris* Hb that have been observed previously. (Supported by NIH grant GM-35847 and NSF grant MCB 9205764)

Su-Pos180

MOLECULAR MECHANISMS FOR SALT-INDUCED STABILIZATION OF THE PARTIALLY FOLDED STATES OF APOMYOGLOBIN ((F. H. Kuntze and B. García-Moreno E.)) Department of Biophysics, Institute for Biophysical Research in Macromolecular Assemblies, Johns Hopkins University, Baltimore, MD 21218

Apomyoglobin is thought to exist in a highly unstructured state under conditions of extreme acidity (pH 2) and low salt concentration. Circular dichroism and NMR experiments reveal that the A, B, G and H helices fold into stable partially folded structures with the addition of salt (Loh, Kay and Baldwin (1995) Proc. Natl. Acad. Sci. Usa. 92, 5446).

To determine the mechanisms of salt-induced stabilization of partially folded states we have calculated the effects of salt on the energetics of 255 structural states constituted by combinations of the 8 helices of apomyoglobin. The calculations were done with the modified Tanford-Kirkwood algorithm; only the free energy owing to electrostatic interactions between ionizable side chains was quantitated. Two types of salt effects were considered: screening, approximated by the Poisson-Boltzmann treatment in the Tanford-Kirkwood algorithm and site-specific anion binding. Anion binding sites were identified directly from the analysis of electrostatic potentials and the energetics of binding were predicted solely from electrostatic considerations.

In agreement with the experimental observations, the calculations have identified the cluster composed of the A, B and G helices as the most stabilized by anions at salt concentrations below 200mM. The neutralization of repulsive clusters by site-specific chloride binding was shown to be the critical determinant of stabilization. In addition, the interactions of the G and H helices are predicted to be greatly enhanced at ionic strengths near 100mM due to screening of long range repulsive interactions.

Su-Pos181

EXCESS ENTHALPIES IN NORMAL AND CROSSLINKED HEMOGLOBINS. ((A. Razynska, Z. Gryczynski, H. Kwansa, H. Gering and E. Bucci)) Dept. of Biochemistry, University of Maryland Medical School at Baltimore MD.

Both Van t' Hoff and calorimetric measurements have demonstrated the enthalpy of oxygenation of hemoglobin varies in the intermediate steps of ligation. The first, second and fourth steps are enthalpy driven, while the third step is entropy driven. This implies large enthalpic excursions produced by the conformational changes of the protein during ligand binding, in excess to the enthalpy of the interaction of oxygen with the iron of the heme. We wanted to investigate whether these excess enthalpies originated from changing hydration of the molecular surface or from internal conformational rearrangements of the protein. We chose a family of crosslinked hemoglobin, where the β82 lysines were bridged by acylation with dicarboxylic residues of increasing length, namely succinyl (4 carbons), adipyl (6 carbons), and sebacyl (10 carbons). Besides the common crosslinking sites, they had oxygen affinities monotonically decreasing with the length of the linker. The standard enthalpies at 25° C of the intermediate steps of oxygenation were estimated, for each crosslinked hemoglobin, by global analyses of at least five isotherms at temperatures between 15° and 37° C. The conformational constraint of the crosslinks did not eliminate the excess enthalpies and failed to show any correlation between the length of the linker and enthalpy distribution at the subsequent steps of oxygenation. Addition of 1.4 M sucrose to sebacyl crosslinked hemoglobin failed to eliminate the excess enthalpies. Sucrose interferes with the hydration of protein surfaces. Therefore it appears that hydration is not the main source of the excess enthalpies.

Su-Pos182

SPECTROSCOPIC STUDIES ON THE SELF-ASSEMBLY OF A *DE NOVO* DESIGNED MODEL OF THE PHOTOSYNTHETIC REACTION CENTER. ((Francesc Rabanal, William F. DeGrado, and P. Leslie Dutton)). The Johnson Research Foundation, Department of Biochemistry and Biophysics, University of Pennsylvania, Philadelphia, PA19104.

A de novo designed heme binding four-α-helix bundle {abbreviated $[\alpha_2]_2$} incorporating a dimeric porphyrin (coproporphyrin I=CP) has been synthesized and characterized as a model of the photosynthetic reaction center. The designed protein, $[CP\text{-}\alpha_2]_2$ consists of two subunits $CP\text{-}\alpha_2$ that self-assemble in aqueous milieu into the four-helix bundle structure thus promoting the porphyrin dimer formation. Furthermore, the dimer-monomer equilibrium of $[CP\text{-}\alpha_2]_2$ can be shifted by addition of cosolvents, thus controlling the state of association of the molecule. A UV-Vis, CD and chromatographic study will be described in support of this assembly process. In addition, the porphyrin moiety is able to be metallated in mild conditions with Cu (II) and Zn (II). Finally, $[CP\text{-}\alpha_2]_2$ also binds up to four-hemes without affecting its UV-Vis spectrum, indicating its probable external appended location.

Su-Pos183

NMR AND UV-VIS SPECTROSCOPIC STUDIES OF NOVEL METAL BINDING SITES IN NANOS, A DEVELOPMENTAL REGULATORY PROTEIN. ((F. Tao, D. Treiber, D. Curtis, R. Lehmann and J. Williamson)) Department of Chemistry, Massachusetts Institute of Technology, and Whitehead Institute for Biomedical Research, Cambridge, MA 02139

The protein nanos plays a crucial part in the segmentation and abdomen formation in the early *Drosophila* embryo. Nanos is required for the localized repression of mRNA translation and the establishment of the anterior-posterior body axis. Phylogenetic analysis shows that there is a high degree of conservation in the C-terminal domain (~72 residues), while little conservation elsewhere in the protein (~400 residues). Biological activity assays show that the C-terminal domain is required, but not sufficient for nanos activity *in vivo*. In contrast, no sequences outside the C-terminal 87 residue region are absolutely required for nanos function. The C-terminal domain has six conserved cysteines and two conserved histidines, that are possible ligands for metal ions. By NMR and UV-Vis spectroscopy, we have demonstrated that the nanos C-terminal domain binds two equivalents of Co(II) or Zn(II), with at least a three order of magnitude preference of Zn(II) over Co(II). Deletion and mutation studies show that metal binding of nanos may be abolished at either one of the binding sites independently. These data suggest that nanos contains two consecutive CCHC type metal binding sites. The sequences intervening the metal ligands are apparently not related to the known CCHC motif in nucleocapsid proteins. Therefore, it may represent a novel zinc finger protein.

Su-Pos184

TITRATION MICROCALORIMETRY AND BINDING STUDIES ON UREASE BY INTERACTION WITH HOMOLOGOUS SERIES OF CATIONIC SURFACTANTS. ((A.A.Moosavi-Movahedi, A.A. Saboury and A.K. Bordbar)) Institute of Biochemistry & Biophysics, University of Tehran, Tehran, Iran, and Dept. of Chemistry, Tarbiat-Modarres University, Tehran, Iran.

The binding of a homologous series of cationic surfactants with jack bean urease have been studied by equilibrium dialysis at pH=10 and two temperatures of 27°C and 37°C. By using the binding capacity concept, a novel method has been applied for resolution and characterization of electrostatic and hydrophobic interactions. Then, by fitting the binding data to the Hill equation with electrostatic and hydrophobic terms, the number of binding sites, binding constants and the amount of co-operativity are obtained and applied in the Wyman binding potential for calculating ΔG, ΔH and ΔS of binding. The trend of variation of binding entropy versus to average number of bound ligand has been interpreted in terms of statistical nature of binding. The interpretation of the binding, spectroscopic and microcalorimetric data show that the predominant unfolding by surfactant occurred at the end of electrostatic binding. Moreover, the heat of these interactions, including binding of surfactants with protein and unfolding of protein, have been measured by a microcalorimeter. Subtraction of binding enthalpies calculated from Wyman binding potential from measured enthalpies. By microcalorimeter shown that the unfolding of this protein occures in two steps with the heat values of 6550 and 650 (kJ / mol) which is independent of surfactant's tail.

Su-Pos185

VOLUMES AND ADIABATIC COMPRESSIBILITIES OF GLOBULAR PROTEINS ((Tigran V. Chalikian and Kenneth J. Breslauer)) Department of Chemistry, Rutgers, The State University of New Jersey, Piscataway, NJ 08855; ((Maxim Totrov and Ruben Abagyan)) The Skirball Institute of Biomolecular Medicine, New York University Medical Center, 540 1st Ave, New York, NY 10016 (Spon. by A. R. Srinivasan)

We report the partial specific volumes, v°, and the partial specific adiabatic compressibilities, k°_S, of 15 globular proteins over a temperature range from 18 to 55 °C. For the subset of 12 proteins with known three-dimensional structures, we have calculated their molecular volumes and the solvent-accessible surface areas of their charged, polar, and nonpolar atomic groups. By applying a linear regression analysis, we have determined, as a function of temperature, the average hydration contributions to v° or k°_S of 1 Å^2 of the charged, polar, and nonpolar solvent-accessible protein surfaces. Comparison of these contributions with those derived from studies on low-molecular weight compounds reveals the following features: (i) The hydration of charged surface atomic groups for a protein is similar to that of charged groups in small organic molecules; (ii) By contrast, the hydration of polar protein surface groups is qualitatively different from that of polar groups in low molecular weight compounds. Perhaps a network of water molecules exist adjacent to the polar surface area of proteins, which involves waters from the second and third coordination spheres; (iii) Nonpolar groups on the protein surface only are hydrated independently at low temperatures. At higher temperatures, some of the waters which solvate nonpolar groups are influenced by neighboring polar groups.

These results will be discussed in terms of models which currently are used to describe the hydration properties of globular proteins.

Su-Pos186

ULTRAVIOLET RESONANCE RAMAN SPECTROSCOPY AS A PROBE OF STRUCTURE AND DYNAMICS IN FILAMENTOUS (*fd, Pf1*) AND ICOSAHEDRAL (*P22*) DNA VIRUSES. ((Zai Qing Wen and George J. Thomas, Jr.)) Division of Cell Biology and Biophysics, School of Biological Sciences, University of Missouri, Kansas City, MO 64110.

Ultraviolet resonance Raman (UVRR) spectroscopy offers a highly selective and sensitive probe of DNA and protein structures in viruses. Employing a recently constructed UVRR spectrometer, equipped with a frequency-doubled continuous-wave argon laser for excitation wavelengths of 257, 244, 238 and 229 nm [Russell *et al.* (1995) *Biophys. J. 68*, 1607-1612), we have obtained spectra of the filamentous viruses *fd* and *Pf1* and of the icosahedral virus *P22*. Using 257 nm excitation, the UVRR spectrum of each virus is dominated by bands of the packaged DNA genome with only minor contributions from tryptophan residues of the coat protein. At 229 nm, on the other hand, the UVRR spectrum is dominated by bands of tryptophan. Tyrosine contributions achieve prominence with 244 and 238 nm excitations. Comprehensive assignment of the UVRR bands has provided a basis for probing DNA-protein interactions and hydrogen exchange dynamics in the native viral assemblies. A remarkably prolific and distinctive DNA profile is obtained for *Pf1*, despite the fact that its DNA genome constitutes only ≈5% of the virion mass. Implications for DNA packaging will be considered. [Supported by NIH grant GM50776.]

Su-Pos187

INFRARED SPECTROSCOPY OF PROTEINS IN AQUEOUS SOLUTION. ((S. Yu. Venyaminov, W. D. Braddock, and F. G. Prendergast)) Department of Pharmacology, Mayo Foundation, Rochester, MN 55905

Fourier transform infrared (FTIR) spectroscopy is a widely used technique for the determination of protein secondary structure and its changes. However, despite its apparent simplicity, there is much controversy regarding the application of this technique. Here we describe methodological aspects of the quantitative measurement and interpretation of FTIR spectra of proteins in aqueous (H_2O and D_2O) solution. For quantitative measurement the correct compensation of the very strong absorbance of water in the range of the protein amide I bend must be done. The most precise optical compensation can be achieved by a comparison of the absorbance of the sample and reference cell in the vicinity of 3645 cm^{-1} (H_2O) and 2770 cm^{-1} (D_2O). The use of a shuttle system allows significant decrease in the influence of such slow changeable parameters as instrument drift, temperature and the water vapor absorbance. The design of a unique short pathlength assembled cell for IR measurements of aqueous solution is described. Maximal signal to noise ratio for the amide I band for any protein concentration can be obtained at an optimal cell pathlength of 3.6 μ (H_2O) and 39μ (D_2O). For data analysis and subsequent physical interpretation, mathematical deconvoution procedures are essential. Details of the appropriate procedure for analysis will be presented and compared to methods commonly employed. The concept of spectrally-consistent protein secondary structure assignment from crystallographic data is discussed as are criteria for choosing the proper number and the nature of IR spectra of reference proteins. (Supported by GM34847-10.)

Su-Pos188

SOLUTION STRUCTURES OF THE TELOMERE BINDING PROTEINS OF *Oxytricha nova* AND THEIR INTERACTION WITH TELOMERIC DNA PROBED BY RAMAN SPECTROSCOPY. ((L. Laporte, J. Stultz and G. J. Thomas, Jr.)) Division of Cell Biology and Biophysics, School of Biological Sciences, University of Missouri, Kansas City, MO 64110.

Telomeres, the DNA-protein complexes which stabilize the termini of eukaryotic chromosomes, consist of repetitive, guanine-rich sequences along the 5' → 3' strand and include a tail protruding beyond the complementary strand by 12-16 nucleotides. The telomere tail is capable of forming different four-stranded (quadruplex) structures containing guanine quartets. Kinetics of duplex-quadruplex and intraquadruplex transformations are generally slow *in vitro* but may be accelerated *in vivo* by specific telomere binding proteins. We report the solution Raman spectra of the α (56 kDa) and ß (41 kDa) subunits of the telomere binding protein of the ciliate *Oxytricha nova*. Both subunits exhibit secondary structures which are rich in ß-strand and relatively thermolabile. Complexes of the subunits with *Oxytricha* telomeric repeats of the form $d(T_4G_4)_n$ and $d(N)_m(T_4G_4)_n$ have also been investigated. The results indicate that subunit binding is coupled with quadruplex structure formation and the affected Raman bands provide information on the protein and DNA residues involved in recognition between *Oxytricha* telomere binding protein and telomeric DNA. [Supported by NIH grant GM54378.]

Su-Pos189

SOLUTION STRUCTURE OF THE C-TERMINAL DOMAIN OF RNA POLYMERASE II: CD OF LONG AND SHORT FRAGMENTS ((Ewa A. Bienkiewicz and Robert W. Woody)) Department of Biochemistry and Molecular Biology, Colorado State University, Fort Collins, CO 80523

The C-terminal domain (CTD) of RNA polymerase II consists of tandem copies of a heptapeptide with the $Y^1S^2P^3T^4S^5P^6S^7$ consensus sequence. This repeat resembles the SPXX motif found in some gene regulatory proteins that adopt a β-turn structure. We have studied CTD fragments using circular dichroism (CD) to test: (1) importance of the putative β-turn points, ie. Ser^2 and Ser^5, (2) dependence of the CTD structure on the length of the polypeptide, and (3) effect of phosphorylation on the CTD structure. The CD analysis of $(SPTSPSY)_8$, $(APTSPSY)_8$, and $(SPTAPSY)_8$ pointed to polyproline II, type I β-turn, and tyrosine as the three major components contributing to the CD signal of CTD. The polyproline II-like conformation predominated in water and at lower TFE concentrations. In contrast, 90% and 100% TFE triggered a dramatic increase in β-turn formation with the concurrent increase in the Tyr CD signal. These results are consistent with the NMR analysis of CTD of Cagas & Corden (Proteins: Struct.Funct.Genet. (1995) 21, 149-160). Replacement of Ser^2 and Ser^5 affected the CTD turn population in water and TFE. The CD of the 1- and 2-repeat of CTD showed a significant dependence of conformation on the chain length. The β-turn structure was favored in short fragments of CTD, whereas the polyproline II component predominated in the 56-residue CTD peptide. Analysis of the phosphorylated CTD fragments is in progress. Overall, the results of this study support the hypothesis that CTD exhibits characteristics of the SPXX transcription factor family.
Supported by NIH Grant GM22994 (RWW) and by a CIRB fellowship (EAB).

Su-Pos190

IN VITRO CHARACTERIZATION OF LIGHT CHAIN AMYLOIDOSIS USING RECOMBINANT LIGHT CHAIN VARIABLE DOMAINS. ((R. Raffen, P. Wilkins Stevens, D.K. Hanson, Y. Deng, M. Berrios-Hammond, F.A. Westholm, M. Schiffer, and F.J. Stevens)) Argonne National Laboratory, Argonne, IL 60439.

Multiple myeloma, a B-cell malignancy, is characterized by the overproduction of a monoclonal population of immunoglobulin light chain protein. In some patients, the light chain protein is soluble and essentially non-pathogenic. At the other extreme, the N-terminal, variable domain (VL) of the light chain is deposited as amyloid, a result that is fatal. The structural characteristics that render certain light chains amyloidogenic are unknown. We have expressed recombinant forms of two VLs, LEN, a non-pathogenic VL, and REC, an amyloidogenic VL. Despite distinct differences in in vivo behavior, the primary structures of the two proteins differ at only 14 positions, thus providing a unique system for identifying structural determinants leading to light chain amyloidosis. We have discerned differences between LEN, REC and several LEN-REC hybrids by examining in vitro characteristics such as dimerization, fibril formation, and stability to chemical denaturation. The results of this study suggest that the amyloid-forming tendency of the REC protein may reside in residues of complementarity-determining loop 1. This research was supported by the US Department of Energy, Office of Health and Environmental Research, under contract W-31-109-ENG-38 and by US Public Health Service grant DK43757.

Su-Pos191

Structural and Mechanistic Studies of Diacylglycerol Kinase, a 13 kDa Integral Membrane Enzyme. ((Charles R. Sanders[1], Prakash Badola[1], Lily Fisher[2], Steven Smith[2], James Bowie[3], Olga Vinogradova[1], and Lech Czerski[1])) [1]Dept. of Physiology and Biophysics, Case Western Reserve University, Cleveland, OH 44106. [2] Dept. of Molecular Biochemistry and Biophysics, Yale University, New Haven, CT 06520. [3]Molecular Biology Institute, UCLA, Los Angeles, CA 90024.

Microbial diacylglycerol kinase (DAGK) contains three transmembrane segments comprising about 80% of its total sequence (Smith et. al., J. Bacter. **176**, 5459-5465, 1994) and catalyzes a topologically complex reaction (MgATP is water soluble, DAG is membrane-associated). In this poster data is presented which indicates that not only is the bilayer-associated protein predominately α-helical, but that the helical segments are well-aligned with the bilayer normal. While the enzyme remains active in neutral micelles, lowering the pH and titrating the micellar enzyme with isopropanol (to 50%) leads a partially unfolded state in which activity is lost and conformational heterogeneity is apparent, but in which detergent-binding capacity and helical secondary structure are maintained. Steady state kinetic analysis combined with inhibition data using a novel bisubstrate analog indicate that DAGK catalyzes phosphoryl transfer by a direct MgATP to DAG pathway rather than by a route which includes a DAGK-phosphate covalent intermediate. Equilibrium binding data (NMR) is also presented which illuminates the putative (Bell and Walsh, Meth. Enzym. **209**, 152-163, 1993) activating roles of the "lipid cofactor" and a second metal ion (beyond that in MgATP).

Su-Pos192

LOCALIZATION OF RESIDUES RESPONSIBLE FOR THE BINDING OF rSkM1 AMINO- AND CARBOXYL-TERMINI. ((Hui Zhang, Sylvia Kolibal, Candace Brady, Weijing Sun, and Sidney A. Cohen)) University of Pennsylvania School of Medicine, Philadelphia, PA 19104.

We previously demonstrated the specific binding of a synthetic peptide encompassing the first thirty residues of the rSkM1 N-terminus to a Maltose Binding Protein (MBP) fusion protein containing the rSkM1 C-terminus (residues 1593-1840). In this study, we first demonstrated identical binding using an N-terminal fusion protein containing the Flag epitope and residues 1-127 of rSkM1. This fusion protein bound specifically and with high affinity (Kd of ~10 nM and 1:1 stoichiometry) to the MBP C-terminal fusion protein. Using both direct and competitive solution phase binding assays, a nested set of peptides encompassing the first 30 residues of the rSkM1 protein were examined for their ability to bind to the MBP C-terminal fusion protein. Peptides 1-30, 7-30, 13-30, and 19-30 but not 24-30 bound specifically and with high affinity to the MBP C-terminal fusion protein, identifying residues 19-24 as the N-terminal region involved in binding to the C-terminus. A similar approach using MBP C-terminal fusion protein deletion mutants and both the 1-30 peptide and the Flag-N-terminal fusion protein identified a partially conserved region in the mid-portion of the C-terminus (residues 1715-1736) which specifically binds to the N-terminus. The N-terminal 19-24 region contains the epitope for L/D3, a monoclonal antibody which differentially labels the surface and T-tubular membranes of fast and slow twitch skeletal muscle cells. We propose that the interaction of N- and C-termini differs in specific membrane environments and may be involved in the subcellular localization of rSkM1 channel protein.

Su-Pos193

STRUCTURAL AND THERMODYNAMIC CHARACTERIZATION OF RBD2 OF HUMAN U1A PROTEIN. ((J. Lu AND K.B. Hall)) Department of Biochemistry and Molecular Biophysics, Washington University School of Medicine, St. Louis, MO 63110.

The RNA Binding Domain (RBD) is one of the most common motifs found in RNA binding proteins. This family of proteins has been shown to bind to various RNA substrates and play important roles in biological processes. We have used two RBDs from human U1A protein as a model system to understand thermodynamic stability, RNA binding affinity and specificity of RBD family. The RBD1 binds very specifically to U1 snRNA stem loop II and plays an important role in pre-mRNA splicing. It also binds to 3'-UTR of its own pre-mRNA for autoregulation of U1A protein. The RBD2 adopts a typical $\beta\alpha\beta-\beta\alpha\beta$ tertiary fold found in other member of this family, but it does not bind any RNA substrates (Lu and Hall, 1995). We have determined NMR tertiary structure of RBD2 and compared its structure and backbone dynamics with those of RBD1. We have also made a number of chimeric proteins between RBD1 and RBD2 and compared their thermodynamic stability and RNA binding properties. These studies should help us identify amino acids that are critical for thermodynamic stability, RNA binding affinity and specificity of RBD family.

Su-Pos194

RADIATION EFFECTS ON THE NATIVE STRUCTURE OF PROTEINS; FRAGMENTATION WITHOUT DISSOCIATION. (J.H. Miller, D.A. Fedoronko, B.D. Hass, M. Myint and E.S. Kempner) NIAMS, NIH, Bethesda MD 20892

Several proteins (phosphoglycerate kinase, peroxidase, glucose 6-phosphate dehydrogenase, avidin and glutamate dehydrogenase) composed of one to six subunits were irradiated in the frozen state. Irradiated proteins were examined by size-exclusion chromatography and by denaturing gel electrophoresis. All these proteins eluted from the column as a single peak even though SDS PAGE showed cleavage of the polypeptide backbone of the monomers. Thus fragmentation of the subunits did not result in dissociation of the oligomeric structure.

Su-Pos195

SURFACE AREA AND VOLUME CHANGE IN PROTEIN FOLDING ((K.J. Frye, C. Perman, D. Shortle[6], and C.A. Royer)) School of Pharmacy, University of Wisconsin-Madison, Madison, WI 53706 and [6]Department of Biological Chemistry, The Johns Hopkins University School of Medicine, Baltimore, MD 21218

When proteins are denatured by chemical denaturants such as guanidine hydrochloride, the value of the change in free energy of unfolding is a linear function of the guanidine hydrochloride concentration the slope of which is referred to as the *m* value. The current opinion is that this *m* value correlates to the change in surface area (ΔA) exposed upon unfolding. In this presentation the pressure-induced denaturation of the model protein staphylococcal nuclease (nuclease) was probed by fluorescence spectroscopy. The unfolding of proteins by high pressure is the result of a decrease in the system volume (ΔV_u). This ΔV_u is also thought to correlate with ΔA. In order to establish whether a correlation exists between the *m* value and ΔA, xylose which is an osmolyte known to stabilize the protein native state was used. The stabilization of the native state occurs through the preferential exclusion of xylose from the protein by water. This preferential exclusion of xylose becomes more energetically unfavorable with increasing exposed surface area. Thus, if the variation in *m* values between a series of nuclease mutants is based on ΔA, then the dependence of the pressure stability of these mutants on xylose concentration should correlate with their measured *m* values. The xylose *m*-value for the m^+ (*m*-value greater than WT) mutant of nuclease, A69T + A90S, does appear to correlate with the guanidine hydrochloride *m*-value, however the volume change upon unfolding is about the same as WT. Thus, there is an interdependence of the *m*-value with the amount of surface area exposed upon unfolding, but not ΔV_u. However, the xylose *m*-value for the m^- (*m*-value less than WT) mutant, H121P, does not correlate with the guanidine hydrochloride *m*-value and the volume change is again about the same as WT.

Su-Pos196

TURBIDIMETRIC STUDIES OF LIMULUS COAGULIN GEL FORMATION. ((T.P. Moody and T.M. Laue)) Dept. of Biochemistry and Molecular Biology, Univ. of New Hampshire, Durham NH 03824.

Blood clots in the horseshoe crab *Limulus polyphemus* form from coagulin, a 16,582 Da product of the protein coagulogen. Coagulin gel formation was monitored using turbidity and its wavelength-dependence. The former provides a measure of the mass concentration of gel and the latter provides structural information. The structural models that describe the gel were limited to Rayleigh scatterers, long rods and long random coils. These structures are predicted to exhibit a wavelength-dependence of -4, -3 and -2, respectively. The turbidity of a Rayleigh scatterer is proportional to the product of its mass concentration and its molecular mass. Given a constant mass:length ratio, the turbidity of a long rod or a long random coil is proportional to its mass concentration. At equal mass concentration, the turbidity of a long rod can be 70 times that of a Rayleigh scatterer, and that of a long random coil can be 90 times that of a long rod of the same mass:length ratio. Gelation exhibits a lag phase, a gel initiation phase and a gel propagation phase. Neither turbidity nor the wavelength-dependence change much during the lag phase, suggesting that only Rayleigh scatterers are present during that phase. The gel initiation phase is the period of greatest change in the wavelength-dependence. It precedes turbidity changes, and probably coincides with rapid changes in the type of species present. The gel propagation phase, characterized by a wavelength-dependence of approximately -2, follows. During that phase, Rayleigh scatterers, long rods and long random coils are probably present, with the latter being the predominant source of the turbidity. Grant acknowledgments: NSF BIR-9314040, NSF DIR-9002027 and NSF DIR-8914571.

Su-Pos197

FORMATION OF SELF-ASSEMBLED MONOLAYER OF *DE NOVO* SYNTHETIC HEMOPEPTIDES ON QUARTZ AND ON GOLD: CHARACTERIZATION BY SPECTROSCOPY AND BY ELECTROCHEMISTRY. ((D. L. Pilloud, F. Rabanal, C. C. Moser and P. L. Dutton)). The Johnson Research Foundation, Department of Biophysics and Biochemistry, School of Medicine, University of Pennsylvania, Philadelphia, PA 19104-6089.

Self-Assembled Monolayers (SAM) of redox peptides on electrodes can be an important tool for the study of electron transfer mechanisms. *De novo* synthetic hemopeptides [1] were successfully chemisorbed onto gold, through the reaction between Cys 1 and the metal, and onto quartz after silanation with 3-mercaptopropyl(trimethoxy)silane. UV-absorption spectroscopy and circular dichroism reveal the presence of alpha-helical peptides. VIS-absorption spectroscopy gives information about the structure of the SAM, distinguishing between physisorbed and ligated hemes. By linear dichroism, the orientation of the hemes relatively to the substrate was determined to be around 40°. Finally, cyclic voltammetry measurements reveal the redox properties of the hemopeptides which can be compared with the results obtained by redox potentiometry in solution.

[1] Robertson D.E.; Farid, R.; Moser, C.C.; Urbauer, J.L.; Mulholland, S.E.; Pidikiti, R.; Lear, J.D.; Wand, A.J.; DeGrado, W.F.; Dutton, P.L. (1994) Nature 368, 425-32

Su-Pos198

SOLVATION FORCES BETWEEN COLLAGEN TRIPLE HELICES IN NONAQUEOUS SOLVENTS. ((N. Kuznetsova[†*], D.C. Rau[*], V.A. Parsegian[*] and S. Leikin[*])) [†]Engelhardt Inst. Mol. Biol., Russ. Acad. of Sci., Moscow, Russia, and [*]LSB/DCRT and ODIR/NIDDK, NIH, Bethesda, MD 20892.

We have previously measured spacing between collagen helices in water with varying osmotic pressure applied by a polymer excluded from the collagen phase. The exponential force-distance curve indicated that hydration forces dominate interactions as in many other systems. To elucidate further the origin of these forces, we have measured the controlled swelling of collagen in nonaqueous solvents. Three qualitative types of swelling curves are observed depending on the hydrogen-bonding ability of the solvent. Plots of excluded polymer weight concentration vs. spacing have an exponential-like shape in water and ethylene glycol, solvents that form hydrogen-bonded networks. A water-like dependence of swelling is also observed in formamide, but only with polymer concentrations large enough to prevent denaturation. In methanol, 2-methoxyethanol, and N-methylformamide (methylated solvents with an impaired hydrogen-bonding ability) swelling curves are no longer exponential-like, but become linear. Further solvent methylation causes complete loss of collagen response to the osmotic stress in ethanol, 2-propanol, and N,N-dimethylformamide, until the stress exceeds some threshold value and removal of solvent becomes favorable. These results provide strong evidence that forces between collagen helices in water are directly mediated by interconnected clusters of hydrogen bonded solvent molecules.

Su-Pos199

RESTORATION OF BIOLOGICAL FUNCTION UPON REFOLDING DOES NOT ENSURE RETURN OF A PROTEIN'S NATIVE STRUCTURE: ROOM TEMPERATURE PHOSPHORESCENCE STUDIES OF BOVINE ß-LACTOGLOBULIN ((Vinod Subramaniam, Ari Gafni and Duncan Steel)) The University of Michigan, Ann Arbor, MI 48109.

When bovine ß-lactoglobulin (ß-LG) was refolded after extensive denaturation in 6M guanidine hydrochloride (GuHCl), the functional activity of the protein, retinol binding, as measured by the enhancement of fluorescence, was completely recovered. In contrast, the room temperature phosphorescence (RTP) lifetime of the refolded protein was ~10ms, significantly shorter than the RTP lifetime of the untreated native protein (~19.4 ms). The lability of the freshly refolded protein was also studied, by following the change in fluorescence intensity at 385 nm upon incubation in 2.5M GuHCl, and it was found that the newly refolded protein is significantly more labile than untreated native protein. In contrast to the observed annealing of *E. coli* alkaline phosphatase (1), we found no changes in the lability or RTP decays of ß-LG over a period of several hours or days. Our results confirm reports by Hattori *et al.* (2), using conformation specific monoclonal antibodies to recognize native-like structure, that certain epitopes in the protein do not return to the native conformation upon refolding. We also use X-ray crystallographic structure data to interpret our results, and present them in the context of slow post-folding 'annealing' events in proteins (1). [Supported by NIA AG09761; ONR N00014-91-J-1938]

1. V. Subramaniam, N. C. H. Bergenhem, A. Gafni, D. G. Steel, *Biochemistry* **34**, 1133-36 (1995).
2. M. Hattori, A. Ametani, Y. Katakura, M. Shimizu, S. Kaminogawa, *J. Biol. Chem.* **268**, 22414-22419 (1993).

Su-Pos200

COOPERATIVE FOLDING OF G-CSF AT LOW pH. ((Carl G. Kolvenbach, Linda O. Narhi, John Philo, Mei Zhang and Tsutomu Arakawa)) Amgen Inc., Thousand Oaks, CA 91320.

Granulocyte-colony stimulating factor (G-CSF), a member of the four helical bundle family of cytokines, retains an unusually stable conformation at low pH. Circular dichroism analyses indicate retention of helical structure at low pH but a loss of native tertiary structure. Upon thermal denaturation at low pH we see the protein undergo a reversible cooperative transition, while at neutral pH it aggregates, yet the initial thermal transition occurs at essentially the same temperature. Sedimentation velocity indicates that the protein exists in a monomeric state at low pH and has only a slightly expanded or elongated conformation relative to that seen at neutral pH. The cooperative melting transition and compact structure both show that the low pH state of G-CSF is not a typical "A-state" or molten globule. Also, one would expect, electrostatically, inter- and intra-molecular interactions at low pH to cause an inherent instability as seen with other cytokines. Thus, G-CSF appears to be unique in its behavior at low pH.

Su-Pos201

FREE ENERGY ANALYSIS OF THE EFFECT OF A CHARGED SIDE CHAIN ON THE STABILITY OF AN α-HELIX ((Li Xiao, A. S. Yang and B. Honig)) Dept. of Biophysics, Columbia University, New York, NY 10032.

The effects of a charged side chain on the stability of a short helical peptide have been studied. A theoretical method originally developed to study α-helix formation was extended to include charged side chains. The approach involves the evaluation of gas phase conformational energies for both coil and helical states, while the solvation effect is treated with a continuum solvation model. The conformation space for coil states contains the main chain and the side chain torsion angles, while for helical states only side chain torsion angles are included. Free energies of helix formation are calculated and analyzed to obtain the pKa shifts of the charged side chain, which are compared to experimental results. Helix is stabilized mainly through hydrogen bond formation between the side chain and main chain atoms.

Su-Pos202

EFFECTS OF CAVITY FORMING MUTATIONS ON THE PHOSPHORESCENCE OF TRYPTOPHAN-109 IN THE CORE OF ALKALINE PHOSPHATASE ((N.C. Bergenhem[†], K.C. Wisser[†], J.A. Schauerte[†§], V.Subramaniam,[†¶], D.G. Steel[†¶],& A. Gafni[†§])) [†]Inst of Gerontology, [§]Dept of Biological Chemistry, [¶]Dept of Physics and Electrical Engineering, Univ of Michigan, Ann Arbor, MI 48109

The existence of long lived room temperature phosphorescence (RTP) in proteins is attributed to the rigidity of the local environment of the phosphorescing tryptophan (Trp) residue. To test this, we used alkaline phosphatase (AP), a protein with an approximately 2 second RTP emitted by Trp 109. Cavity forming mutants of AP were produced by replacing alanine residues with glycine residues in the immediate vicinity of Trp 109. It was expected that creating cavities near Trp 109 would alter the rigidity of the core, which could be monitored by RTP studies. Significant alterations in tryptophan phosphorescence properties were detected in these AP mutants, whose RTP lifetimes were significantly shorter than the 2 second lifetime observed for the wild-type. RTP studies also reveal significant diffrences between the two AP mutants and the wild-type AP in the temperature dependencies of their phosphorescence decay times. Our data shows the known break in the Arrhenius plot for the wild-type AP at 24 °C first described by Vanderkooi, et al (Proc. SPIE, 1640;473-477(1992)). However the mutants show an analogous break at a significantly lower temperature. This analysis provides information on the activation barriers to triplet state non-radiative processes, and changes within the protein that alter these activation barriers. The transition may reflect a structural change in the protein that alters the isolation of the core from the solvent.
(Supported by NIA AG09761)

Su-Pos203

PROTEIN FOLDING STUDIES OF TYROSINE-TO-PHENYLALANINE SUBSTITUTED MUTANTS OF RIBONUCLEASE A. ((D. Juminaga, R. Garduno-Juarez, M.A. McDonald, and H.A. Scheraga.)) Baker Laboratory of Chemistry, Cornell University, Ithaca, NY 14853-1301.

We have made three mutants of bovine pancreatic ribonuclease A, Y25F, Y92F, and Y97F, which correspond to phenylalanine substitutions of the three buried tyrosine residues in the native structure. Values of the molar extinction coefficient of these mutants at 275 nm are consistent with Tyr-25 and Tyr-97 being more buried than Tyr-92. Thermal unfolding and catalytic activity measurements indicate that the mutation of Tyr-25 or Tyr-97 significantly lowers the structural stability and catalytic activity of the native protein, while the mutation of Tyr-92 shows only a slight decrease of catalytic activity and no lost of structural stability. Single-jump experiments monitored by fluorescence indicate that the unfolding of disulfide-intact Y92F and Y25F consist of both fast and slow phases. This suggests that other tyrosines, in addition to Tyr-92 and Tyr-25, give rise to the fluorescence intensity change observed in the slow phase.

Su-Pos204

A HIGHER ORDER STRUCTURE AND ENERGETICS OF PEPTIDES *IN VACUO* REVEALED BY MASS SPECTROMETRY.

((I.A. Kaltashov, C. Fenselau)) Dept. of Chemistry and Biochemistry, University of Maryland Baltimore County, Baltimore, MD 21228.

Solvent-protein interactions have been traditionally thought to play a central role in folding proteins and maintaining their native conformations. Experimental techniques used traditionally to study higher order structure (NMR, X-ray crystallography, etc.) do not provide analysis of intrinsic structures of single biopolymers unaffected by neighboring molecules in solutions and crystals. We have recently employed mass spectrometry to develop a method that allows determination of conformations of biopolymers in a solvent-free environment [1]. Experimental measurement of the electrostatic repulsion in multiply protonated peptides provides intercharge distances, from which molecular geometry can be deduced with support from molecular modelling. The method has been initially tested on peptides, which were determined to possess rather rigid structures in the absence of solvent.

Thermochemical measurements have now been made on multiply charged melittin, a 26-meric peptide. These indicate that melittin is likely to maintain its α-helical structure in a solvent-free environment. This surprising result may provide an insight on the delicate balance between electrostatic repulsion and weak intramolecular forces.

[1] I.A.Kaltashov, D.Fabris, C.Fenselau. *J. Phys. Chem.* 1995, 99, 10046.

ANION CHANNELS

Su-Pos205

VOLTAGE-DEPENDENT CHANGES OF ANION AND TAURINE SELECTIVITY OF PHOSPHOLEMMAN CHANNEL MOLECULES.

((Gopal C. Kowdley, Zhenhui Chen, Larry R. Jones, Gabor Szabo, J. Randall Moorman)) Indiana University, Indianapolis, IN; University of Virginia, Charlottesville, VA.

Phospholemman (PLM), a 72 amino acid membrane protein, forms large conductance ion channels in planar lipid bilayers. These channels have the unique ability to switch in a voltage-dependent manner between conformations with different selectivities for anions and cations. In addition, these channels show a high degree of selectivity for the sulfonic amino acid taurine. We now find that PLM channels also exhibit transitions between conformations with different selectivities among anions. Currents were recorded in bi-anionic conditions with equimolar Na on the two sides of the membrane. The voltage protocol was a ramp for 5 sec from -100 mV to 0 mV followed by 5 sec at 0 mV. Leak currents have been subtracted. The current with a negative reversal potential during the ramp and positive value at 0 mV is relatively taurine-selective (T; 230 pS; $P_{taurine}$: P_{Cl} 5.4); the other is more Cl-selective (Cl; 170 pS; $P_{taurine}$: P_{Cl} 0.5). The voltage-dependence of the taurine-selective conformation is the same as that of the previously described cation-selective conformation, suggesting that they may be the same.

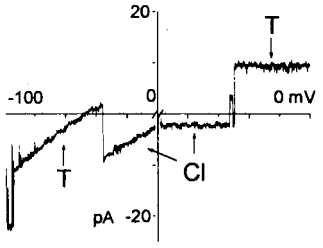

Su-Pos206

STRUCTURAL CHARACTERIZATION OF PHOSPHOLEMMAN BY MASS SPECTROMETRY, ELECTROPHORESIS, CD, AND EPR SPECTROSCOPY.

((G. H. Addona, S. H. Andrews, L. R. Jones* and D. S. Cafiso)). Department of Chemistry, University of Virginia, Charlottesville, VA 22901. *Department of Medicine and Pharmacology, Indiana University School of Medicine, Indianapolis, IN 46202.

Phospholemman (PLM), a 72 residue protein from muscle tissue, is a major kinase substrate that forms a small anion selective channel. PLM has an 18 residue hydrophobic domain and two cysteines. Mass spectrometry of DTT-reduced and unreduced PLM yields a single mass peak at 8409 Da for the reduced sample, equal to the calculated molecular weight, and a major peak at 16820 Da for the unreduced sample. By SDS-PAGE; the major band in the reduced sample corresponded to an M_r of 9 kDa and in the unreduced sample to 17 kDa. The unreduced samples included minor bands at higher M_r of 31 and 41 kDa. These higher bands indicate preferential aggregation states of PLM monomers. Evidence for membrane aggregation can also be obtained from the EPR spectra of PLM spin labeled at cysteines 40 and 42. Spin-labeled PLM was also analyzed by power saturation EPR. The Φ value, based on $\Delta P_{1/2}$ ratios, located these cysteines at the membrane surface consistent with the nearby location of a stop-transfer sequence. The CD of PLM yielded a helical content of approximately 31% in either the reduced or unreduced sample. This helical content and the placement of the cysteines, is consistent with the hydrophobic domain in a transmembrane α-helical configuration, and suggests a model for the channel structure.

Su-Pos207

SOME AGENTS INFLUENCING PERMEATION THROUGH THE RAT SKELETAL MUSCLE Cl^- CHANNEL.

((D.StJ. Astill, G.Y. Rychkov, M.L. Roberts, S.H. Bryant† and A.H. Bretag)) CABS, Univ. of South Australia and Physiology Department, Univ. of Adelaide, AUSTRALIA; and †Pharmacology & Cell Biophysics, Univ. of Cincinnati, USA

The Cl^- channel, rClC-1, was expressed in cultured Sf-9 insect cells using the baculovirus system. Whole-cell patch-clamping from a holding potential of -30 mV revealed large inwardly rectifying currents with saturating outward currents in response to depolarising voltage steps and rapidly deactivating inward currents for hyperpolarising steps. Action of blocking agents was assessed from dose-response curves for peak instantaneous currents induced by hyperpolarising voltage steps to -100mV with the following results: anthracene-9-carboxylate (A9C, IC50 = 21 μM), perrhenate (IC50 = 1.1mM) and zinc (IC50 = 2.2 mM). Cadmium has an effect similar to that of zinc and, like A9C, does not alter current kinetics, being rapidly (within seconds) effective on external application and readily reversible. A9C appears to act via a binding site that is normally occupied by Cl^- as the permeating anion, since block is enhanced by low extracellular Cl^- concentrations (Cl^- replaced by glutamate). Several other agents, including niflumate, perrhenate and 2,4-dichlorphenoxyacetate alter current kinetics in addition to their blocking action. The R(+) enantiomer of 2-(4-chlorophenoxy)-propionate, in contrast to the S(-) and other agents tested, increases both instantaneous and steady-state inward currents at very low concentrations (10nM to 10μM).

Su-Pos208

Ca^{2+}-ACTIVATED Cl^- CHANNELS IN CELLS FROM TRACHEAL SMOOTH MUSCLE OF THE GUINEA-PIG.

(Y. Imaizumi, S. Henmi, K. Muraki and M. Watanabe) Dept. of Chem. Pharmacol. Nagoya City Univ., Nagoya 467, Japan (Spon. by W. Giles)

In single smooth muscle cells freshly isolated from guinea-pig trachea, application of 10 mM caffeine induced a phasic inward Cl current at a holding potential of -60 mV when the pipette solution contained mainly CsCl. Occasionally, openings of large conductance single channels were recorded during caffeine-induced macroscopic currents. The opening of large conductance channel was also observed in about 5% patches examined in the cell-attached mode just after application of caffeine under conditions were Ca^{2+}-activated K^+ channels were blocked by tetraethylammonium (TEA). In the inside-out mode, channel activity with a conductance of 340 pS was occasionally observed in pCa 6.0 solution but not in pCa 7.0 solution under conditions of symmetrical 130 mM TEA Cl. This channel activity ran down within several minutes. To avoid this after the cell-attached mode was established, the cell was permeabilized by applying B-escin from a separate pipette. Under these conditions, opening of the large conductance channel was observed for more than 10 min following elevation of $[Ca^{2+}]_i$. The reversal potential of this current depended on the transmembrane gradient of Cl concentration but not on that of cations. The open probability of this channel at +40 mV increased from 0.1 to 0.8 when $[Ca^{2+}]_i$ was raised from pCa 7.0 to 5.0. This Cl channel current contributes in part to caffeine-induced macroscopic Cl current in tracheal smooth muscle cells of the guinea-pig.

Su-Pos209

IDENTIFICATION AND ROLE OF Cl CHANNELS IN BASAL MEMBRANES OF ELECTRORECEPTIVE AMPULLARY EPITHELIUM FROM SKATES. Jin Lu and Harvey M. Fishman, Department of Physiology & Biophysics, University of Texas Medical Branch, Galveston, TX 77555-0641

A small current oscillation (1 nA) originating in basal membranes of the ampullary epithelium, isolated from skates, is essential for electroreception (Lu and Fishman, Biophys. J. 69: *in press*, 1995). We identified the types of basal membrane ion channels necessary for generation of the oscillation by use of blockers and ion substitutions. From spectral analysis of the current through a voltage-clamped isolated organ at 20°C, the fundamental frequency of oscillation was 32 Hz. The oscillation ceased 8 min after changing the basal-side solution to a Cl-free solution, and reappeared 10 min after return to control saline solution. Both DIDS (100 μM, a Cl channel blocker) and niflumic acid (0.5 mM, a specific blocker of Cl(Ca) channels) when added to the basal solution abolished the oscillation within minutes. Rapid suppression of the oscillation by both niflumic acid and DIDS is consistent with the presence of Cl(Ca) channels. Also, after elimination of the oscillation, the electrical sensitivity of an organ was markedly reduced (Lu and Fishman, op. cit.). These results suggest that Cl(Ca) channels: (1) are present in basal membranes of electroreceptor cells of the ampullary epithelium, and (2) are necessary for the generation of an oscillation which is important in synaptic transmission from presynaptic (basal) membranes to afferent nerves.
Supported by ONR grant N00014-90-J-1137

Su-Pos210

$[Na^+]_i$ -DEPENDENT ACTIVATION OF Ca^{2+} -ACTIVATED CHLORIDE CURRENT IN RABBIT VENTRICULAR MYOCYTES. ((S. KAWANO, A. KURUMA and M. HIRAOKA,))
Department of Cardiovascular Diseases, Medical Research Institute. Tokyo Medical and Dental University, Tokyo , Japan.

Ca^{2+}-activated chloride current, $I_{Cl(Ca)}$, could be activated by Ca^{2+}-induced Ca^{2+} release mechanism (CICR). In cardiac myocyte, it is known that CICR can be triggered by not only Ca^{2+} current (I_{Ca}) but also Na^+/Ca^{2+} exchanger. In this study, we examined how Na^+/Ca^{2+} exchanger contributed to the activation processes of $I_{Cl(Ca)}$. By using patch clamp method, we recorded whole cell currents in single ventricular myocytes from rabbit hearts. While perfusing the cells internally with 1 μM free Ca^{2+} and various concentrations of Na^+_i (5, 10, and 20 mM), $I_{Cl(Ca)}$ could be observed after blocking I_{Ca} by nicardipine (5 μM) but abolished by Ni^{2+}, indicating the activation by Na^+/Ca^{2+} exchange. The amplitudes of $I_{Cl(Ca)}$ activated by exchanger were augumented with increasing $[Na^+]_i$ in a concentration dependent manner. The contributions of exchanger to $I_{Cl(Ca)}$ activation were 26 %, 50 % and 83 % of total $I_{Cl(Ca)}$ in 5, 10 and 20 mM $[Na^+]_i$, respectively. However, total $I_{Cl(Ca)}$ was nearly constant amplitude at each $[Na^+]_i$ and appeared not to be additive to the I_{Ca} -dependent and exchanger-dependent components. Therefore, we conclude that both I_{Ca} and Na^+/Ca^{2+} exchanger could activate $I_{Cl(Ca)}$, and both systems operate as back-up for Ca^{2+} entry into cardiac cells.

Su-Pos211

Na^+/Ca^{2+} EXCHANGE CONTRIBUTES TO THE ACTIVATION OF CA^{2+}-ACTIVATED CHLORIDE CURRENT IN RABBIT VENTRICULAR MYOCYTES. ((A. KURUMA, M. HIRAOKA, and S. KAWANO))
Department of Cardiovascular Diseases, Medical Research Institute. Tokyo Medical and Dental University, Tokyo , Japan.

Ca^{2+}-activated chloride current, $I_{Cl(Ca)}$, could be activated by Ca^{2+}-induced Ca^{2+} release mechanism (CICR), which is mediated by Ca^{2+} current, (I_{Ca}), and Ca^{2+} release from sarcoplasmic reticulum. In this study, we examined whether Ca^{2+} entry through Na^+/Ca^{2+} exchange might contribute to the activation process of $I_{Cl(Ca)}$. We used single ventricular myocytes from rabbit hearts and recorded whole cell currents by patch clamp methods. While the cells were internally perfused with the solution contained 1 μM free Ca^{2+} and no Na^+, nicardipine (5 μM) completely blocked both I_{Ca} and $I_{Cl(Ca)}$. However, when cells were loaded with 20 mM Na^+_i, $I_{Cl(Ca)}$ was not blocked by application of nicardipine, inspite of complete inhibition of I_{Ca}. The kinetic properties of $I_{Cl(Ca)}$ in Na^+-loaded cells showed slow activation and inactivation compared with those in Na^+-nonloaded cells. In the presence of nicardipine, $I_{Cl(Ca)}$ in Na^+ loaded cells was completely blocked by the elimination of Na^+ or Ca^{2+} from bath solutions, or the application of TTX or Ni^{2+}, suggesting contributions of Na^+/Ca^{2+} exchange. The current was also blocked by the bath application of caffeine, ryanodine or thapsigargin. We conclude that in Na^+-loaded conditions $I_{Cl(Ca)}$ can be activated by CICR triggere via not only I_{Ca} but also Na^+/Ca^{2+} exchange.

Su-Pos212

ALTERED VOLTAGE-DEPENDENT ACTIVATION OF A SKELETAL MUSCLE Cl^- CHANNEL CAUSES MYOTONIA IN THE FAINTING GOAT. ((C. L. Beck, Ch. Fahlke, and A. L. George)) Vanderbilt University, Nashville, TN 37232.

Voltage-gated Cl^- channels are essential for the normal excitability of skeletal muscle fibers. This principle was established by studies of the myotonic (or fainting) goat, an animal affected by a dominantly inherited syndrome characterized by diminished sarcolemmal Cl^- conductance (g_{Cl}) leading to hyperexcitability, repetitive action potential generation, and delayed muscle relaxation. Similar phenotypes characterize the recessive ADR mouse and both recessive and dominant human myotonia congenita. Mutations in the mouse and human skeletal muscle Cl^- channel isoform, ClC-1, have been identified to explain the molecular genetics of these syndromes. Similarly, we have detected a missense mutation in the myotonic goat skeletal muscle chloride channel (gClC-1) that results in the substitution of proline for a highly conserved alanine residue within the carboxy-terminus of the protein. To ascertain the effects of this substitution on Cl^- channel function, we created the mutation (A885P) in a recombinant human skeletal muscle chloride channel (hClC-1) and examined its functional properties in *Xenopus* oocytes by two-electrode voltage clamp recording. Chloride currents recorded from oocytes expressing either wild-type (WT) hClC-1 or A885P were similar with respect to maximal amplitude, general features of their gating kinetics, and I–V relationships. However, the mutant exhibited a dramatic ~ +65 mV shift in the midpoint of steady-state activation. This shift results in a substantially decreased open probability of the mutant relative to WT within the physiological voltage range and is the likely cause of the decreased g_{Cl} in myotonic muscle. Thus, dominant myotonia may be caused by a change-of-function rather than a loss-of-function Cl^- channel mutation.

Su-Pos213

THE PHENOL DERIVATIVES GOSSYPOL AND NDGA BLOCK CHLORIDE CHANNELS ACTIVATED AFTER CELL SWELLING ((Martin Gschwentner, Alex Susanna, Sabine Hofer, Andreas Jungwirth[§], Julian Frick[§] and Markus Paulmichl)) Department of Physiology, Fritz-Pregl-Str. 3, University of Innsbruck, A-6020 Innsbruck, and [§]Department of Urology, SLKA, Müllner Hauptstr., A-5020, Salzburg, Austria, Europe.

Reduction of extracellular osmolarity is, in eukaryotic cells, accompanied by cytoplasmatic swelling. The concerted activation of chloride and potassium channels is a prerequisite for the cells under this condition to regulate the volume back to resting conditions. I_{Cln}, a cloned chloride channel identified to be crucial for regulatory volume decrease (RVD), can be blocked by NPPB, a substance structurally related to the phenol derivatives gossypol, a compound isolated from cotton seeds, and NDGA (nordihydroguaiaretic acid). Here we show that gossypol and NDGA are able to selectively block the swelling-dependent chloride channels in NIH 3T3 fibroblasts (IC_{50} ≈4 μM and ≈3 μM, resp.) and the depolarization of the membrane potential observed in fibroblasts after reduction of extracellular osmolarity. The cAMP-dependent chloride current elicited in CaCo cells is much less sensitive to the two substances tested. The binding site for the two phenol derivatives to I_{Cln} seems to be distinct from but closely related to the nucleotide binding site identified as GxGxG, a glycine repeat located at the predicted outer mouth of the I_{Cln} channel protein. This conclusion was drawn from experiments where both substances were added in the presence of TDP, a nucleotide known to bind to the presumed nucleotide binding site but unable to block the swelling dependent chloride current. In conclusion, gossypol as well as NDGA are able to directly impede swelling-dependent chloride channels in NIH 3T3 fibroblasts.

Su-Pos214

EXPRESSION OF MOUSE *mdr1a* P-GLYCOPROTEIN INCREASES THE RATE OF ACTIVATION OF SWELLING-ACTIVATED CHLORIDE CURRENTS((T.D.Bond, C.F.Higgins, M.A.Valverde)) NDCB, Univ. of Oxford, Oxford, OX3 9DU, UK. (Spon. by D.N.Sheppard)

Regulatory Volume Decrease (RVD) in hyposmotically swollen cells has been shown to result from the concomitant exit of chloride and potassium and osmotically driven water. A type of swelling-activated chloride conductance, thought to be involved in RVD, has been electrophysiologically characterised as an outwardly rectifying, DIDS and tamoxifen sensitive conductance. Recent evidence suggests that human multidrug-resistance (MDR) P-glycoprotein may function as a regulator of this type of swelling-activated chloride current. We have now investigated whether the murine MDR P-glycoproteins also regulate this conductance. In rodents three closely related MDR homologues have been identified (*mdr1a, mdr1b* and *mdr2*) although only the products of *mdr1a* and *mdr1b* confer drug resistance. A swelling-activated chloride conductance was examined in Chinese Hamster Ovary (LR73) cells permanently transfected with *mdr1a* (LR-1a) and *mdr1b* (LR-1b) full length cDNAs using the whole-cell patch clamp technique. Cells were exposed to solutions of varying tonicities (10, 20, 40% hyposmotic) and the swelling-activated chloride conductances monitored. These chloride currents were inhibited by tamoxifen (10μM), dideoxyforskolin (100μM) and DIDS (100μM) in all three cell lines. LR-1a cells developed larger currents after a 3 minute exposure to small changes (7-20%) in bath osmolarity than both parental (LR73) and LR-1b cells. However, no differences in the magnitude of currents were observed among the three cell lines after exposure to a larger reduction (40%) in bath osmolarity. Similarly, once this swelling-activated chloride conductance reaches a steady state value (approx. 10 min.) no difference in the magnitude of currents was seen in all three cell lines at low (20%) hypotonic shocks (LR73: 80±11pA/pF(n=5); LR-1a: 89±11pA/pF(n=5); LR-1b: 85±17pA/pF(n=3)). A Ca^{2+} dependent, tamoxifen resistant potassium conductance was also identified in these cells. This conductance was not affected by changes in bath osmolarity and/or expression of the mouse P-glycoproteins. These observations suggests that P-glycoprotein-1a expression shifts to the left the time and stimulus response curves of the swelling-activated chloride channel without affecting the steady-state level.

Su-Pos215

PERMEATION PROPERTIES OF VOLUME REGULATED ANION CURRENT IS DEPENDENT ON ANIONIC COMPOSITION. ((I. Levitan and S.S. Garber)) Medical College of PA & Hahnemann Univ., Philadelphia, PA 19129.

Volume regulated Cl^- currents in human myeloma cells are induced by exposure to an extracellular hyposmotic solution. We have addressed the hypothesis that glutamate competes with Cl^- through the same permeation pathway. Reversal potential (V_r) and conductance were measured when the molar ratio of glutamate and Cl^- ions ([Glu^-]/([Glu^-]+[Cl^-]) was varied from 0.0 to 1.0 in extracellular solutions of constant ionic strength. The pipette solution was invariant, containing 120 mM Glu^- + 0.2 mM Cl^-. The Glu^-/Cl^- permeability ratio (P_{Glu^-/Cl^-}), calculated from V_r, was 0.17 ± 0.02 with a molar ratio of 0.0. Increasing the molar ratio to 0.1 or 0.2 resulted in a of P_{Glu^-/Cl^-} to 0.27 ± 0.08 and 0.29 ± 0.04, respectively. Further increasing the molar ratio ≥ 0.3 returns P_{Glu^-/Cl^-} back to 0.17 ± 0.06. The anomalous mole fraction dependence of P_{Glu^-/Cl^-} suggests that this volume regulated Cl^- channel can be occupied by more than one anion at a time. This result implies that Glu^- and Cl^- complete for the same permeation pathway. The conductance of the volume regulated current saturates at Glu^-/Cl^- molar ratios ≤ 0.4 and decreases as the molar ratio approaches 1.0. Volume regulated currents in this cell line exhibit voltage dependent inactivation independent of extracellular anionic composition. The midpoint of inactivation shifted from 90 mV ± 3 mV for a molar ratio of 0.0 to a less depolarized volume of 68 mV ± 3 mV for molar ratio of 1.0. Together, these results show that extracellular anionic composition has a direct effect on the functional properties of volume regulated anion currents. Supported by NIH DK46672 and an AHA Established Investigator Fellowship.

Su-Pos216

GLUTAMATE INDUCES LARGE CONDUCTANCE ANION CHANNEL ACTIVITY IN ASTROCYTES. ((E. Scemes and D.C. Spray)) Dept. Neurosci., A. Einstein Coll. Med., Bronx, NY and Dept. Physiol., Univ. Sao Paulo, Brazil.

Large conductance anion channels have been described in a variety of cell types, including astrocytes, where their role is generally believed to lie in cell volume regulation. We have previously shown that astrocyte large conductance (360-400 pS) anion channels are not activated during the time course (3-5 min) of astrocyte regulatory volume decrease following moderate hyposmotic shock (Scemes et al, Soc. Neurosci. Abst. 21:878, 1995). We have now investigated whether action of another swelling-inducing agent, glutamate, involves activation of these channels. Astrocytes were exposed to l- or d-glutamate (100 μM) and channel activity was recorded using patch clamp techniques. Large anion channel activity was not observed in cell-attached (N=6) recordings from astrocytes exposed to l-glutamate but was recorded in 55% (5 of 9) of the patches at about 5-7 min after application of d-glutamate. After washing out either glutamate steroisomer, channel activity was present in 70-90% (11 of 16) of the excised (inside-out or outside-out) patches of astrocytes. Such channel activities had a similar slope conductance (350-400 pS) and voltage dependence ($V_0 = \pm 35$ mV) as those seen in 17% (7 of 41) of the excised patches of untreated astrocytes. Under inside-out patch configuration, l-glutamate did not affect the conductance or the voltage-dependence of the large anion channels. These results show that large conductance anion channel activity is induced by astrocyte exposure to glutamate, suggesting their participation in processes underlying excitoxicity.

Su-Pos217

EXTRACELLULAR CATIONS MODIFY VOLTAGE-DEPENDENT INACTIVATION OF A CELL SWELLING-ACTIVATED Cl^- CHANNEL. ((J. Anderson, M. Madan and D. Fedida)) Dept. of Physiology, Queen's University, Kingston, Ont., CANADA K7M 3N6.

In a human small cell lung cancer cell line (H69AR), we characterized the time- and voltage-dependent inactivation of a swelling-activated Cl^- current using single channel and whole-cell patch clamp techniques. Cells were swelled in 210 mOsm solutions containing either NaCl (NaCl-210) or N-methyl-D-glucamine (NMDG)-Cl (NMDG-210) as the major ionic species. Pipette solutions contained 130 CsCl or CsAsp, HEPES, EGTA and ATP/GTP. Inactivation of the current was best fit with a dual exponential function plus a maintained, non-inactivating current component. In NaCl-210 (1 Mg^{2+}), the slow time constant of inactivation was voltage-dependent (3.1 ± 0.7 s at +60 mV; 1.3 ± 0.4 s at +100 mV) while the fast time constant was independent of voltage (180 ± 40 msec at +60 mV, 210 ± 70 msec at +100 mV). The midpoint of inactivation ($V_{0.5}$) was 64 ± 8 mV and the slope factor (s) was 9.7 ± 0.4 mV. Substitution of intracellular Cl^- by aspartate did not affect inactivation. In NMDG-210 (0 Mg^{2+}), inactivation was slower, much less complete (larger non-inactivating component) and the steady-state inactivation relationship was shifted to depolarized potentials ($V_{0.5}$ = 81 ± 9 mV, s = 16.7 ± 9 mV). This effect could be so profound that some cells showed no significant inactivation at depolarizations greater than +100 mV. Addition of 10 mM Mg^{2+} to NMDG-210 caused a marked return of the steady-state inactivation curve back to the left ($V_{0.5}$ = 63 ± 9 mV, s = 9.3 ± 0.3 mV). Kinetic analysis of single channels revealed 2 open times and at least 2 closed time distributions. Addition of NMDG-210 moved the channel to a predominantly long-lived dwell state while addition of Mg^{2+} shifted channel gating to predominantly short open lifetimes. Voltage-dependent inactivation of this swelling-activated, outwardly rectifying Cl^- current is determined by the ability of extracellular cations to affect gating of this channel. Supported by M.R.C., Canadian Cancer Society.

Su-Pos218

VOLUME-SENSITIVE CHLORIDE CURRENTS (I_{Cl^-}) IN HUMAN MONOCYTE-DERIVED MACROPHAGES (HMDM). ((G.R. Ehring)) Dept. of Physiology and Biophysics, UC Irvine, CA 92717

Cell-swelling induced by either hyperosmotic internal solutions or hypo-osmotic bath solutions activated an outwardly rectifying chloride conductance in HMDM. In symmetrical (150 mM) Cl^- solutions the current reversed at 0 mV; substitution of glutamate or aspartate for the Cl^- in the internal solution shifted the reversal potential to -50 mV indicating the anion selectivity of this current. I_{Cl^-} was blocked by NPPB (IC_{50} = 50 μM); NPPB block was not affected by voltage. DIDS blocked I_{Cl^-} in a voltage-dependent manner

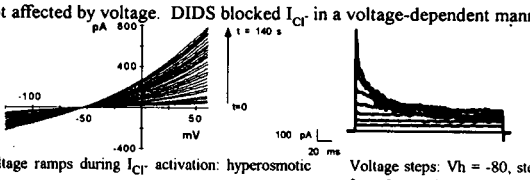

Voltage ramps during I_{Cl^-} activation: hyperosmotic CsGlu internal, M.R. bath. Break in at t = 0.

Voltage steps: Vh = -80, steps from 0 to + 140 mV.

(IC_{50} = 25 μM at +40 mV and > 500 μM at -40 mV). Unlike I_{Cl^-} reported in T and B lymphocytes and neutrophils, I_{Cl^-} in HMDM showed time- and voltage-dependent inactivation during steps to > +40 mV. The voltage for 50% inactivation was ~ 60 mV. Supported by a grant from Pfizer, Inc.

Su-Pos219

PURINERGICALLY STIMULATED Cl CHANNELS, BUT NOT cAMP STIMULATED ONES, ARE COUPLED TO MUCIN SECRETION IN HT29-Cl.16E. ((X.W. Guo, D. Merlin, C. Laboisse and U. Hopfer)) Dept. of Physiology and Biophysics, CWRU, Cleveland, OH 44106 and Université de Nantes, Faculté de Médecine, Groupe de Recherche Fonctions Sécrétoires des Epitheliums Digestifs (CJF INSERM 1994-04), F-44035 Nantes, France.

To obtain information about the coupling of Cl and mucin secretion, simultaneous Cl conductance and capacitance measurements were made in the mucin-secreting cell line HT29-Cl.16E and its sister cell line, HT29-Cl.19A, which lacks mucin secretion, but otherwise closely resembles Cl.16E. The whole cell patch clamp method was employed with the phase tracking method for the capacitance measurements. Purinergic stimulation with 200 μM extracellular ATP transiently increased the Cl conductance in both cell lines, but only the capacitance in the mucin-secreting Cl.16E: Peak Cl conductances increased from baseline 1.3±0.5 nS to 18 ±.5 nS in Cl.16E and from 1.2±0.5 nS to 24±2 nS in Cl.19A with a life-time of about 40 sec; the cell capacitance was increased by 17% from a baseline of 22±1 pF in Cl.16E, but only 1% from a baseline of 18±1 pF in Cl.19A. These results are consistent with the presence of mucin granules that fuse with plasma membrane in Cl.16E, but not in Cl.19A. To probe the location of the purinergically stimulated Cl conductance, 100 nM wortmannin was applied as inhibitor of granule fusion. This compound inhibited 50% of the purinergically stimulated Cl conductance in Cl.16E, but had no effect in Cl.19A. At the same time, wortmannin inhibited 80% of the capacitance increase stimulated by extracellular ATP in Cl.16E. These results indicate that 1) wortmannin does not directly inhibit activation of Cl conductance; 2) more than 50% of the purinergically activated Cl conductance reaches the plasma membrane through fusion of granules; 3) the residual Cl conductance is constitutively located in the plasma membrane. In the same Cl.16E cell line, elevation of cAMP by 10 μM Forskolin increased Cl conductance by 7 nS, while increasing capacitance by less than 1%. These results indicate that the cAMP-activated Cl conductance is also located in the plasma membrane and not in the granule membrane. The conclusion about the location of cAMP-activated Cl conductance is consistent with previously reported results that the short-circuit current in monolayers stimulated by intracellular cAMP and supermaximal doses of a purinergic agonist is additive even though the granule fusion, measured as mucin release, is driven predominantly by the purinergic agonist. Supported by the grants from the Cystic Fibrosis Foundation and NIH (HL-07714).

Su-Pos220

DIRECT EVIDENCE OF DOWN-REGULATION OF CALCIUM-DEPENDENT CHLORIDE CURRENT BY INOSITOL(3,4,5,6) TETRAKISPHOSPHATE IN CFPAC-1 CELLS. ((M.W.Y. Ho[1], S.B. Shears[2], K. Bruzik[3], M. Duszyk[4], and A.S. French[5])) [1]Depts. of Physiology & [4]Medicine, University of Alberta, Edmonton, Alberta, Canada., [2]Inositol Lipid Section, NIEHS, Research Triangle Park, NC, USA., [3]Dept. of Medicinal Chemistry, University of Chicago, Chicago, IL, USA., [5]Dept. of Physiology & Biophysics, Dalhousie University, Halifax, Nova Scotia, Canada.

Activation of purinergic receptors by 10^{-6}M ATP induced a calcium (Ca^{2+})-dependent whole cell chloride current in CFPAC-1 cells. This current showed strong outward rectification and could be blocked by 50 μM DIDS. By-products from the activated inositol phosphate cascade had several different effects on the current. Addition of 10 μM Ins(3,4,5,6)P_4 to the pipet solution completely blocked the action of ATP, whereas Ins(1,4,5,6)P_4 had no effect on whole cell current. However, other inositol tetrakisphosphates such as Ins(1,3,4,5)P_4 and Ins(1,3,4,6)P_4 enhanced the effects of ATP. These results suggest that inositol tetrakisphosphates play an important role in regulating the ATP-activated Ca^{2+}-dependent chloride channels.
Supported by the Canadian Cystic Fibrosis Foundation and the Alberta Heritage Foundation for Medical Research.

Su-Pos221

THE EFFECT OF DIVALENT CATIONS ON CFTR GATING. ((K. L. Gunderson and R. R. Kopito)) Stanford University, Stanford, CA 94305.

Previous studies on CFTR gating suggest that ATP hydrolysis at NBF1 and NBF2 play a key role in opening and closing the channel. Most hydrolysis reactions use divalent cations as a cofactor to facilitate hydrolysis, with a strong preference for magnesium ions over calcium ions. We examined the effect of replacing MgATP (1mM) with CaATP (1 mM) on CFTR gating kinetics. The major change in gating kinetics was a dramatic decrease in the closing rate of CFTR, leading to prolonged open burst durations. The mean open burst duration increased at least tenfold compared with the MgATP induced open burst duration (>5 sec vs. 500 msec). In addition, we examined the effect of LaATP and TbATP, where La and Tb are analogs of Ca^{2+}, and observed a much greater effect on the open burst duration of CFTR (>> tenfold increase). The lanthanides may serve as a useful set of probes for characterizing the structure and function of the purified CFTR molecule. We also investigated the effect of Zn^{2+} on CFTR gating. Zn^{2+} covalently modifies the channel, changing CFTR's gating kinetics even after Zn^{2+} has been washed out and replaced with Mg^{2+}. Addition of Zn^{2+} leads to a semi-permanent decrease in both the the opening and the closing rate of the channel. Upon washout of Zn^{2+} and addition of MgATP, the channel retains its altered gating kinetics. This effect was immediately reversible upon addition of DTT. These data suggest that Zn^{2+} covalently interacts with cysteine sulfhydryl residues to modify both the opening and closing rate of the channel.

Su-Pos222

ATP CONDUCTANCE OF THE CFTR CHLORIDE CHANNEL.
((R. Grygorczyk, J.A. Tabcharani and J.W. Hanrahan))
Department of Physiology, McGill University, Montréal, Québec, Canada H3G 1Y6.

CFTR is a low-conductance Cl channel which mediates cAMP-stimulated Cl secretion by epithelia. It has also been reported to have substantial conductance in high ATP solutions (~5 pS) and is proposed to mediate ATP efflux during autocrine regulation of other apical membrane Cl channels. The aim of this study was to measure the ATP conductance of wild-type CFTR stably expressed in Chinese hamster ovary cells. In the cell-attached configuration with 100 mM Mg-ATP solution in the pipette and 140 mM NaCl in the bath, exposing cells to forskolin (10 μM) or forskolin + 8-Br-cAMP (500 μM) caused the activation of a low-conductance channel with kinetics identical to those of CFTR. These single channel currents were negative at the resting membrane potential (pipette potential V_p=0 mV), consistent with Cl diffusion from the cell into the pipette. The transitions decreased in amplitude but did not reverse direction when V_p was clamped at negative potentials (≤-80 mV) to increase the driving force for inward ATP flow. There was also no reversal when currents were recorded using excised, inside-out patches under essentially biionic conditions (Cl_{in}/ATP_{out} or ATP_{in}/Cl_{out}), although PKA-activated chloride currents were clearly observed in the same patches. With 154 mM NaCl solution in the bath and a mixture of 81 mM ATP and 77 mM Cl in the pipette, the single channel I/V curve reversed near the predicted equilibrium potential for chloride. Finally, in the whole-cell configuration with NaCl in the bath and 100 mM MgATP or TrisATP in the pipette, cAMP-stimulated cells had time-independent, outwardly rectifying currents consistent with Cl selectivity. The whole-cell currents did reverse near -60 mV under these conditions, however the inward current at -100 mV was less than -10 pA/cell, which is approximately the leak current expected for a typical (10 gigaohm) seal between the plasma membrane and glass pipette. In summary, we found no evidence for CFTR-mediated electrodiffusion of ATP. *Supported by the Canadian CFF, MRC(Canada) and NIH(NIDDK).*

Su-Pos223

VOLTAGE DEPENDENT BLOCK OF SINGLE CFTR CHANNELS BY INTRACELLULAR ANIONS. **((Paul Linsdell and John W. Hanrahan)) Dept. Physiology, McGill University, Montréal, Québec, Canada.**

CFTR is a low conductance Cl channel regulated by phosphorylation and ATP. In symmetrical Cl solutions, single CFTR channels exhibit a linear I-V relationship; however, replacement of intracellular Cl by larger anions leads to an outward current rectification stronger than that predicted by the Goldman-Hodgkin-Katz relationship. Using single channel recording from Chinese hamster ovary cells stably expressing CFTR, we have found that both glutamate and gluconate ions cause a rapid, voltage-dependent block of CFTR when applied to the inside, but not the outside of excised patches. Both anions appear to interact with a site 30-50% of the way through the membrane electric field from the inside. The voltage dependence of block was dependent on external Cl concentration, consistent with the multi-ion nature of the CFTR pore. Our results suggest that outward rectification of single CFTR currents results from a combination of asymmetrical Cl concentrations and voltage-dependent block by intracellular anions. In addition, we find that high concentrations of intracellular sucrose, sorbitol and urea cause a voltage-independent decrease in CFTR conductance, consistent with a rapid block of the channel by these osmolytes. ***Supported by MRC, Canadian CF Foundation, and NIH(NIDDK).***

Su-Pos224

MUTATION OF PHOSPHORYLATION SITES ALTERS ATP DEPENDENT REGULATION OF CFTR. ((M.C. Winter, M.J. Welsh)) Howard Hughes Medical Institute, University of Iowa, Iowa City, IA 52242.

The activity of CFTR Cl channels is regulated by two processes, PKA phosphorylation of the R domain and binding and hydrolysis of ATP by the nucleotide binding domains (NBDs). To examine the relationship between these two processes, we mutated several PKA phosphorylation sites and studied the expressed channels with the excised patch clamp technique. We found that in the presence of PKA and 1mM ATP, mutation of various sites had different effects on open-state probability (Po): wt 0.42; S660A 0.30; S737A 0.42; S795A 0.19; S660,737,795,813A 0.19. The mutants had a mean burst duration similar to that of wild-type CFTR. Thus the mutants altered Po by altering the duration of the long closed times between bursts. Our previous work showed that the duration of long closed times between bursts is controlled by ATP concentration. Therefore we asked whether mutation of phosphorylation sites would alter ATP-dependent regulation. We found that mutation of the phosphorylation sites altered the relationship between ATP concentration and Po. The ATP concentration required to generate half-maximal activity (EC50) was (in μM): wt 60; S660A 900; S737A 200; S795A 3000. However maximum Po (Pmax) at high ATP concentrations was approximately the same for wild-type and variant channels (Po ~ 0.53). Alteration of EC50 without a change in Pmax suggests that the phosphorylation state of CFTR affects binding of ATP to the NBDs. If a step either prior or subsequent to ATP binding were altered, we would have expected a change in both EC50 and Pmax. These data suggest a complex interaction between the R domain and the NBDs and suggest that the R domain serves as more than just a "plug" to control channel gating.

Su-Pos225

IDENTIFICATION OF CHANNEL-LINING RESIDUES IN THE M6 MEMBRANE-SPANNING SEGMENT OF CFTR AND THE POSITION OF THE ANION-SELECTIVITY FILTER. ((Myles H. Akabas and Min Cheung)) Ctr. for Mol. Rec, Columbia Univ., New York, NY, 10032.

In order to understand the structural bases of ion conduction and selectivity in CFTR we sought to identify the amino acid residues in and flanking the M6 membrane spanning segment (329-353) that line the ion channel of CFTR. Using the scanning cysteine accessibility method we found that charged sulfhydryl-specific reagents, derivatives of methanethiosulfonate, irreversibly altered conduction in oocytes expressing the mutants I331C, L333C, R334C, K335C, F337C, S341C, I344C, T351C, R352C, and Q353C (the mutant R347C has not yet been tested). We infer that the side chains of the corresponding wild-type residues are exposed in the channel lumen. The exposed residues from F337 to I344 form a stripe on an α helix suggesting that this region may be α helical. The exposure of 3 consecutive residues at the cytoplasmic end of M6 implies that this region does not have a fixed α helical secondary structure. By measuring the relative rates of reaction of the negatively charged MTSES and the positively charged MTSEA with channel-lining residues we are locating the position of the anion selectivity filter. Supported by NIH NS30808, the New York Heart Association and the Klingenstein Foundation.

Su-Pos226

DISTRIBUTION OF CONDUCTANCE STATES REVEALS A POSSIBLE MULTIMERIC STRUCTURE OF CFTR CHLORIDE CHANNEL. ((Jiying Zhao, Tao Tao and Jianjie Ma)) Dept of Physiology and Biophysics, Case Western Reserve Univ., Cleveland, Ohio 44106. (Spon. by J. Whittembury)

To study regulation of conductance states of the CFTR channel, we expressed the wild type CFTR protein in HEK 293 cells, and isolated microsomal membrane vesicles for reconstitution studies in lipid bilayer membranes. We found that the CFTR channel contained at least three conductance states (H, M and L), which, under certain conditions, could gate independently from each other. In 200 mM KCl, both H (8.6±0.6 pS) and L (2.7±0.3 pS) states could be measured in stable single channel recordings, while M (~6 pS) could not. Spontaneous transitions between H and L were slow; it took 4.5 min. for L→H, and 3.2 min. for H→L. Similar phenomena were also observed with endogenous CFTR channels in T84 cells. At high salt conditions (1.5 M KCl), the M state (9.7±0.4 pS), as well as the H (14.8±0.6 pS) and L (3.6±0.4 pS) states, could be measured independently in separate experiments. A chaotropic agent, perchlorate, applied to the intracellular solution (10 mM), caused irreversible transition of the channel from H to L. The existence of multiple stable conductance states associated with the CFTR channel suggests that either a single CFTR molecule can exist in multiple configurations with distinct conductances for Cl ions, or the CFTR channel may contain multimers of the 170 kDa CFTR protein which aggregate or separate to form different conductance states of the Cl channel.

Su-Pos227

RECTIFICATION OF CFTR CHLORIDE CHANNEL MEDIATED BY EXTRACELLULAR DIVALENT CATIONS. ((B. Zerhusen, J. Zhao, T. Tao, J. Xie, M.L. Drumm*, P.B. Davis and J. Ma)) Dept. of Physiology & Biophysics, and Pediatrics*, Case Western Reserve Univ., Cleveland, OH.

Patch clamp studies identify the cystic fibrosis transmembrane conductance regulator (CFTR) as a linear conductance Cl channel. We report here distinct rectification of the CFTR channel reconstituted in lipid bilayer membranes. Under symmetrical ionic condition of 200 mM KCl (with 1 mM $MgCl_2$ in *cis*-intracellular and 0 $MgCl_2$ in *trans*-extracellular solutions), inward currents (*cis*→*trans* Cl movement) through a single CFTR channel were always larger than the outward currents (i=-0.68±0.03 pA, V=-80 mV; i=0.56±0.04 pA, V=+80 mV). The linear I-V relationship of the CFTR channel could be restored through addition of divalent cations to the *trans* solution. In the presence of 5 mM $[Mg]_o$ or $[Ca]_o$, the I-V curve became linear with a slope conductance of 8.6±0.6 pS. The dose responses for $[Mg]_o$ and $[Ca]_o$ had half dissociation constants of 152±81 μM and 290±129 μM, respectively. Rectification of the CFTR channel seemed to be due to negative surface charges on the channel protein, since in pure neutral phospholipid bilayers (PE), clear rectification of the channel could also be observed when the extracellular solution did not contain divalent cations. The CFTR protein contains clusters of negatively charged amino acids on several extracellular loops joining the transmembrane segments, which could constitute the putative binding sites for Ca and Mg. Supported by NIH, CFF, and AHA.

Su-Pos228

MODULATION OF CFTR CHANNEL BY MEMBRANE SURFACE CHARGES. ((Tao Tao, Junxia Xie, Mitch L. Drumm*, Jiying Zhao, Pamela B. Davis and Jianjie Ma)) Dept. of Physiol. & Biophys., and Pediatrics*, Case Western Reserve University, Cleveland, OH. (Spon. by D. Dearborn)

The effect of surface charges on the function of CFTR channels was studied in the bilayer reconstitution system. The bilayer membranes were formed with a lipid mixture of phosphatidylethanolamine (PE), phosphatidylserine (PS) and cholesterol (CL). We found that both Cl conductance and open probability of the CFTR channel were sensitive to negative charges on the bilayer membrane. The inward, as well as the outward, currents through a single CFTR channel increased significantly (~30%), when the lipid composition of the bilayers was changed from PE:PS:CL=6:6:1 to 12:0:1. Open probability of the channel followed inversely with negative charges on the bilayer (Po=0.45, 0.33, and 0.05 in PE:PS=12:0, 6:6, and 1:11). The conductance-activity relationship of the CFTR channel saturated at a maximum conductance of 16.7±0.7 pS with half Cl concentrations of 148±20 mM in PE:PS:CL = 6:6:1. The steep dependence of CFTR channel on Cl concentration and surface charge could account for the different conductance values (7-12 pS) reported in literature. Our data indicate that the conduction pore of the CFTR channel lies well within the region of the lipid membrane. Thus, hydrophilic portions of the CFTR molecule (nucleotide-binding folds and regulatory domain) would constitute mostly mobile structures, which could regulate the Cl conductance pathway through direct electrostatic or allosteric mechanisms.

Su-Pos229

MUTATION OF THE NARROW REGION OF THE CFTR CHANNEL PORE. ((Paul Linsdell, Johanna M. Rommens, Yue-Xian Hou, Xiu-Bao Chang, Lap-Chee Tsui, John R. Riordan and John W. Hanrahan))
Dept. Physiology, McGill University, Montréal, PQ; Research Institute, Hospital for Sick Children, Toronto, ON; and Mayo Clinic, Scottsdale, AZ.

CFTR is a phosphorylation-regulated and nucleotide-dependent Cl channel. Several lines of evidence suggest that the sixth membrane-spanning region of CFTR (TM6) is a major constituent of the channel pore. Mutation of a threonine residue at position 338 in TM6 is associated with an unusual, mild cystic fibrosis phenotype. Since threonine side-chains have been implicated in the formation of ion channel permeation pathways, we have examined the role of this and an adjacent threonine residue in CFTR channel function using the Chinese hamster ovary cell expression system. Mutation of both these residues to alanines (the TT338,339AA mutant) led to an approximately 25% increase in single channel conductance with symmetrical 150mM Cl solutions. Saturating conductance seen at higher Cl concentrations was similarly increased. In addition, TT338,339AA channels had increased permeability to several large extracellular anions, consistent with an increase in the size of the narrowest part of the pore. We suggest that one or both of these threonine residues normally line a constriction in the permeation pathway of CFTR, and that interaction between permeating Cl ions and this narrow region slows flux through the pore. *Supported by MRC, CCFF and NIH(NIDDK).*

Su-Pos230

EXPRESSION OF PHOSPHOLEMMAN 1-43 INDUCES CHLORIDE CURRENTS IN *XENOPUS* OOCYTES ((J. Paul Mounsey, Zhenhui Chen, J. Edward John, J. Randall Moorman, Larry R. Jones)) University of Birmingham, UK; University of Virginia, Charlottesville, VA; Indiana University, Indianapolis, IN.

Phospholemman (PLM) induces Cl currents when expressed in *Xenopus* oocytes and forms anion channels when reconstituted in phospholipid bilayers. It has a single transmembrane domain with intracellular and extracellular domains: at 72 aa in length, it is the smallest membrane protein known to form ion channels. To investigate whether the cytoplasmic domain is a necessary part of the ion pore, we expressed mRNA encoding only the transmembrane domain and extracellular peptide of PLM (PLM 1-43) in *Xenopus* oocytes. The Figure shows hyperpolarization-activated oocyte currents recorded during two-microelectrode voltage clamp. The currents induced by expression of PLM 1-43 (center) and intact PLM (right) have similar kinetics, threshold, voltage dependence of activation, and reversal potential-dependence on external [Cl]. The similarity of the currents suggests that the PLM molecule does not require the cytoplasmic tail for function. The finding of a membrane current induced by PLM 1-43 establishes a new estimate of the minimum size required for an ion channel subunit.

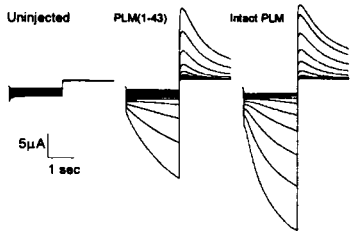

MODULATION OF CHANNELS

Su-Pos231

Acetylcholine inhibits voltage-dependent Ca^{2+} channels in mouse pancreatic B-cells. Gilon P[1,2,3], Yakel J[2], Gromada J[1], Zhu Y[2], Henquin JC[3] and Rorsman P[1].
[1]Islet Cell Physiology, Novo Nordisk A/S, Denmark. [2]Laboratory of Cellular and Molecular Pharmacology, NIH, North Carolina. [3]Laboratoire d'Endocrinologie et de Métabolisme, UCL, Belgium.

Acetylcholine (ACh) stimulates insulin secretion by activating muscarinic receptors in B-cells. However, it has recently been reported that ACh exerts both stimulatory and inhibitory effects on the concentration of cytoplasmic Ca^{2+} ($[Ca^{2+}]_i$). In the present study, we have tested the hypothesis that ACh lowers $[Ca^{2+}]_i$ by inhibiting the voltage-dependent Ca^{2+} channels. Voltage-clamp Ca^{2+}-currents were recorded in individual mouse pancreatic B-cells using the standard whole-cell configuration. ACh (2.5 - 250 μM) reversibly and dose-dependently inhibited the Ca^{2+} current elicited by depolarizations from -80 mV to 0 mV. The maximum inhibition, observed at concentrations >25 μM, averaged 30%. The effect was blocked by atropine (10 μM). Indicative of an involvement of G-proteins, the inhibitory effect of ACh on the Ca^{2+} current was more pronounced and irreversible after inclusion of 10 μM GTPγS in the pipette solution (dialyzing the cell interior) and was prevented by 2 mM GDPβS in the pipette. However, overnight pretreatement of the cells with either pertussis or cholera toxin (500 ng/ml) both failed to prevent the effect of ACh on the Ca^{2+}-current. The effect of ACh was not due to the activation of PKC as suggested by the observation that TPA (500 nM) failed to reproduce the inhibitory action. Likewise, it is unlikely to result from Ca^{2+}-induced inhibition of the Ca^{2+} current as: 1) the effect remained observable when Ba^{2+} was used as the charge carrier; and 2) all intracellular solutions contained 10 mM EGTA to buffer $[Ca^{2+}]_i$ to very low concentrations. The effects of ACh on the Ca^{2+}current were not prevented by including 100 μM $(2,4,5)IP_3$ or 1 mg/ml heparin in the pipette solution suggesting that ACh-induced elevation of IP_3 does not account for the action on the Ca^{2+}-current . In conclusion, ACh inhibits voltage-dependent Ca^{2+} current by a Ca^{2+}-independent mechanism following activation of a pertussis toxin- and cholera toxin-insensitive G protein.

Su-Pos232

PURINERGIC MODULATION OF A VOLTAGE GATED POTASSIUM CHANNEL IN RAT BROWN ADIPOCYTES. ((S.M. Wilson & P.A. Pappone)) Univ. of California, Davis 95616.

We found that stimulation of P_{2y} purinergic receptors with 20 nM - 10 μM extracellular ATP induced a 50 - 100% decrease in voltage gated potassium (IKv) currents evoked from a -60 mV holding potential in rat brown adipocytes. This IKv current decrease developed over several minutes following ATP exposure in whole cell patch voltage clamped cells with a nucleotide-free internal pipette solution. The IKv membrane current decrease is due to hyperpolarizing shifts in the V1/2 of steady state inactivation which ranged from -14 to greater than -60 mV. The voltage dependence of activation was shifted negative also, but by a lesser amount, 0 to - 27 mV in the same cells (n=13).

The response of the brown adipocytes to extracellular ATP was dependent upon the cytosolic integrity. In whole cell experiments with the nucleotide-free internal pipette solution the effects of external ATP exposure were irreversible. Adding mM ATP to the pipette solution required a 5 fold increase in the extracellular ATP dose to induce a measurable IKv current decrease. Furthermore, in perforated patch clamped cells IKv current only transiently decreased when ATP was applied, suggesting that a non-membrane bound component may be involved in modulating the purinergic response.